NASA Contractor Report 178116

1N-19604

Development of Composite Tube Protective Coatings

H. Dursch, and C. Hendricks

Boeing Aerospace Company

Seattle, Wa 98124

Contract NAS1-16854

July 1986

(NASA-CR-178116) DEVELOPMENT CF COMPOSITE TUBE PROTECTIVE COATINGS Final Report (Boeing Aerospace Co., Seattle, Wash.) 109 p CSCL 11G

N86-29989

Unclas

G3/27 43540

NASA

National Aeronautics and
Space Administration

Langley Research Center
Hampton, Virginia 23665-5225

NASA Contractor Report 178116

Development of Composite Tube Protective Coatings

H. Dursch, and C. Hendricks

Boeing Aerospace Company

Seattle, Wa 98124

Contract NAS1-16854

July 1986

NASA

National Aeronautics and
Space Administration

Langley Research Center
Hampton, Virginia 23665-5225

FOREWORD

This report describes the work accomplished by the Boeing Aerospace Company under Contract NAS1-16854, Task 4, "Development of Composite Tube Protective Coatings". The contract was sponsored by the National Aeronautics and Space Administration, Langley Research Center.

Mr. Louis A. Teichman was the NASA Technical Monitor. The Materials and Processes Technology organization of the Boeing Aerospace Company was responsible for the work performed in Task 4. Mr. Carl L. Hendricks was program manager; Mr. Harry W. Dursch was the technical leader. The following personnel provided critical support to various task activities.

Ethel A. Greyerbiehl	Manufacturing R&D, coordination of composite tube fabrication.
Warren R. Lance	Performed structural analysis.
Walter L. Plagemann	Coordination of analyses to determine coating optical properties, and examination of tubes for microcracks.
Mark S. Pollack	Manufacturing, preparation of aluminum foil anodized surfaces.

CONTENTS

CONTENTS (Cont'd)

Figures

Figures (Cont'd)

Figures (Cont'd)

1.0 INTRODUCTION AND SUMMARY

INTRODUCTION

Contract NAS1-16854 between the National Aeronautics and Space Administration, Langley Research Center, and the Boeing Aerospace Company was established for the purpose of researching the effects of simulated space environments on spacecraft materials, especially advanced composites. The contract is of the task assignment type. Four tasks were authorized for performance on the contract with Task 1 beginning on September 30, 1981 and Task 4 ending on May 16, 1986. This document reports the results of Task 4 conducted during the period from May 5, 1985 to May 16, 1986.

The objective of Task 4 was to evaluate protective coatings for graphite/epoxy (Gr/Ep) tubular structures for a manned Space Station. There are many requirements for these tubes, including high stiffness, dimensional stability, close tolerances in dimensions, and stability in the low Earth orbit (LEO) environment. To accomplish the goals of this contract, the structural, optical, and environmental properties of Gr/Ep composite tubes for use in erectable Space Station applications had to be defined.

The required structural properties of the tubes were defined from Space Station and Boeing documentation and meetings with NASA Langley personnel. No new test analyses were performed. Using Gr/Ep properties generated by tests conducted by the industry, an analysis of the predicted composite mechanical and thermal properties in a tube configuration was generated with a Boeing-developed computer program (INCAP). This analysis determined the ply orientation and prepreg required to meet the structural properties.

The success of the composite tube truss structure for the Space Station depends on its ability to endure long-term exposure to various LEO environmental factors such as atomic oxygen, thermal cycling, charged-particle radiation, ultraviolet radiation, micrometeroids, and space debris. The atomic oxygen environment at LEO is especially severe and has been observed to cause significant degradation of exposed spacecraft surfaces. The recombination of atomic oxygen absorbed on the Gr/Ep surfaces causes substantial erosion of the Gr/Ep. The atomic oxygen also causes optical properties of organic coatings to increase their solar absorptance and the diffuse component of their reflectance. A consideration of LEO environmental effects on protectively coated Gr/Ep structures must also take into account combined effects, such as micrometeroid penetration, which would allow a mechanism for atomic oxygen degradation of the coating or Gr/Ep composite.

Concepts for protectively coating the Gr/Ep tubes from the LEO environment include the use of metal foils and electroplating. The metal foil evaluated was primarily aluminum foil that had been anodized or had a vacuum-deposited coating applied prior to wrapping onto the Gr/Ep tube. Adhesive systems were evaluated for bonding the foils, and composite surface treatments were evaluated for the promotion of electroplating adherence. The various protective coatings were optimized to possess the targeted optical values, which included a nonspecular reflectance to eliminate any problems associated with astronauts working with mirror-like surfaces.

The various protective coatings were applied to the Gr/Ep tubes and then subjected to simulated LEO environmental testing to evaluate the coatings and the coated tubes survivability in LEO. The evaluation of the coatings included abrasion resistance, atomic oxygen resistance, surface preparation required, formation of microcracks in the tubes, changes in optical properties and adhesion after testing, coating uniformity, and pin hole density.

Four 8-ft-long Gr/Ep tubes were fabricated and coated with the optimized protective coating. These full-scale tubes, along with a representative Space Station truss structure joint, were submitted to NASA LaRC at the end of this contract.

SUMMARY

This program was divided into four parts:

Part 1 - System Definition
Part 2 - Coating Concept Selection and Evaluation
Part 3 - Scale-up and Assembly
Part 4 - Reporting

Part 1: System Definition. Two primary areas required definition. The first was to define the structural configuration of the composite tubes and the second was to define the LEO environment. Structural configuration included (1) selecting the composite materials to be used for tube construction and the necessary procurement controls, (2) establishing the structural configuration of the tubes, and (3) determining the tape ply orientation to meet the structural requirements that were established. The prepreg and composite ply sequence selected was a P75S/934 $(0_2, \pm 20, 0_2)_s$ layup. This layup meets the primary requirements of high composite stiffness (longitudinal tensile modulus $\geq$ 40 Msi), relatively large data base, and commercial availability. Definition of the LEO environment included (1) determining the temperature extremes experienced by coated and uncoated composite tubes, (2) definition of the solar radiation type and amount, (3) determination of the flux and energy of atomic oxygen, and (4) estimation of the potential effects from micrometeroids and space debris.

Part 2: Coating Concept Selection and Evaluation. This part of the task comprised the main emphasis of the contract. Part 2 concentrated on selecting and evaluating candidate protective coatings for the composite tubular concepts. A total of eleven concepts were screen tested for processing properties and optical characteristics. The initial evaluation narrowed the list to five coatings:

a. Sputtered 1 micron SiO_2/sputtered 3000Å Al/Al foil.
b. Phosphoric acid anodized Al foil.
c. Chromic acid anodized Al foil.
d. Electroplated nickel.
e. SiO_x/electroplated nickel.

These five coatings were evaluated for (1) adherence of the coating to the composite tube under a combined vacuum and thermal environment and under a thermal cycling environment, (2) surface preparation required for coating of the composite tubes, (3) compatibility of coefficient of thermal expansion of the coating with that of the composite tubes, (4) abrasion resistance and changes in optical properties under handling conditions, (5) optical properties in the as-formulated state and after thermal/vacuum exposure, and (6) atomic oxygen resistance.

Part 3: Scale-up and Assembly. During this part of the program, two selected coatings-chromic acid anodized Al foil and SiO_2/Al/Al foil-were further evaluated to demonstrate feasibility, quality, reliability, and environmental durability. Four 8-ft-long by 2-in-diameter tubes wrapped with chromic acid anodized Al foil were fabricated. The anodized Al foil was 0.002-in-thick, had an AM-O solar absorptance of 0.22 and a thermal emittance of 0.23. It also had a very high nonspecular reflectance. These four full-scale tubes, fitted with representative Space Station erectable truss structure end-fittings, were submitted to NASA LaRC. Figure 1.0-1 shows the assembled truss structure.

Part 4: Reporting. A kickoff meeting was held at NASA LaRC on June 4, 1985, to inform NASA personnel of our proposed program approach. Three different interim progress reports were delivered to NASA LaRC during the duration of this contract. An oral presentation of this final report was given at NASA LaRC on May 5, 1986, to NASA personnel.

The program test results demonstrated that both phosphoric acid and chromic acid anodized aluminum foils possess retention of adhesion to the composite tubes and stability of optical properties when subjected to atomic oxygen and thermal cycling representative of the LEO environment. SiO_2/Al coatings sputtered onto Al foils also resulted in an excellent coating with respect to optical and adhesion properties and resistance to simulated LEO environment. However, the large vacuum chamber requirements for deposition made it less desirable than the anodized Al coatings. The electroplated Ni possessed unacceptable adhesion loss to the Gr/Ep tube during atomic oxygen testing.

An investigation into the relative toughness (microcrack resistance during thermal cycling) of the $(0_2, \pm 20, 0_2)_s$ Gr/Ep tubes was also undertaken. The tubes were subjected to a total of 550 1-hr thermal cycles to determine if the thermal cycling at LEO would cause any formation of microcracks. The temperature range was +120°F to -150°F. After the cycling was completed, the tubes were examined for microcracks using 50X-200X magnification and X-ray analysis. No microcracks were found in any of the Gr/Ep tubes. The use of low-angle off-axis plies required to meet the stiffness requirements of the Space Station seems to have minimized the microcracking phenomenon.

ORIGINAL PAGE IS
OF POOR QUALITY

Figure 1.0-1 Four 8-ft Graphite/Epoxy Tubes Latched Together

2.0 SYSTEM DEFINITION

The objective of this task was to define the structural and environmental properties required of composite tubes for use in Space Station truss applications. This information was generated from Boeing data and Space Station documentation.

2.1 STRUCTURAL DEFINITION

This section defines the structural properties required for the composite tubes. Properties that were defined included required material, recommended construction techniques, structural configuration and ply orientation, and the resulting mechanical and thermal properties.

2.1.1 Selected Composite Material

The composite material selected for tube fabrication was P75S/934 Gr/Ep supplied as a unidirectional 0.005-in-thick prepreg tape by Fiberite Corporation. P75S is a high modulus graphite fiber manufactured by Union Carbide; 934 is an epoxy resin manufactured by Fiberite. This material has a relatively mature data base generated from work completed by Boeing on the Optical Telescope Assembly and other space programs. The prepreg was procured to Boeing Specification BMS 8-247, "Graphite Fiber Preimpregnated With Epoxy Resin, Unidirectional Tape, 350^{o}F Cure."

The P75S/934 Gr/Ep composite was selected to meet the primary requirements of high composite stiffness (longitudinal tensile modulus $\geq$ 40 Msi), relatively large data base, and commercial availability. Other competing high modulus fibers, such as P100 or GY70 combined with candidate resins such as BP907 (American Cyanamid), 5245 (Narmco), and ERLX 1962 (Union Carbide), have not been produced and evaluated in commercial quantities and represented a high risk for this program.

2.1.2 Structural Configuration

The structural configuration of the composite tubes was derived from the Space Station configuration document published by NASA (ref. 1). Based on this document and inputs from meetings with NASA Langley personnel, the full-scale composite tube configuration selected for the deliverable tubes was 8-ft in length with an I.D. of 2.0 in.

2.1.3 Composite Ply Orientation

The composite ply orientation selected was $(0_2, \pm 20, 0_2)_s$. This selection was based on analysis results of P75S/934 composite ply orientations using a Boeing-developed computer program called INCAP. The analysis methods contained in INCAP are based on classical lamination theory; the base material properties of P75S/934 were developed from results of industry test data. INCAP plots are shown for the tensile modulus in the longitudinal and hoop (x and y) directions; shear modulus and coefficient of thermal expansion (CTE) in the x and y direction vs θ for various ply stacking sequences. Three basic ply stacking sequences were analyzed: $(0_2, \pm\theta, 0_2)_s$, $(\theta, 0, -\theta, 0, \theta, 0)_s$ and $(\pm\theta, 0_2 \mp\theta)_s$. The plots of the mechanical properties versus θ are shown in figures 2.1.3-1 through 2.1.3-5. Figure 2.1.3-6 summarizes these figures and also includes Euler buckling and ultimate strength values. Although the $(\theta, 0_5)_s$ layups had the required stiffness and strength, they were eliminated from consideration because of the shear-extensional coupling that would occur in the unbalanced layup. Shear-extensional coupling is the shearing of the off-axis plies during extension, which induces moments in the laminate. A balanced layup has counteracting plies $(\pm\theta)$ that eliminate this phenomenon.

Crushing strengths of the various layups were also determined. This was done to simulate maximum handling stresses that could occur during assembly. Because the ultimate strength of the composite tube in the longitudinal direction is many times greater than in the hoop direction, the greater the off-axis ply angles, the better the crushing resistance. It was determined that, while all layups with all θ's $\leq$20 deg were marginal, layups with all θ's $\leq$10 deg were too easily crushed to warrant further consideration. A point load of 5 lbs was used to represent the gripping force that could occur during assembly.

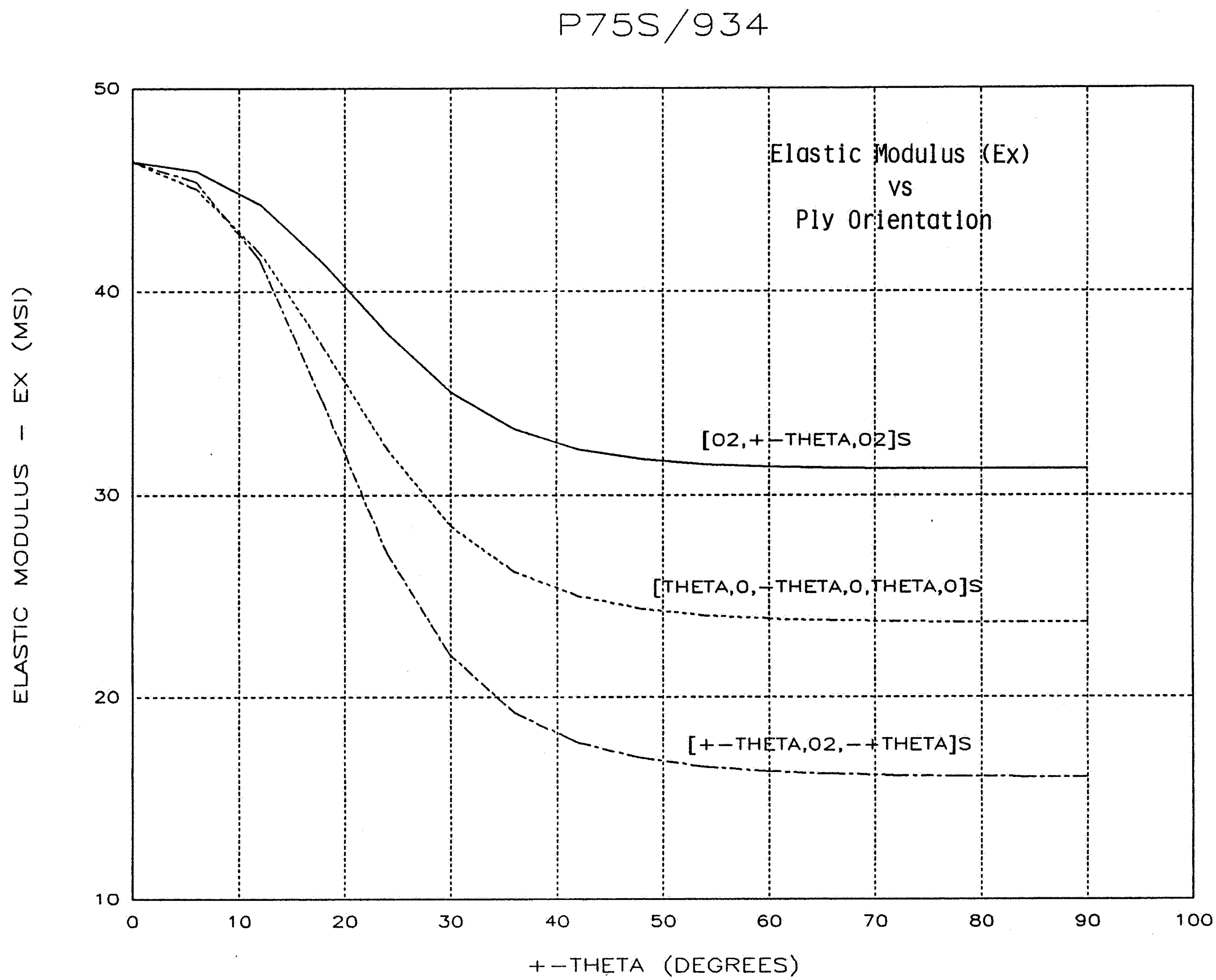

Figure 2.1.3-1 Elastic Modulus (Ex) Versus Ply Orientation

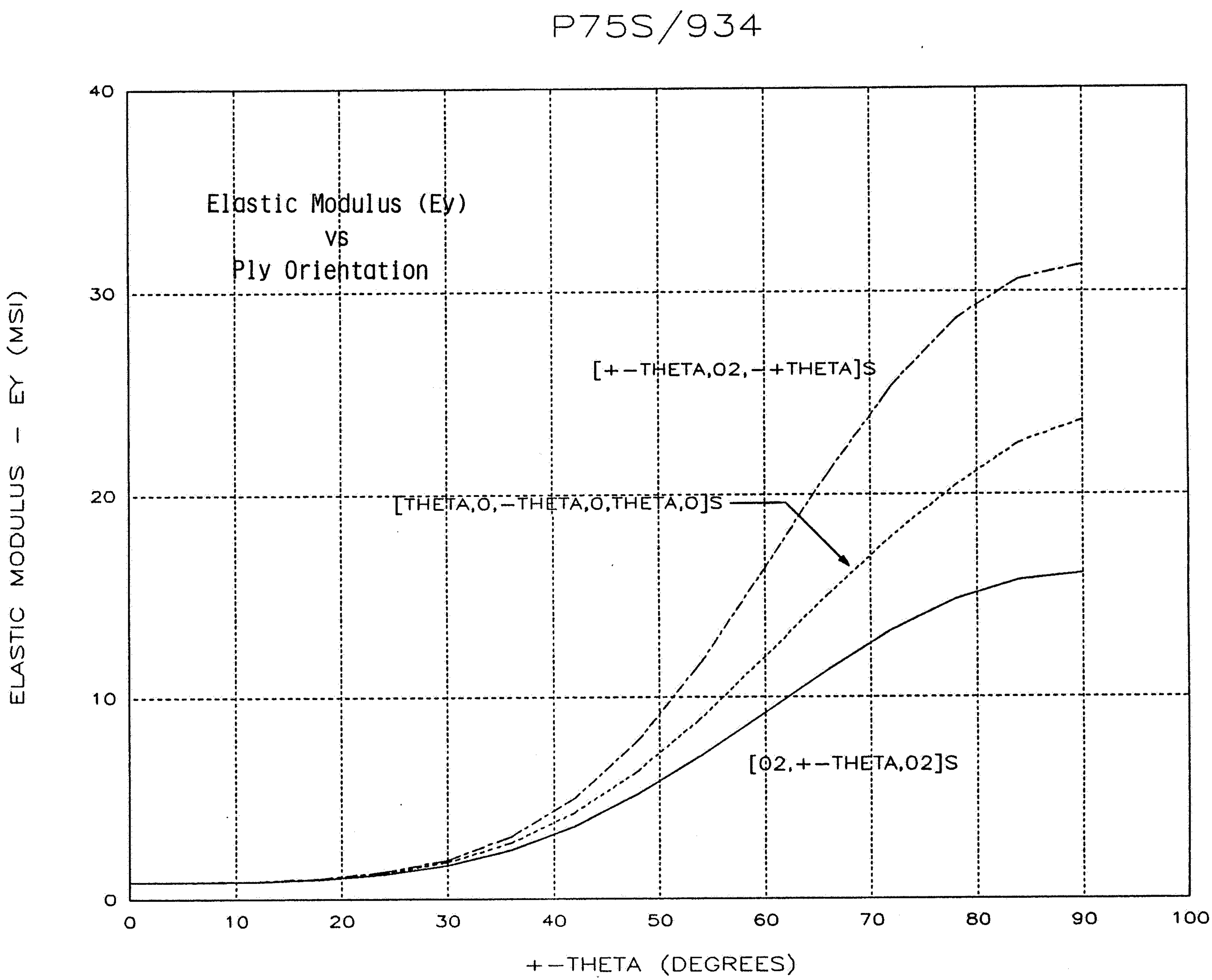

Figure 2.1.3-2 **Elastic Modulus (Ey) Versus Ply Orientation**

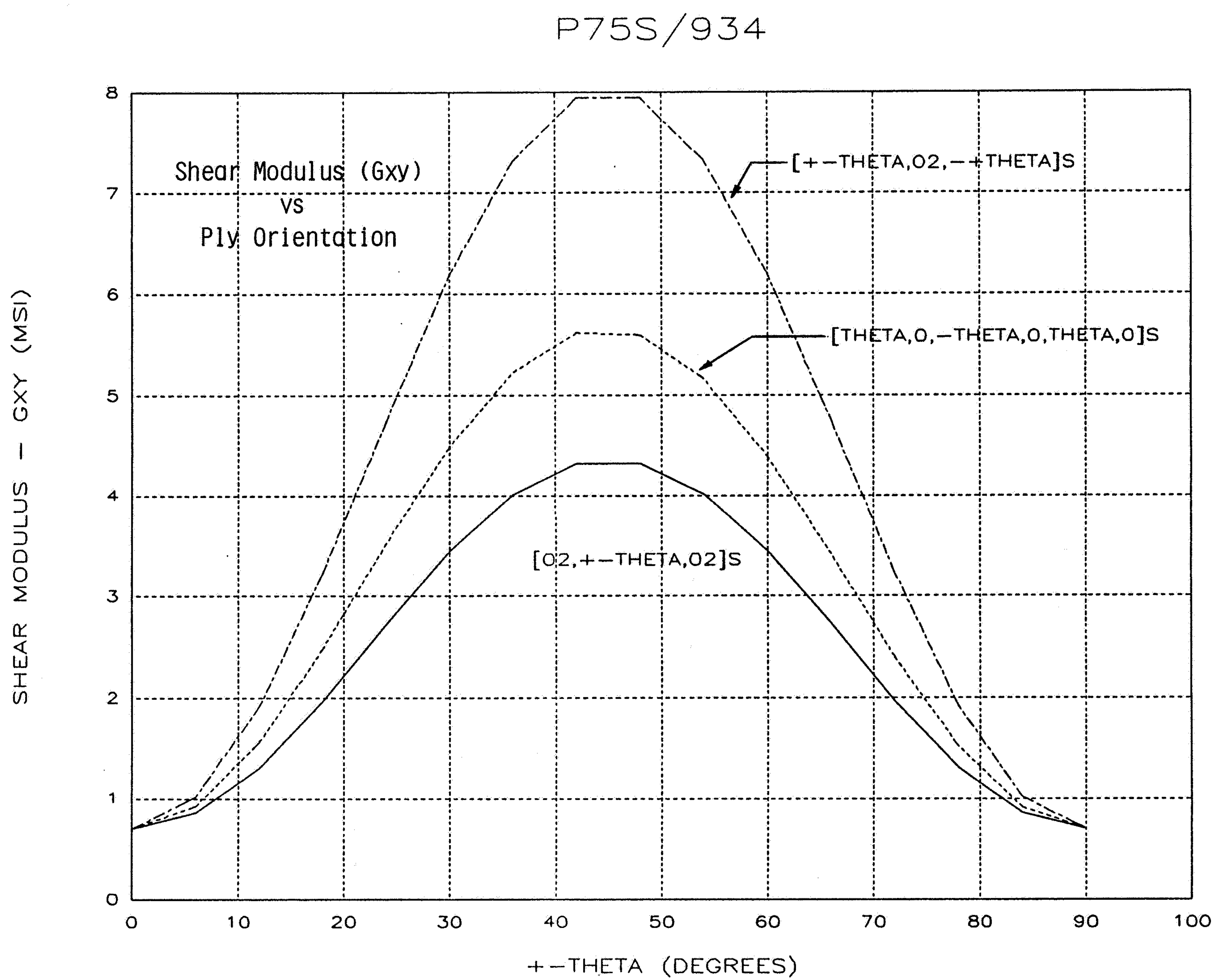

Figure 2.1.3-3 Shear Modulus (Gxy) Versus Ply Orientation

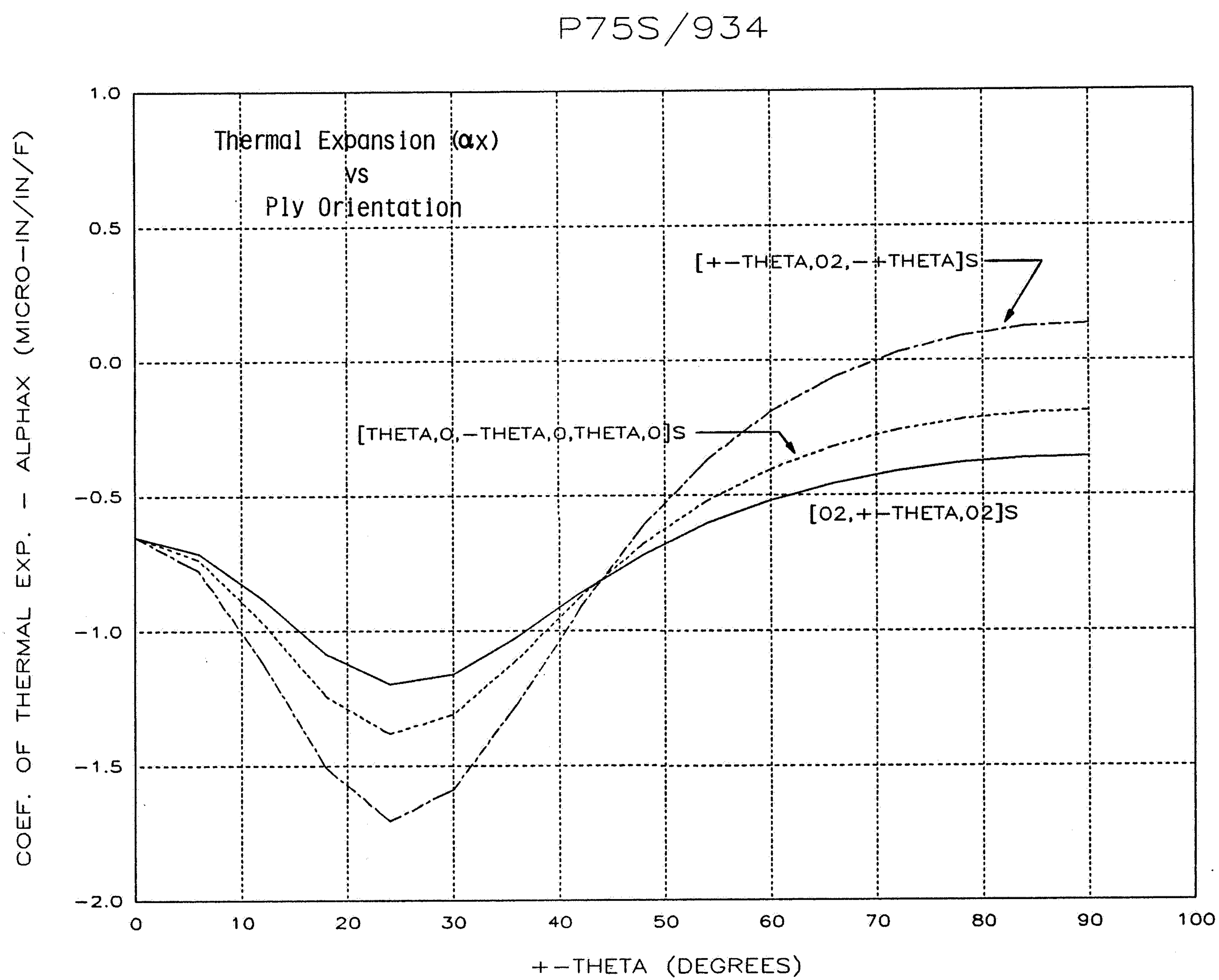

Figure 2.1.3-4 **Thermal Expansion (αx) Versus Ply Orientation**

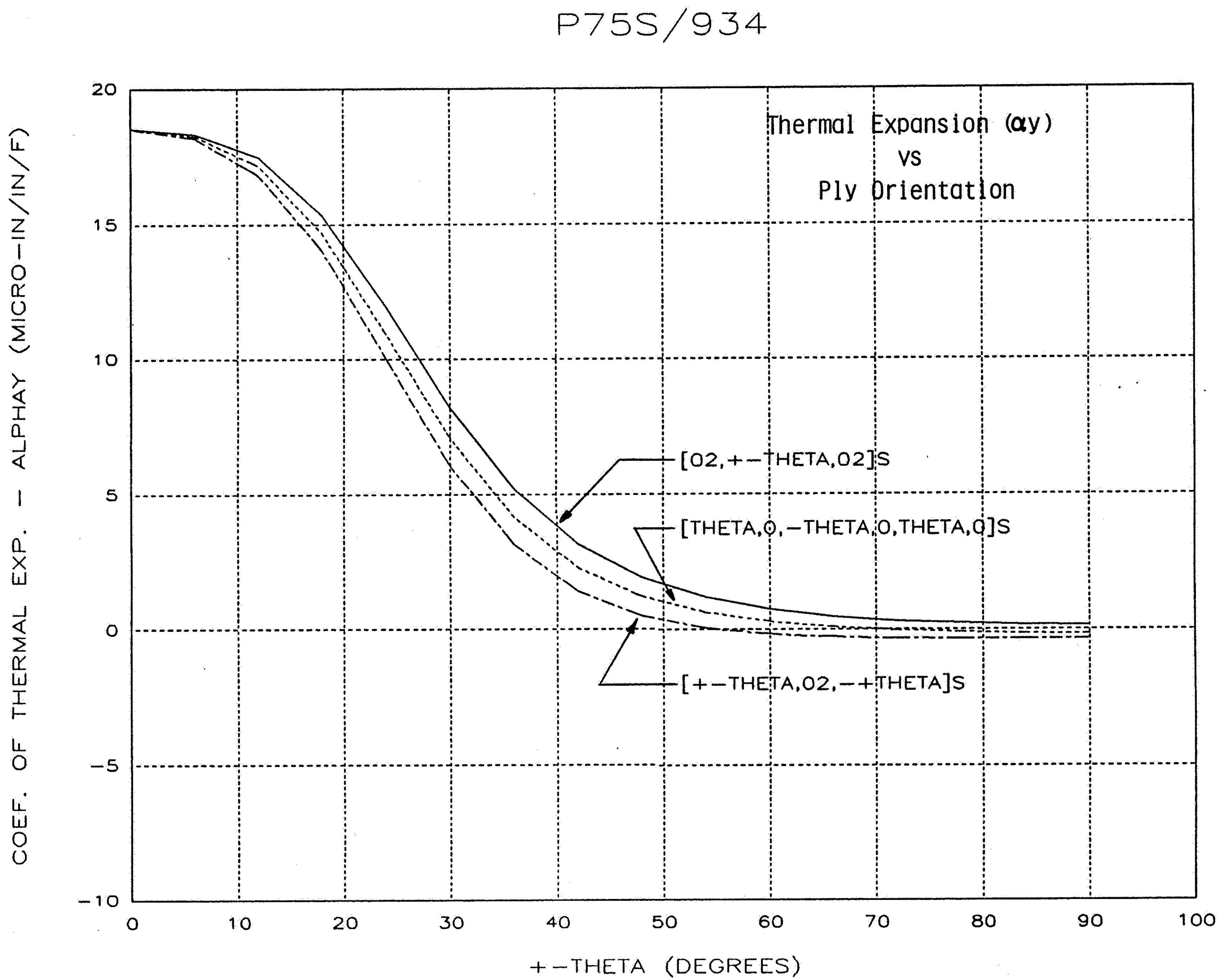

Figure 2.1.3-5 **Thermal Expansion (αy) Versus Ply Orientation**

Layup	Ex (Msi)	Ey (Msi)	Gxy (Msi)	αx (μin/in)	αy (μin/in)	F_L^{tu} (ksi)	F_T^{tu} (ksi)	Euler Buckling Load (lb) (L=8 ft)
$(0_2, \pm10, 0_2)_s$	45	0.8	1.1	-0.8	17.5	105	2.4	9900
$(0_2, \pm15, 0_2)_s$	42.5	0.9	1.6	-1.0	17	100	2.5	9400
$(0_2, \pm20, 0_2)_s$	40	1.0	2.2	-1.1	14	95	2.7	8800
$(0_2, \pm30, 0_2)_s$	35	1.7	3.5	-1.2	8	80	4.0	7700
(10, 0, -10, 0, 10, 0)s	42.5	0.8	1.4	-0.9	17	95	2.5	9400
(20, 0, -20, 0, 20, 0)s	35.5	1.0	2.9	-1.3	13.5	80	2.7	7800
(30,0, -30, 0, 30, 0)s	28	1.8	4.5	-1.3	7	65	4.0	6200
$(\pm10, 0_2, \mp10)_s$	42.5	0.8	1.6	-1.0	16.5	102	3.0	9400
$(\pm20, 0_2, \mp 20)_s$	32	1.0	3.8	-1.6	12.5	74	4.4	7100
$(\pm30, 0_2, \mp 30)_s$	22	1.8	6.2	-1.6	6	52	8.6	4900

Figure 2.1.3-6. Composite Matrix Properties

With a minumum of 40 Msi required for the longitudinal tensile modulus, the only two remaining layups are $(0_2, \pm 15, 0_2)_s$ and $(0_2, \pm 20, 0_2)_s$. Of these two layups, the $(0_2, \pm 20, 0_2)_s$ was chosen because of its lower CTE in the hoop direction and the increased shear modulus. This layup also effectively increased the crushing strength of the tubes compared to the $(0_2, \pm 15, 0_2)_s$ layup.

The thermal expansion of the selected layup (fig. 2.1.3-6) is -1.1 in/in and 14.0 in/in in the longitudinal and hoop direction respectively. No difficulty is expected to be caused by the high-hoop CTE if the tube is wrapped with Al foil or if Al end fittings are used, because the CTE of Al is closely matched to the hoop CTE of this tube layup.

Figures 2.1.3-7 through 2.1.3-11 show the effect on the mechanical and thermal expansion properties caused by wrapping the $(0_2, \pm\ , 0_2)_s$ P75S/934 Gr/Ep tubes with 0.002-in-thick Al foil and the 0.005-in-thick epoxy adhesive used to bond the foil to the tube surface. Figure 2.1.3-7 shows that with foil and adhesive on the exterior surface of the tube, the longitudinal tensile modulus decreases from 40 Msi to 38 Msi for a $(0_2, \pm 20, 0_2)_s$ layup. Figure 2.1.3-12 summarizes the results.

The weight of the bare $(0_2, \pm 20, 0_2)_s$, 2-in ID, P75S/934 tube is 0.30 lb/lineal ft. The addition of 0.002-in-thick Al foil and 0.005-in-thick epoxy to the exterior surface increases the weight of the tube to 0.33 lb/lineal ft. If 0.003-in-thick epoxy is used instead of the 0.005-in-thick epoxy, the weight of the tube becomes 0.32 lb/lineal ft. The protective coatings and the primer used to improve the epoxy/Al foil bond adds negligible weight to the Gr/Ep tubes.

2.1.4 Fabrication of Gr/Ep Tubes

The construction technique selected for fabrication of composite tubes for this program was convolute wrapping. It had the advantages of high speed and efficient wrapping of superior quality composite tubes. The Gr/Ep plies are cut to size from the roll of prepreg before wrapping. Each ply is approximately 0.030-in wider than the previous one to take into account the increasing circumference of the tube as the various plies are applied. The plies are then wrapped onto a mandrel using a rolling table. Before the initial ply is applied, the mandrel has had several coats of releasing agents applied to ensure release of the cured composite tube. The

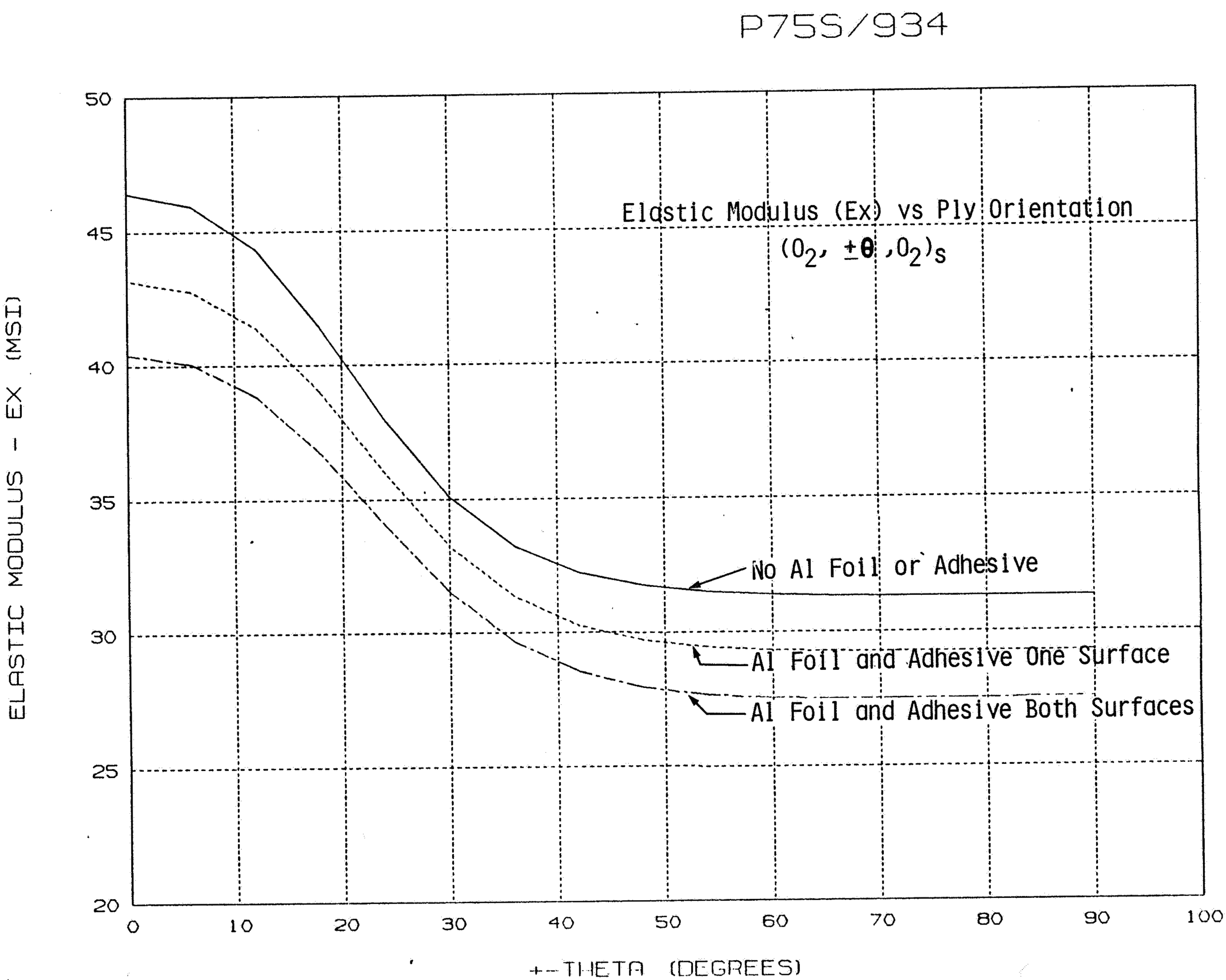

Figure 2.1.3-7 **Elastic Modulus (Ex) With and Without Al Foil and Adhesive**

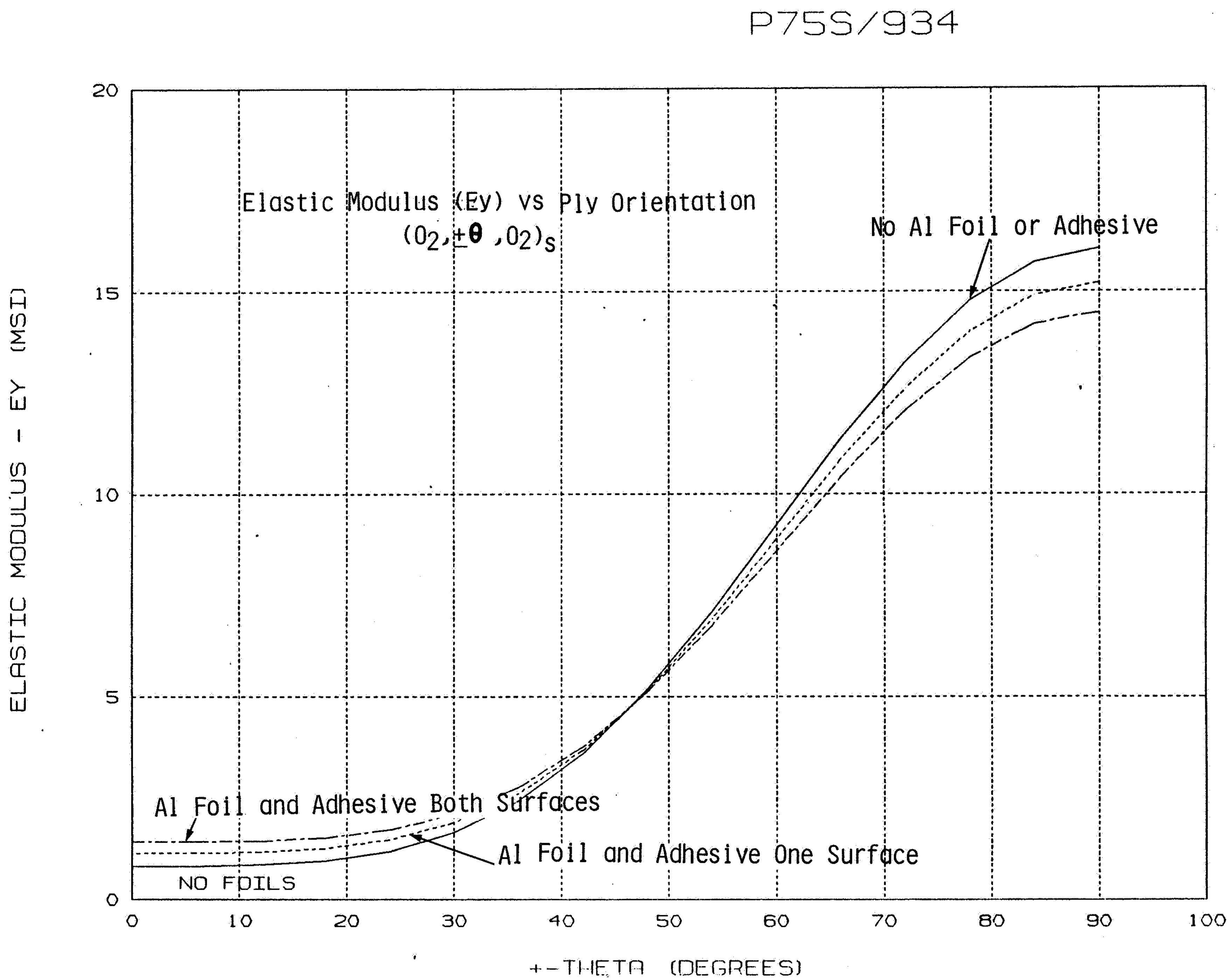

Figure 2.1.3-8 Elastic Modulus (Ey) With and Without Al Foil and Adhesive

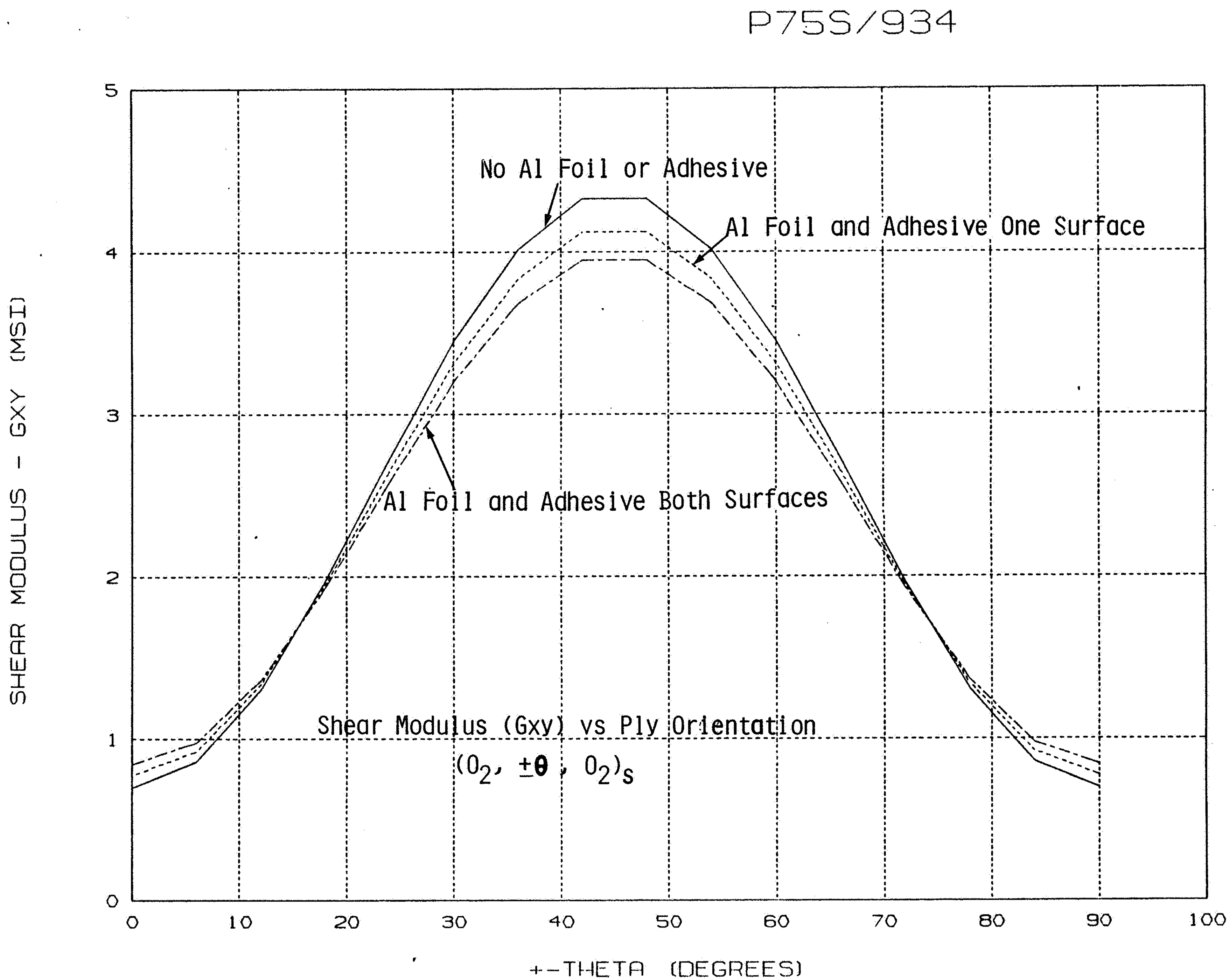

Figure 2.1.3-9 **Shear Modulus (Gxy) With and Without Al Foil and Adhesive**

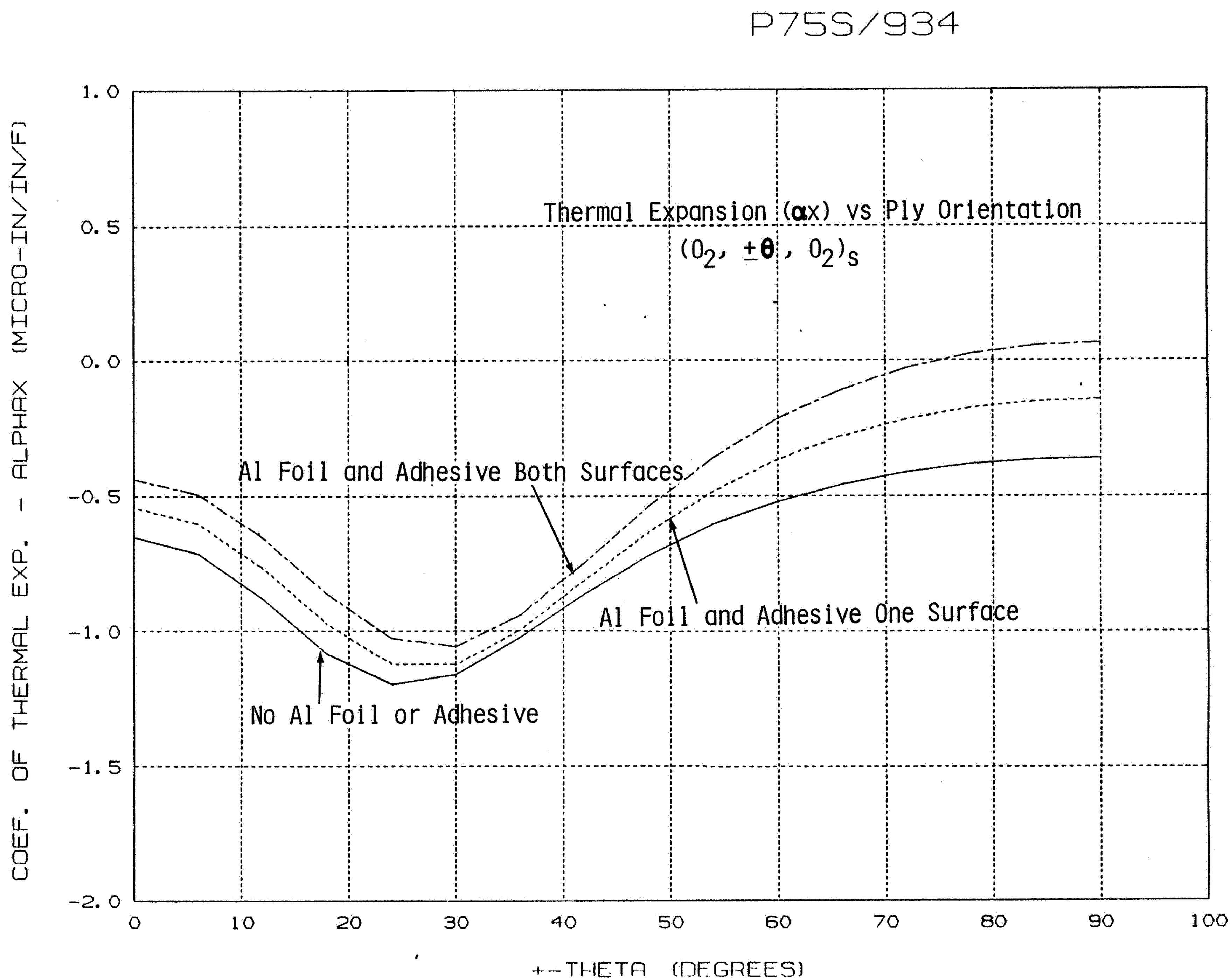

Figure 2.1.3-10 **Thermal Expansion (αx) With and Without Al Foil and Adhesive**

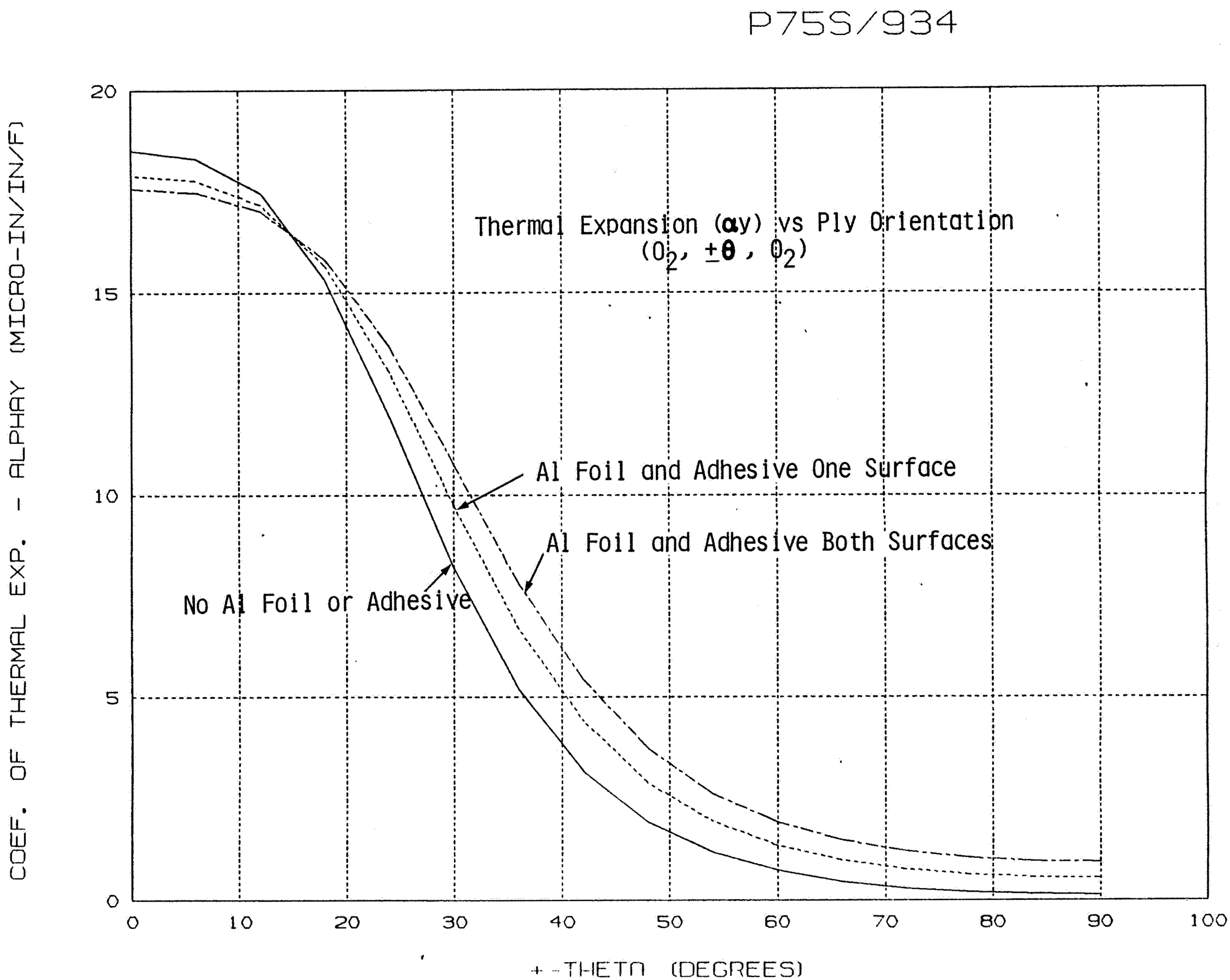

Figure 2.1.3-11 **Thermal Expansion (αy) With and Without Al Foil and Adhesive**

Layup	Ex (Msi)	Ey (Msi)	Gxy (Msi)	αx (μin/in)	αy (μin/in)
$(0_2, \pm 20, 0_2)_s$	40	1.0	2.2	-1.1	14
$(0_2, \pm 20, 0_2)_s$ with foil on one surface	38	1.3	2.2	-1.0	15
$(0_2\ \pm 20, 0_2)_s$ with foil on both surfaces	36	1.6	2.2	-0.9	15

Figure 2.1.3-12. Composite Tube Matrix Properties

(with and without 0.002-in Al foil bonded to the tube using 0.005-in epoxy adhesive)

wrapped mandrel is vacuum bagged, thermocoupled, and then cured in an autoclave. This fabrication method and cure cycle are a standard process at Boeing and were used for all the tubes fabricated during this contract. The tubes were 4-ft-long and, after curing, were cut into 1-ft lengths before having the various coatings applied. Several 8-ft tubes were also fabricated, including the four delivered to NASA LaRC for Part 3 (Scale-up and Assembly) of this contract.

An adhesive layer consisting of 0.005-in, 350°F cure, sheet epoxy was used to bond the Al foil to the last ply of each tube. 0.003-in-thick sheet epoxy could be used, but the small amount required for this program didn't justify the amount required by the vendor for a minimum purchase. The foil and adhesive were wrapped onto the tube using the same technique as wrapping a 0-deg ply. To give a more textured (diffuse) surface to the foil surface, the four 8-ft-long tubes had fiberglass roving spiral wrapped on the exterior surface of the foil. The tubes were then vacuum bagged and cured using the same cycle as was used for bare tubes.

2.1.5 Space-Erectable End Fitting

The NASA SOW required that each of the four 8-ft-long Gr/Ep tubes delivered to NASA be fitted with a "typical space-erectable structural end fitting." Boeing purchased (from Star Net, a division of Space Structures) an end-fitting that meets NASA's requirements.

The hub and stud assembly (fig. 2.1.5-1) represents a corner of an interlocking network of Gr/Ep struts and aluminum hubs that can easily be erected by a single astronaut without tools. Threaded aluminum inserts are bonded to the inside of each Gr/Ep tube using 350°F cure epoxy and 0.006-in shims to control the bondline. The inserts had been cleaned, phosphoric acid anodized, and primed to increase the bond strength. An end view of the bonded insert is shown in figure 2.1.5-2. The latching mechanism is then screwed into the Gr/Ep tube and a locking ring is tightened to hold the devise in place. Strut attachment to the hub assembly begins by attaching the latching device at the end of the strut (fig. 2.1.5-3) to the hub assembly. The strut and hub are mated and a locking collar is moved forward and rotated to secure the strut to the hub.

ORIGINAL PAGE IS
OF POOR QUALITY

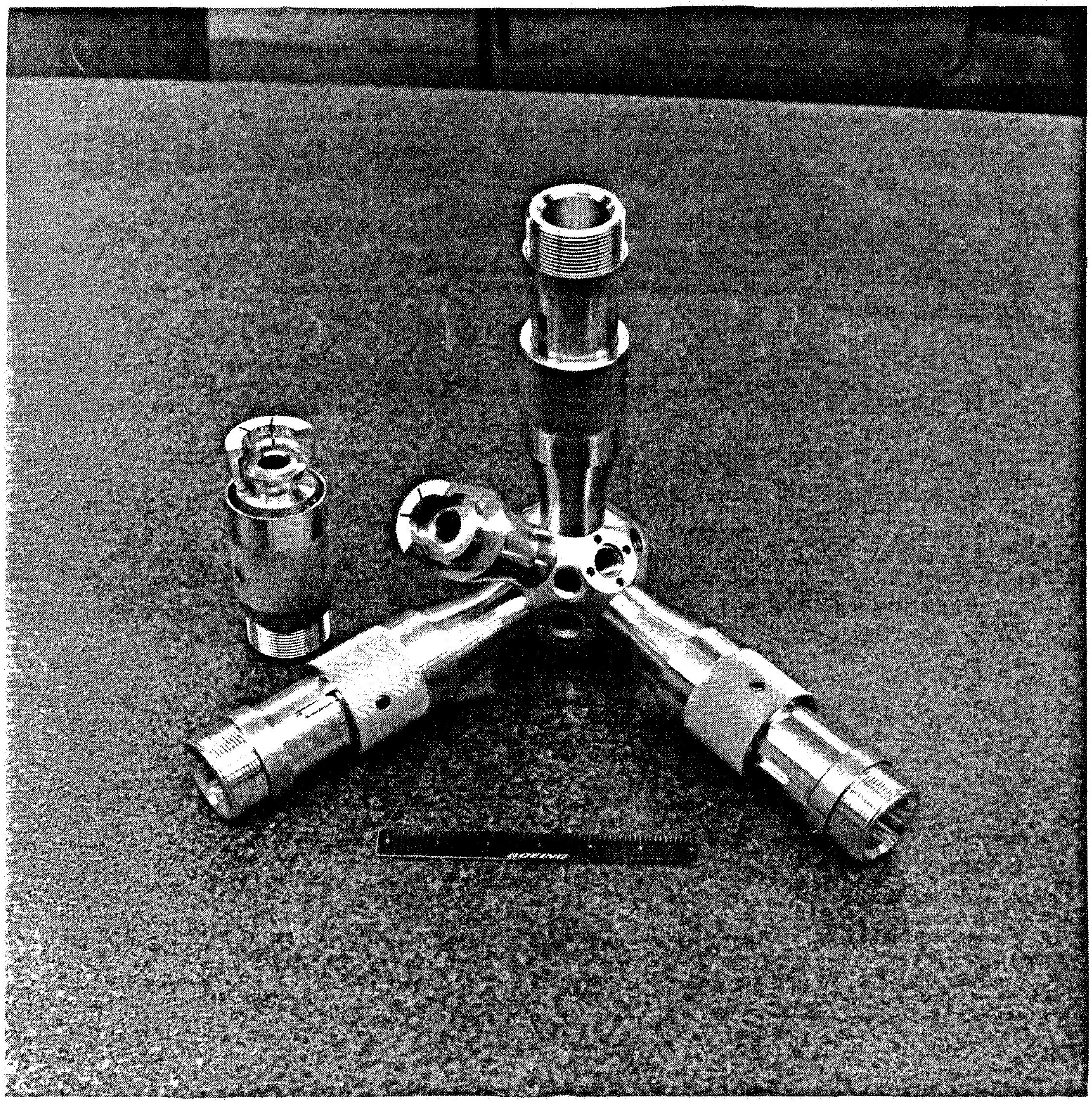

Figure 2.1.5-1 Space-Erectable End Fitting

Figure 2.1.5-2 Bonded Insert

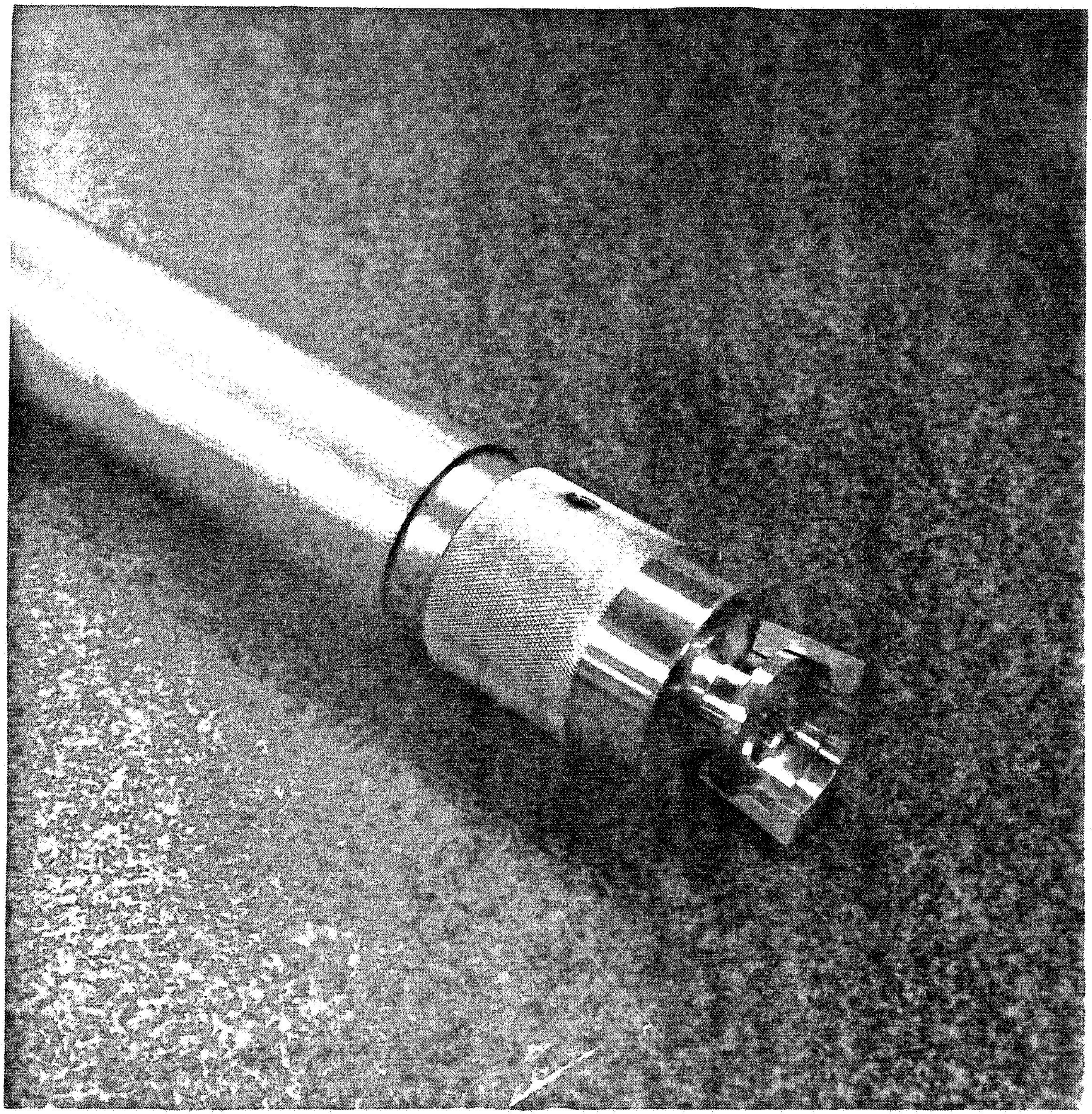

Figure 2.1.5-3 Latching Assembly

2.2 LOW EARTH ORBIT ENVIRONMENTAL PARAMETERS

The success of the Space Station will be directly related to its ability to endure long-term exposure to the LEO environment. The various parameters that make up this environment are temperature cycling caused by the 94-min orbit, solar radiation, atomic oxygen, vacuum, micrometeoroids, and space debris. Much of this environment has been shown to be both reactive and degrading to spacecraft materials. Most of the environmental data in this section was obtained from reference 2.

2.2.1 Temperature Extremes

Figure 2.2.1-1 shows the predicted temperature cycle that a 0.060-in-thick, 2-in-diameter, uncoated, $(0_2, \pm 20, 0_2)_s$ layup Gr/Ep tube would achieve in LEO. With the incident solar flux normal to the tube, the front surface would reach a maximum temperature of +155°F and the back surface would reach a maximum temperature of +25°F. During the shadowed portion of the orbit, the tube front and back surface would achieve minimum temperatures of -155°F and -170°F, respectively.

2.2.2 Solar Radiation

Figure 2.2.2-1 shows the results of an orbital radiation study conducted in 1978. This figure shows the daily charged-particle flux and radiation levels that can be expected near Space Station altitude of 500 km. Another component of the LEO is solar electromagnetic radiation. Of the total solar electromagnetic spectrum, ultraviolet causes the largest effect on materials. The UV for the LEO is spectrally matched to that of the AM-0 spectrum because of the absence of any atmospheric attenuation at this altitude.

2.2.3 Atomic Oxygen

The natural environment at LEO is composed primarily of 0 (atomic oxygen), N_2, and He. The flux of these constituents that would impinge on an orbiting platform as a function of altitude is shown in figure 2.2-3-1. The atomic oxygen bombards frontal areas at orbital speeds of 8 km/sec and its flux varies from 10^{13} to 10^{15} atoms/cm^2-sec over a solar cycle. The chemical activity of atomic oxygen with

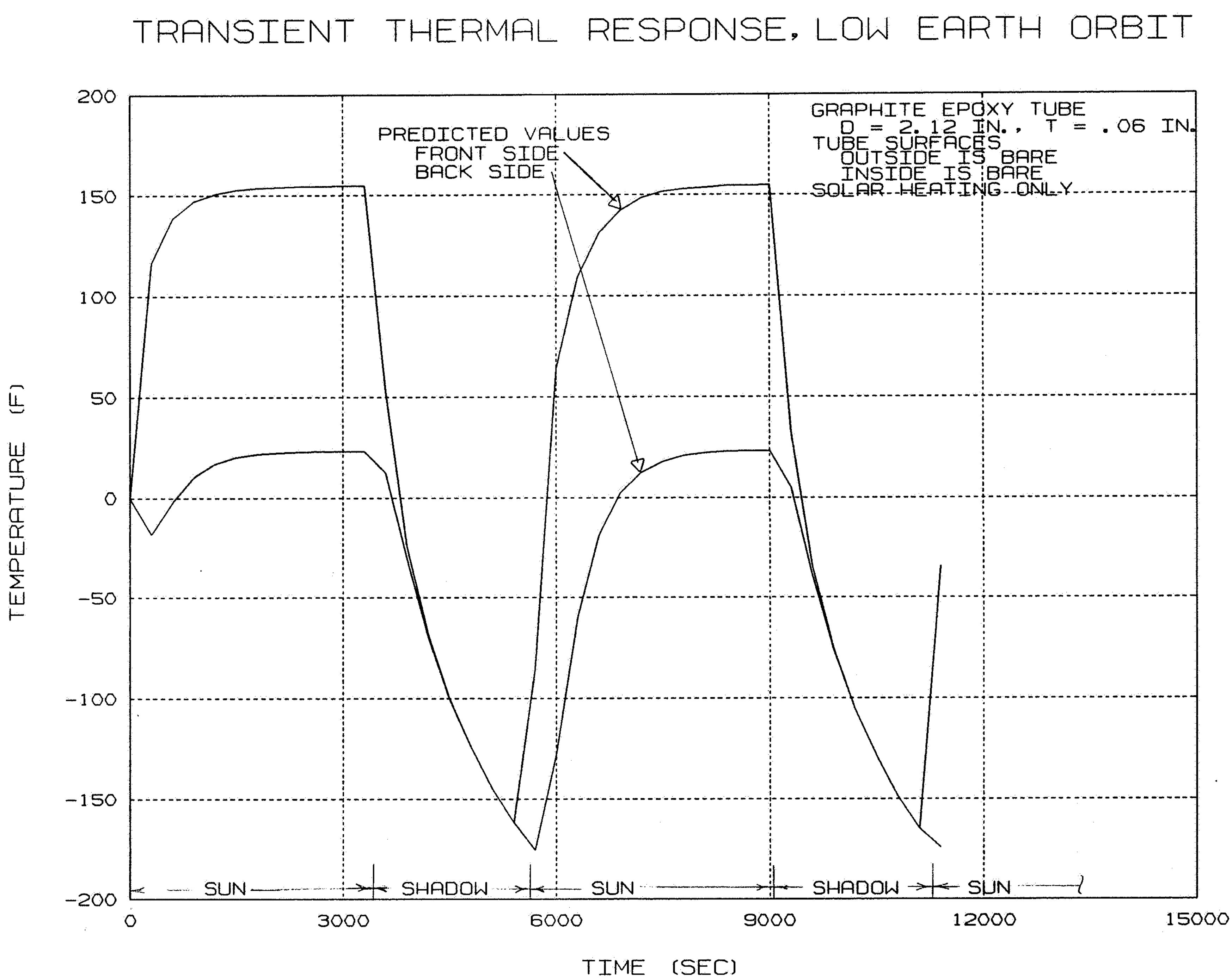

Figure 2.2.1-1 **Predicted LEO Temperature for Bare Gr/Ep Tube**

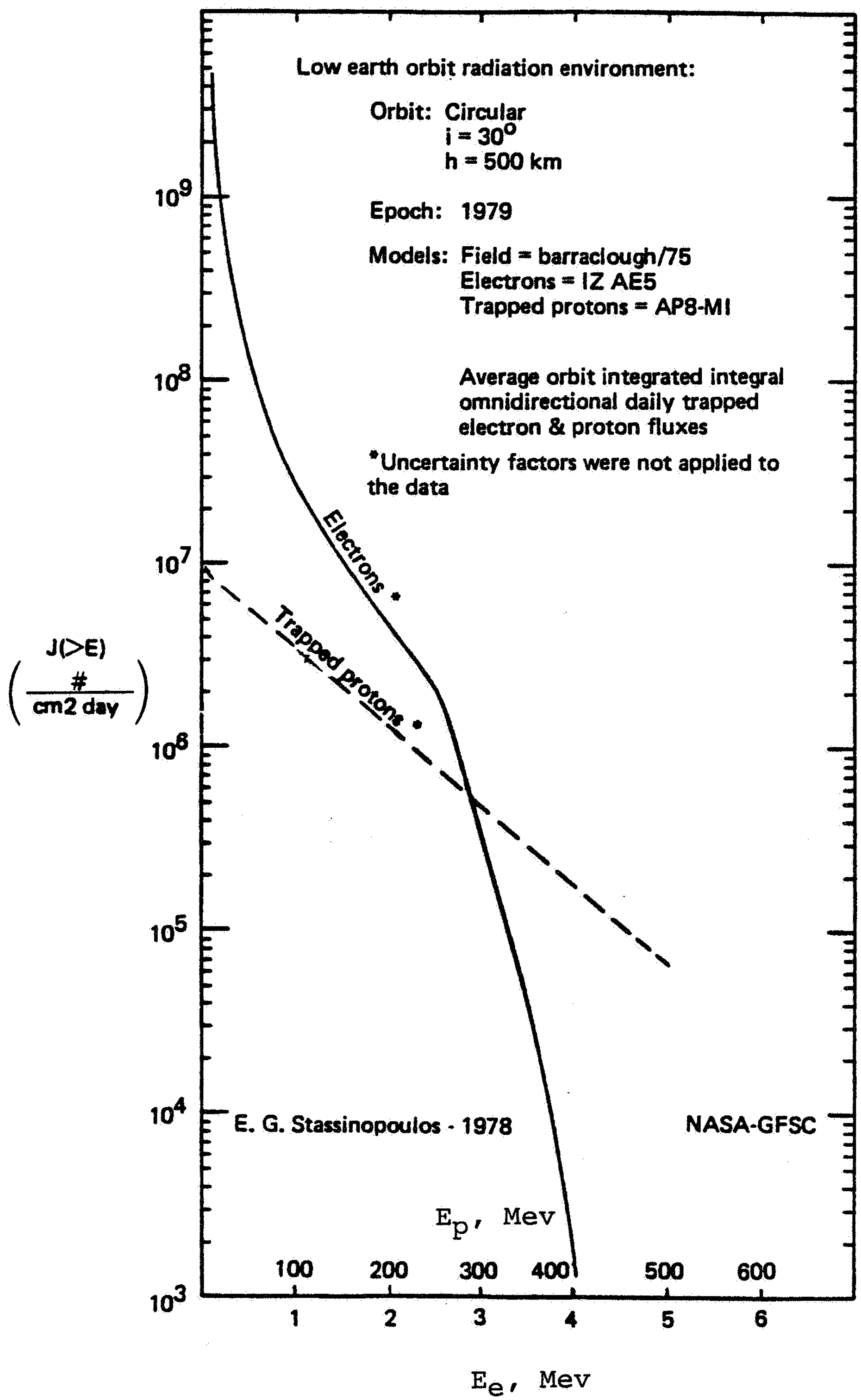

Figure 2.2.2-1 Charged Particle Flux Versus Energy

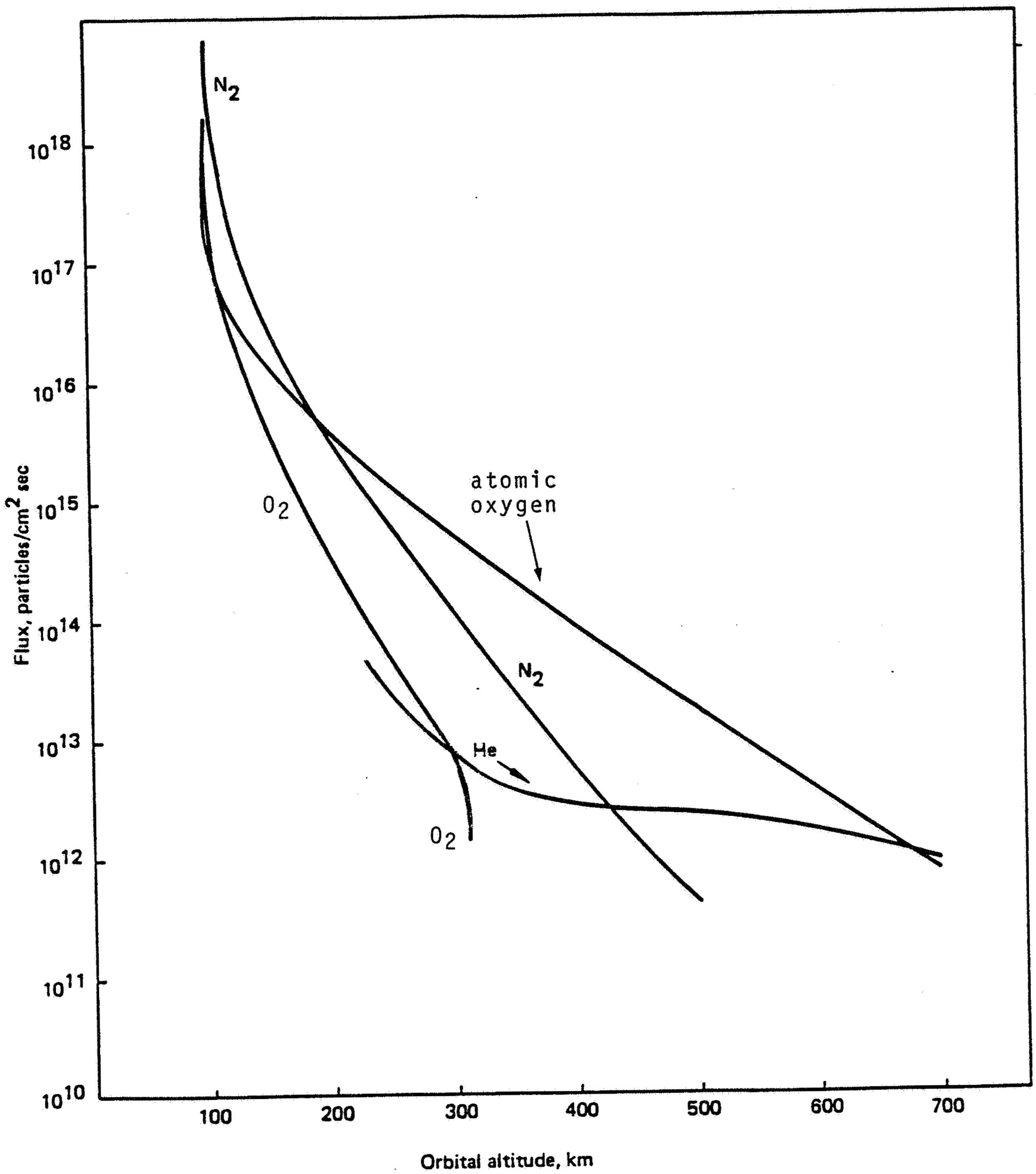

Figure 2.2.3-1 Flux Composition as a Function of Orbital Altitude

5eV of directed energy causes substantial erosion of many common organic materials normally used on spacecraft exteriors. Figure 2.2.3-2 shows the effects of atomic oxygen on several materials based on general observations compiled from actual flight data.

2.2.4 Micrometeoroids and Space Debris

A consideration of the LEO environmental effects on materials must also include the combined effects of micrometeroids (and space debris) with atomic oxygen. The threat from micrometeroids and space debris is shown in figure 2.2.4-1. A typical micrometeroid impact hole is on the order of 2-to 5-microns in diameter. This hole would allow a pathway for penetration of atomic oxygen through the coating to the substrate. The small hole size would be difficult to detect on coated structural elements. The damage in a micrometeroid field is cumulative and will tend to accelerate any degradation of the coating and substrate. To simulate the potential damage caused by the impact of micrometeroids and/or space debris, we will put pinholes of know size in several of the coated test specimens. The specimens will then be placed alongside defect-free specimens during the atomic oxygen exposure.

- Carbon coatings loss significant - totally lost on some surfaces on STS-3 and STS-4.
- Osmium losses significant - forms osmium tetroxide with high vapor pressure, reflectivity decreases of factors of 3 or 4.
- Organics lose same amount within factor of 2 each other.
- Silver degradation produces flakes - easily removed - turns to non-conductive oxide.
- S13GLO (RTV602 + Pigment) has no noticeable degradation.
- Other glossy paints become diffuse.
- Diffuse reflectance increases, specular decreases.
- Surfaces facing away from direct flux are effected by scattered atomic oxygen-less by factors on the order of 3 or 4 for GFU-8 mass loss and less by factor of 2 for osmium reflectivity.
- Samples show cosine dependence on flux.
- Teflon loses about ½ that of Kapton-mylar similar to Kapton.
- Changes from 135 nmi altitudes to 270 nmi altitudes should show reduction by a factor of 30.
- Reaction efficiencies vary with total fluence.
  - Reaction efficiency doubled between STS-5 and STS-8 and fluence tripled.
- Temperature dependence does not exist for oxygen interactions material loss.
- Kevlar rope loses 40 percent tensile strength.
- Results observed are for on the order of 40 hours exposure on each flight.
- Concentration can vary 6 orders of magnitude between 300 and 900 km and can vary 5 orders of magnitude at 900 km.
- Reactions observed on:
  - Skylab foils (ATM Sunshield) (435 km)
  - Discoverers 26 and 32 (228-810 km range) (QCMS)
  - OGO-6 (397-1098 km)
  - DMSP (4 Satellites) (1976-1979) (830 km)
  - TIROS-N (870 km)
  - NOAA-A (870 km)
  - NIMBUS-7

Figure 2.2.3-2 Atomic Oxygen Degradation Effects - General Observations

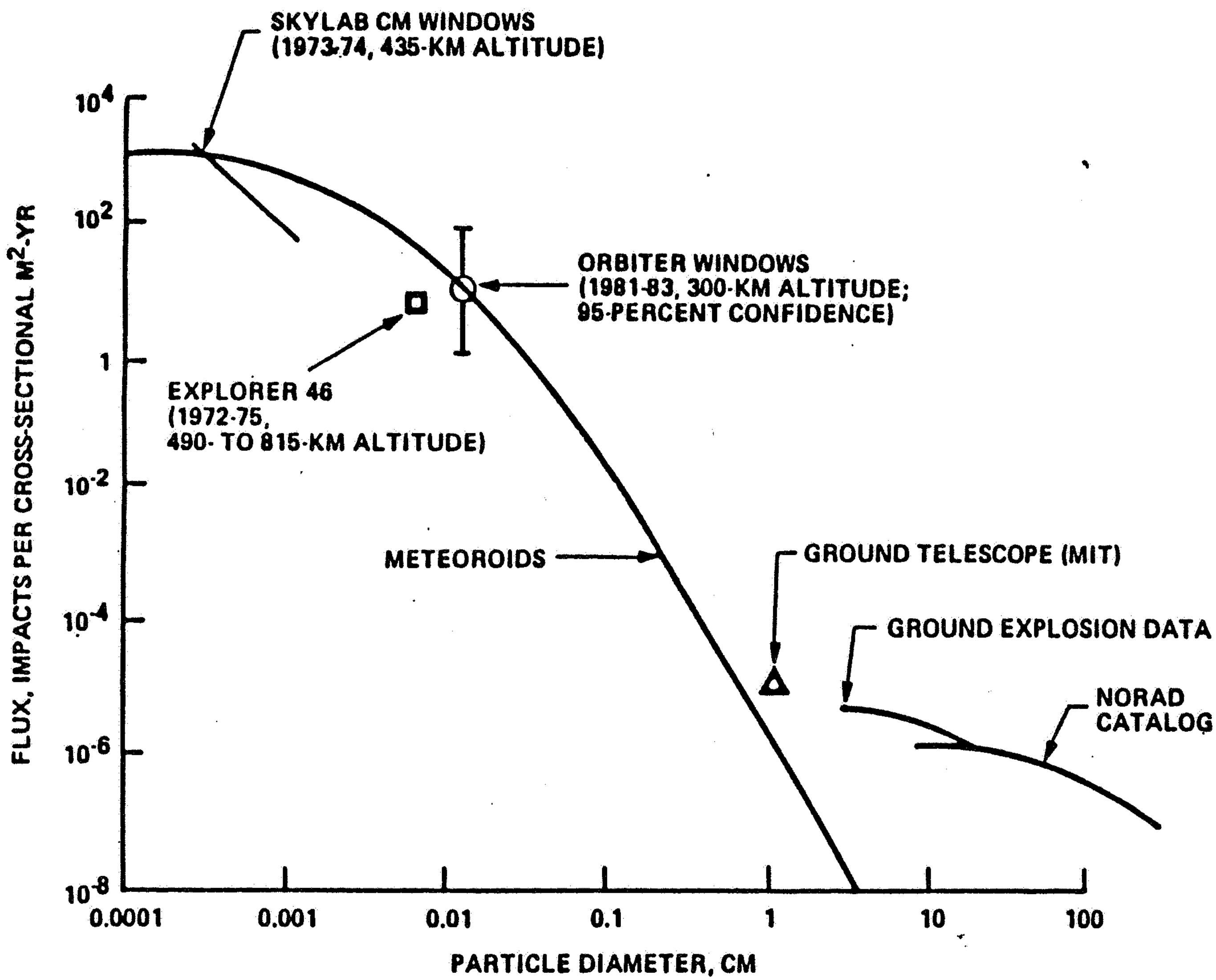

Figure 2.2.4-1 *Existing Orbital Debris Measurements Compared to Meteoroid Flux (From SST/AD-1)*

3.0 COATING CONCEPT AND SELECTION

This task comprised the main emphasis of the contract. Several concepts for protectively coating the Gr/Ep tubes (defined in sec. 2.0) were evaluated. These coatings were tested under simulated LEO conditions to select the coating that demonstrated the most promise. Section 3.1 describes the coating concepts and the results in achieving the targeted optical and adhesion values of each coating along with the various processing required to apply the respective coating to the metal foil or directly to the Gr/Ep tube. Section 3.2 describes the techniques used to determine the optical, adhesion, and microcrack properties of the coatings and coated tubes. Section 3.3 describes the simulated LEO environmental tests performed and the respective test results. Figure 3.0-1 shows the overall test plan that was used to evaluate the protective coatings.

3.1 COATINGS SELECTED FOR EVALUATION

Coatings selected for evaluation were; anodized Al foil, Al foil sputter-coated with Al and SiO_2, alodined Al foil, electroplated nickel (with and without SiO_x coatings) and inorganic sol gel solutions. These coatings offered the potential to protect the Gr/Ep tubes from the LEO environment and exhibit stability themselves to the LEO environment and handling requirements.

Except for the large area (1 ft^2) $Si0_2$ depositions and the $Si0_x$ depositions, all the above coatings were applied by various Boeing laboratories. Because of the lack of large-area $Si0_2$ sputtering targets within Boeing, eight 1-ft^2 specimens of sputtered Al on Al foil were sent to Circuits Processing Apparatus (CPA), Fremont, California for RF magnetron sputtering of $Si0_2$. Battelle Columbus deposited the $Si0_x$ coatings onto the Gr/Ep tubes electroplated with nickel.

3.1.1 Target Optical Values

The target optical values selected as goals for the protective coatings were an AM-O solar absorptance (α) = 0.20 to 0.35 and a thermal emittance (ε) = 0.15 to 0.25. The low values of α reduce the maximum tube temperatures when the tubes are exposed to direct or albedo radiation, and the low values of ε will reduce the

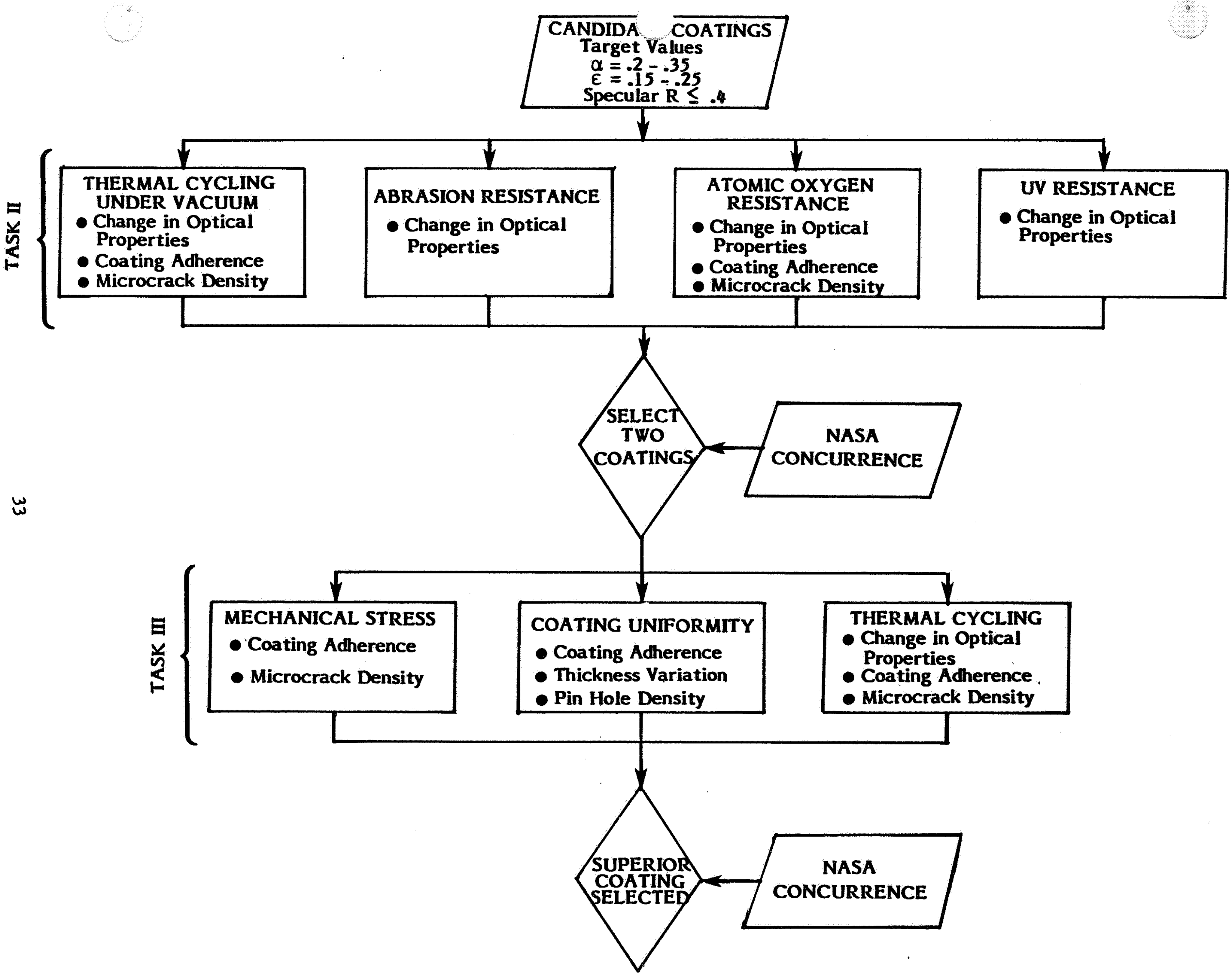

Figure 3.0-1 Test Plan

minimum temperatures when the tubes are exposed to deep space. A low specular reflectance, while maintaining the α and ε within the range of targeted ranges, was also a design goal. This would provide the astronauts with a non-mirror like surface to work with. Figure 3.1.1-1 shows the predicted temperature range that a Gr/Ep tube, wrapped with Al foil possessing the required optical values, would undergo in a LEO orbit. The maximum temperature is on the front side and is predicted to be 65°F and the minimum temperature would be -55°F and is located on the backside of the tube.

3.1.2 Aluminum Foil Selection

To evaluate the effects of thickness and temper of Al foil on fabricating and curing of Gr/Ep tubes, representative tubes were wrapped with 0.001, 0.0015, 0.002, 0.003 and 0.005-in thick Al foil. All the foil evaluated was series 1145 Al. This Al alloy possesses purities of greater than 99% Al and is characterized by excellent corrosion resistance, high thermal and electrical conductivity, low mechanical strengths, and excellent workability. The 1145 Al foil had a temper of 1145-0 (fully annealed) or 1145-H19 (fully strain-hardened). These were the only tempers available without a large volume order.

As expected, the thinner and softer the foil, the more difficult it was to wrap the 2-in-diameter tubes with consistent, successful results. The thin, fully soft foils would form wrinkles and/or pin holes during the wrapping process, which couldn't be avoided. The pin holes allowed the epoxy resin to bleed through the foil during curing. These pin holes would also be expected to cause localized deterioration of the Gr/Ep tube by atomic oxygen when exposed to the LEO environment. The 0.002-in-thick, 1145-H19 Al foil was selected as the lightest weight Al foil that could be consistently wrapped onto the 2-in diameter tubes without flaws and also provide the highest reliability.

3.1.3 Anodized Aluminum Foil

The anodizing of Al foil was performed within Boeing using various production facilities. Boeing has two industry-accepted specifications that control anodizing of Al foils: BAC 5555, "Phosphoric Acid Anodizing of Aluminum for Structural Bonding" and BAC 5884, "Chromic and Sulfuric Acid Anodizing of Aluminum Alloys." These specifications also include the cleaning of the foil, which is

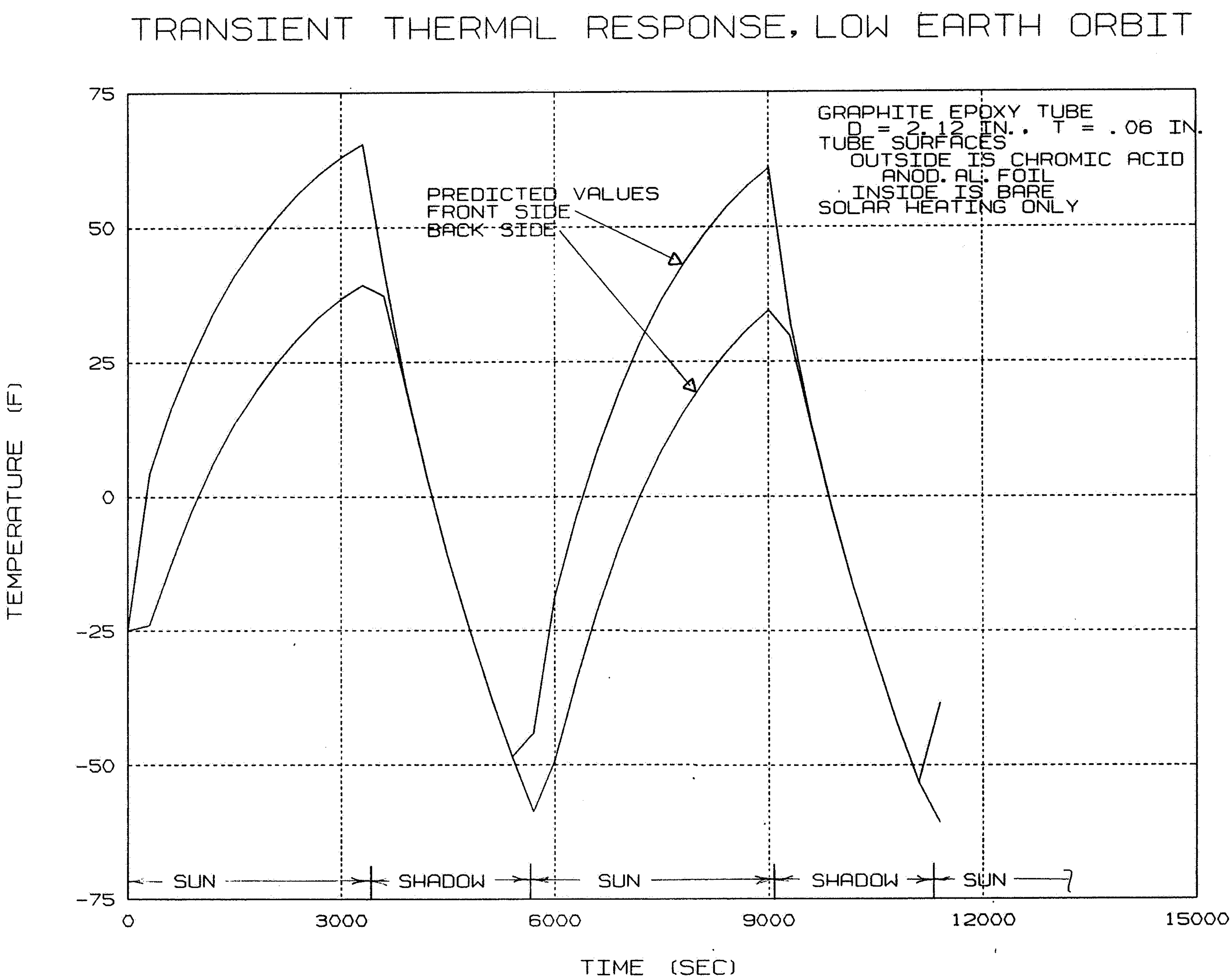

Figure 3.1.1-1 **Predicted LEO Temperature Range**

required to ensure a satisfactory anodizing. The specifications required that the foils be anodized in the following sequence:

a. Vapor degreased.
b. Placed in racking.
c. Alkaline cleaned.
d. Hot water rinse.
e. Deoxidized.
f. Cold water rinse.
g. Anodize.
h. Cold water rinse.
i. Dryed (warm air).

After the foil is vapor degreased, a metal rack is clamped to the perimeter of the foil to provide a secure electrical contact. The racking was kept to a minimum because the foil under the racking doesn't anodize. This unanodized portion is trimmed off after the anodizing process is completed. The racking also provides a means for handling the foil during the various cleaning processes performed prior to the anodizing. Sections of Al foil (1 ft^2) were anodized per Boeing specification. After the anodizing was complete, 1-in^2 samples were cut from the 1-ft^2 sections to determine the optical values. This established the control optical values that could be achieved by following the anodizing parameters of the Boeing specifications. Follow-up samples were then fabricated using modified anodizing parameters in an attempt to achieve the target optical values. The parameters modified were the immersion time in the acid solution and/or the ramp time to desired voltage. (The immersion time is defined as the amount of time the specimen is immersed in the acid solution while at full voltage. The ramp time is defined as the time it takes to arrive at full voltage). During the ramping, the foil is immersed in the acid solution. Because the anodizing was performed in production tanks, it was impossible to modify the various acid solution/water percentages. The anodizing process deviated from the Boeing specifications only at the end of the process. The standard processing of anodized parts requires them to be sealed by immersing the parts in 170°F water. These weren't done on the Al foil because of the expected adverse effects on the Al foil bonding strengths (ref. 3). Figure 3.1.3-1 shows the tanks used to clean and chromic acid anodize the Al foil. The akaline cleaning and deoxidizing tanks are in the foreground. These

ORIGINAL PAGE IS
OF POOR QUALITY

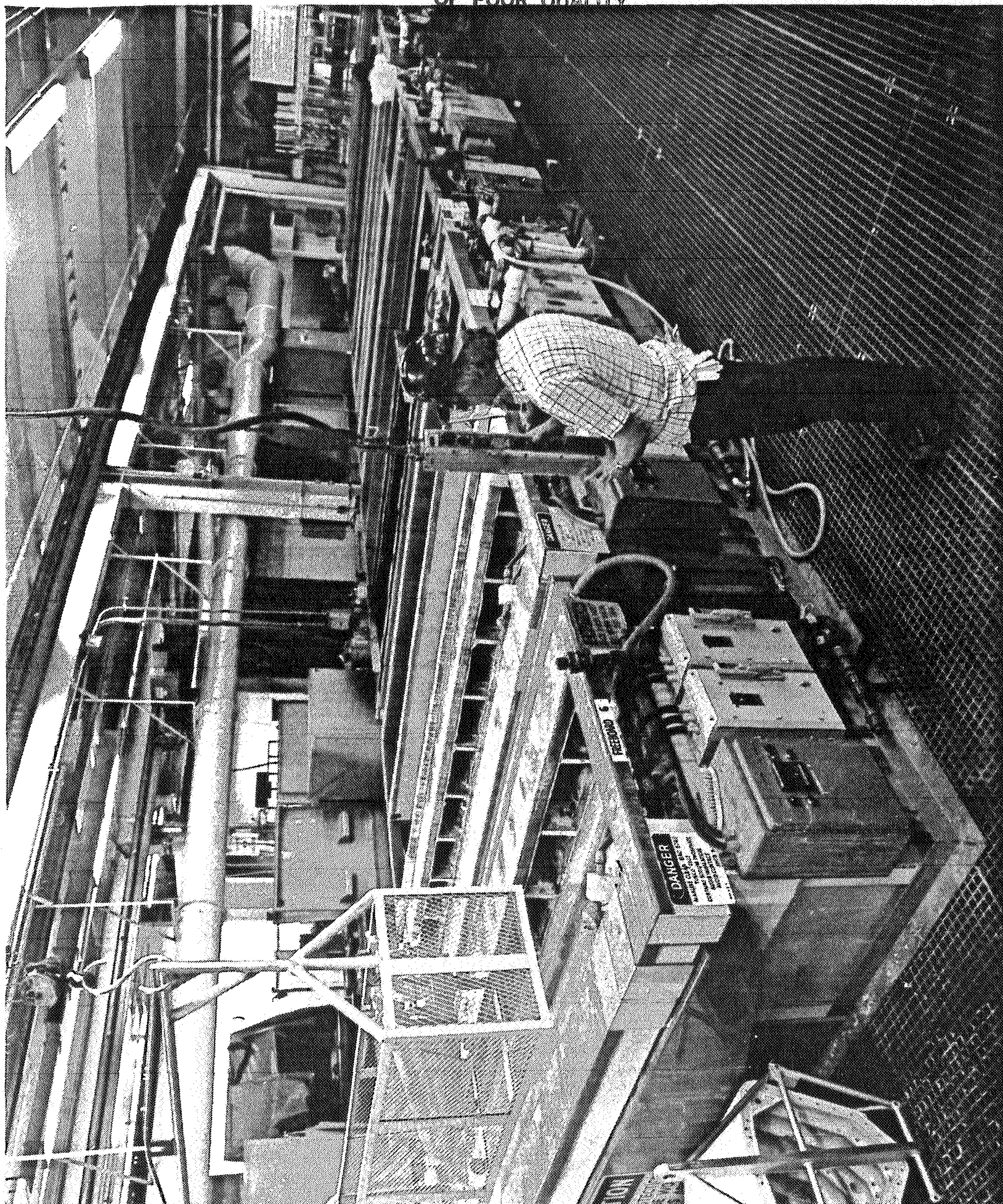

Figure 3.1.3-1 Chromic Acid Anodizing Facility

tanks were also used to clean and chromic acid anodize the 4-ft-long and 8-ft-long sections of Al foil required for the longer Gr/Ep tubes. Figure 3.1.3-2 shows the tanks used to phosphoric acid anodize the foils. The tank used to vapor degrease the foils is in the foreground.

As shown in figure 3.1.3-3, the optical properties of the phosphoric and chromic acid anodizing could be tailored to achieve the targeted optical values. The sulfuric acid anodizing was unable to achieve the desired emittance even though the immersion time was lowered to 5 minutes. All the anodized foils had excellent uniformity in optical properties and were free from pin holes and other flaws.

Commercially anodized Al foil was also evaluated to determine if any of the commercially available foils achieved the targeted optical values. Almost all of the off-the-shelf anodized foils were dyed, sulfuric acid anodized. As shown in figure 3.1.3-4, none of these samples came very close to achieving the target optical values. Al foil with surfaces abraided ("scratch brushed") before being clear sulfuric acid anodized had optical values closest to the optical goals. For example, samples of 0.003-in Al foil that had been scratch brushed prior to anodizing possessed a $\alpha = 0.40$ and a $\varepsilon = 0.69$. These foils had been roll coated anodized by being immersed for 3 to 5 min in a sulfuric acid solution and then sealed for 3 to 5 min in 170°F water. This foil also possessed the least specular reflectance of any of the foils evaluated, as discussed in section 3.1.10.

Anodizing of Al foil is currently state-of-the-art in the industry. For example, sulfuric acid anodizing of 0.003-in Al foil is currently being done by a roll-to-roll coating process at line speeds ranging from 5 to 20 ft/min on foil widths up to 36 in. However, difficulty could be encountered in purchasing large enough volumes of anodizing foil to interest the industry in varying the acid solution and/or processing parameters. If the roll coating of anodized foil is cost prohibitive because of the production changes, Al foil can easily be anodized in a batch process. For example, Boeing has a 61,000-gal, 110-ft-long chromic acid anodizing tank that could be used for batch processing of foil.

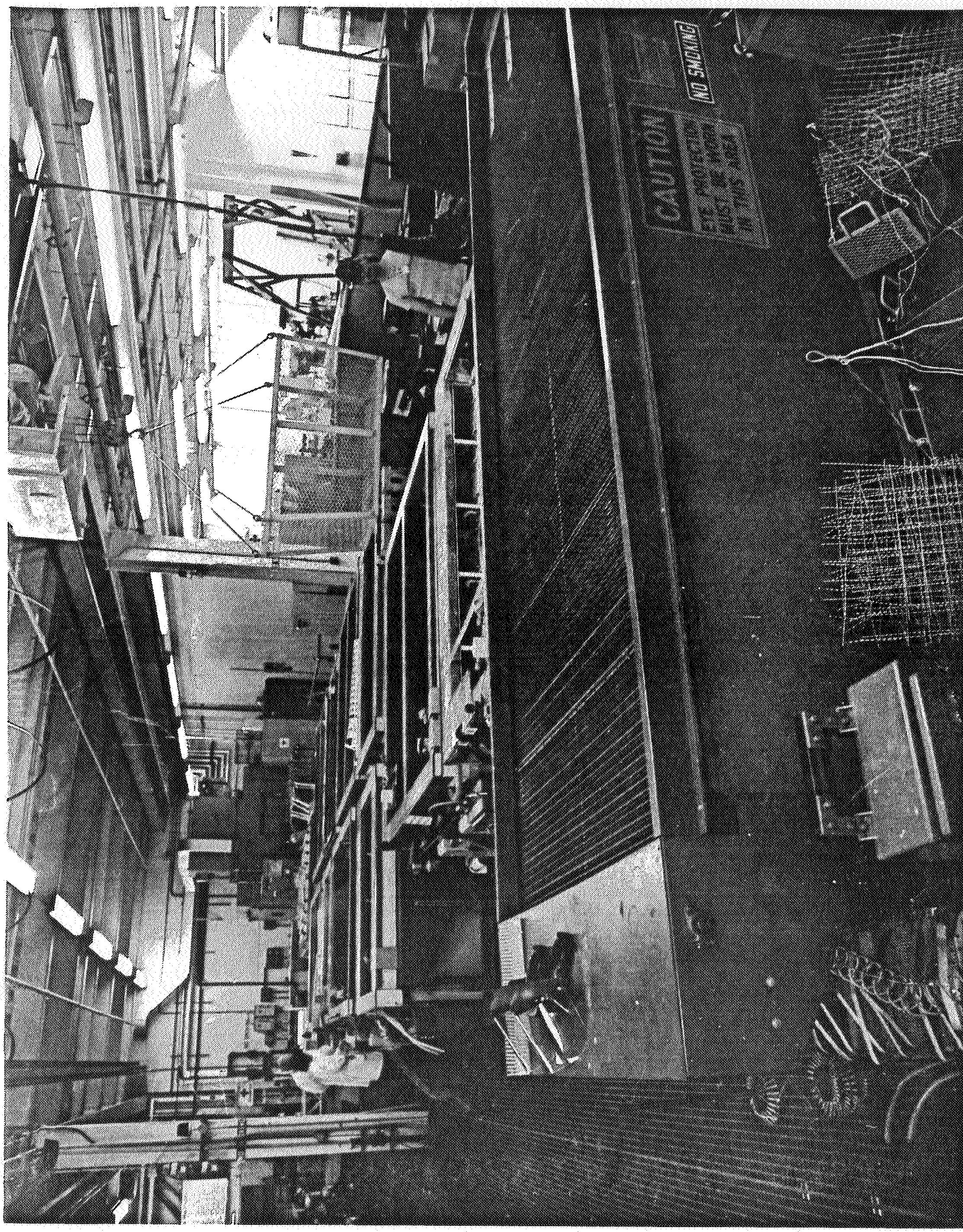

Figure 3.1.3-7 Phosphoric Acid Anodizing Facility

	Sample	α	ε	α/ε
1.	Sulfuric Acid Anodized Al Foil BAC 5884; Type II, Class I Sulfuric Acid/H_2O = 30% by weight immersion time = 30 min	0.32	0.75	0.43
2.	Same as above except immersion time = 11 min	0.28	0.68	0.41
3.	Same as above except immersion time = 5 min	0.24	0.69	0.35
4.	Chromic Acid Anodized Al Foil BAC 5884; Type I, Class I Chromic Acid/H_2O = 5% by weight immersion time = 55 min ramp time to 22 volts = 5 min	0.52	0.67	0.78
5.	Same as above except immersion time = 15 min	0.21	0.15	1.40
6.	Same as above except immersion time = 10 min ramp time = 10 min	0.22	0.14	1.57
7.	Same as above except immersion time = 5 min ramp time = 15 min	0.21	0.11	1.91
8.	Same as above except immersion time = 10 min ramp time = 15 min	0.22	0.19	1.16
9.	Same as above except immersion time = 15 min ramp time = 15 min	0.22	0.23	0.96
10.	Same as above except immersion time = 20 min ramp time = 15 min	0.27	0.29	0.93
11.	Phosphoric Acid Anodized Al Foil BAC 5555 Phosphoric acid/H_2O = 14% weight immersion time = 20 min	0.31	0.12	2.58
12.	Same as above except immersion time = 50 min	0.26	0.15	1.73
13.	Same as above except H_2O sealed	0.25	0.16	1.56

Figure 3.1.3-3.

Solar Absorptance and Thermal Emittance of Anodized 0.002-in Aluminum Foil

Dyed Al Foil Sample	α	ε
Black Matte	0.67	0.80
Black Med Etch	0.63	0.78
Warning Red Matte	0.54	0.77
Warning Red Satin	0.53	0.76
Fire Red Matte	0.53	0.72
Fire Red Glossy	0.44	--
Blue Matte	0.70	0.75
Blue Glossy	0.60	--
Green Matte	0.65	0.75
Green Glossy	0.58	--
Purple Matte	0.54	0.70
Purple Glossy	0.43	--
Gold Satin	0.44	0.70
Gold Brush	0.49	0.70
Clear Glossy	0.13	--
Clear Satin	0.23	0.69

Figure 3.1.3-4

Solar Absorptance and Thermal Emittance of Dyed, Sulfuric Acid Anodized Aluminum Foil

3.1.4 Vacuum-Deposited SiO_2/Vacuum-Deposited Al/Al Foil

Several iterations of vacuum-deposited SiO_2 and sputtered Al coatings were deposited onto Al foil in the Boeing Aerospace Thin Film Laboratory to determine the thicknesses required to obtain the targeted optical values. Figure 3.1.4-1 shows the optical results of these deposited coatings. As shown in this figure, the overall ε can be tailored by controlling the thickness of the deposited SiO_2, and the overall α can be tailored by controlling the thickness of the sputtered Al.

It was found that, using Al foil as a substrate, deposited Al layers of less than 1000 Å exhibit little if any grain growth, therefore no change in reflectance. Deposited Al thicknesses greater than 1000 Å develop increasing grain structure and, as a result, the reflectance decreases (increased absorptance) as the grain structure increases. The optimized thicknesses proved to be 1-micron of SiO_2 and 3000 Å of Al. All thickness measurements were made with a profilometer.

Except for sample #5, the SiO_2 was deposited using the RF sputtering process and a SiO_2 (quartz) target. For sample #5, the SiO_2 was deposited using an electron beam source. All the Al was DC magnetron sputtered. Samples #1 through #5 were deposited 4-in^2 specimens of Al foil, which was the largest substrate size that could be uniformly deposited with SiO_2 by Boeing. Because 1-ft^2 specimens were needed to wrap the 1-ft-long Gr/Ep tubes, Circuits Processing Apparatus (CPA), Fremont, CA was subcontracted to RF magnetron sputter 1 micron of SiO_2 onto eight Boeing-supplied, 1-ft^2 specimens of Al foil that had 3000 Å of Al sputtered deposited on them in Boeing's Thin Film Laboratory.

CPA found that, during deposition of the SiO_2, the Al foil substrate buckled and distorted due to the heat buildup in the foil. Because of this, CPA had to lower the deposition rate to 15 Å/sec, which required eight passes under the 5.5-in-long by 15-in-wide target at 3-in/min to achieve the required 1-micron of SiO_2. The SiO_2 coatings possessed uniform optical properties and very few imperfections in the coatings were observed under visual examination.

Flexibility of the 1-micron layer of SiO_2 on Al foil was a concern because the coated foils would be wrapped around 2-in diameter tubes. To determine the flexibility of the SiO_2 layer, coated foils were wrapped around 2-in and 0.5-in

Sample	α	ε	α/ε
1) 3000 Å Al/Al Foil	0.30	0.04	7.50
2) 1 micron SiO_2/500 Å Al/Al Foil	0.22	0.24	0.92
3) 1 micron SiO_2/1000 Å Al/Al Foil	0.23	0.26	0.88
4) 1 micron SiO_2/3000 Å Al/Al Foil	0.31	0.25	1.24
5) 1.2 micron SiO_2/3000 Å Al/Al Foil	0.32	0.32	1.00
6) 1 micron SiO_2 (Deposited by CPA/ 3000 Å Al/Al Foil	0.32	0.15	2.13
7) Same as above, but measured elsewhere on the same specimen	0.34	0.18	1.89

Figure 3.1.4-1

Solar Absorptance and Thermal Emittance of SiO_2/ Sputtered Aluminum/0.002-in Aluminum Foil

diameter tubes and then examined under a dark field microscope at a magnification of 50X. No crazing or cracking of the SiO_2 was found in the foils wrapped around either tube.

3.1.5 Alodined Al Foil

To evaluate the alodined coating process, samples of Al foil were alodined per BAC Specification 5719. This specification is divided into two classes: class 1200, which has had a dye added to the solution; and class 1000, which is a clear solution. A sixth sample was provided by American Cyanamid which uses alodined Al foil as a corrosion barrier for their honeycomb products. Figure 3.1.5-1 shows the results of the optical evaluations of the alodined foils. As the results indicate, the α was satisfactory, but the alodining processes had no effect on increasing the ϵ above that of the bare Al foil. Therefore, no alodined samples were considered for further evaluation.

3.1.6 Electroplated Coatings

Electroplating was selected as a potential protective coating because of its low cost application methods, good uniformity, and ability to coat irregular-shaped surfaces such as end fittings. Nickel plating also provides good corrosion resistance. However, the stability of optical values during exposure to the LEO environment requires investigation. Boeing has several specifications that pertain to the electroplating of Gr/Ep. The two major specifications are BAC 5746, "Nickel Plating, Electrodeposited" and BAC 5226, "Plating on Carbon-Reinforced Composite Parts."

The exterior surfaces of the Gr/Ep tubes were sanded prior to plating which improves adhesion of the various solutions to the tubes. The interior surfaces were not abraided, therefore, the various plating solutions didn't adhere. This kept the overall weight of the tubes to a minimum. Because Gr/Ep is a relatively poor electrically conductive material, the tubes were immersed in an electroless copper solution to provide a conductive surface for the electroplating process. All the tubes had a 0.0001-in base layer of electroless copper applied by immersing in a copper solution prior to electroplating. Figure 3.1.6-1 shows the results of a variety of plating processes.

	Sample	α	ε	α/ε
1)	Alodined Al Foil BAC 5719; Class A, Type 1200 (Dyed) immersion time = 30 sec	0.32	0.04	8.00
2)	Same as above except immersion time = 60 sec	0.36	0.05	7.20
3)	Same as above except immersion time = 75 sec	0.37	0.05	7.40
4)	Alodined Al Foil BAC 5719; Class B, Type 1000 (Clear) immersion time = 60 sec	0.18	0.04	4.50
5)	Same as above except immersion time = 120 sec	0.19	0.04	4.75
6)	American Cyanamid Alodined Al Foil	--	0.04	--

Figure 3.1.5-1

Solar Absorptance and Thermal Emittance of Alodined 0.002-in Aluminum Foil

Solar Absorptance and Thermal Emittance of Electroplated Gr/Ep Tubes

	Sample	α	ε	α/ε
1)	0.001-in layer electroplated Ni/electroless Cu	0.47	0.12	3.92
2)	Same as above except brighteners added to Ni bath	0.37	0.12	3.08
3)	Same as above except flash coating 0.0001-in layer of brightened Ni	0.46	0.13	3.54

Solar Absorptance and Thermal Emittance of SiO_x Coated/Electroplated Nickel, Gr/Ep Tubes

1)	Bare Al Foil	0.10	0.04	2.50
2)	0.5 micron SiO_x/Al Foil	0.17	0.20	0.85
3)	1 micron SiO_x/Al Foil	0.17	0.47	0.36
4)	1.5 micron SiO_x/Al Foil	0.18	0.48	0.38
5)	2 micron SiO_x/Al Foil	0.19	0.53	0.36
6)	1 micron SiO_x/.001 layer brightened Ni	0.49	0.52	0.94
7)	1 micron SiO_x/.0001 layer brightened Ni	0.53	0.55	0.96

Figure 3.1.6-1

Solar Absorptance and Thermal Emittance of Gr/Ep Tubes

The coatings were tested for adhesion by using the tape peel test. This test is based on ASTM D 3359, "Measuring Adhesion by the Tape Test." The test is used to establish whether the adhesion of a coating to a substrate is at an adequate level. Semitransparent pressure-sensitive tape is placed over the desired area and rubbed firmly into place to ensure good contact with the coating. The tape is then rapidly peeled off. Both the tape and substrate are examined to determine if any coating has been removed. All the electroplated coatings had, at the very least, good adhesion as determined by this test because none of the nickel was removed by the tape.

The optical results from the initial electroplated sample (#1) exhibited a need to decrease the α. To do this, a chemical brightner was added to the plating solution. Sample #2 is the result of this effort. Samples #1 and #2 had an electroplated nickel layer of 0.001-in. A second method was tried to lower the α by changing the immersion time in the plating solution. Sample #3 had a "flash" coating of nickel which was less than 0.0001-in-thick. Several other tubes were plated with intermediate layers comprised of varying thicknesses of electroplated copper but, because these had no effect on the overall optical properties, they were not further evaluated.

3.1.7 $Si0_x$/Electroplated Nickel

To increase the ϵ of the electroplated nickel, Gr/Ep tubes with 0.001-in and 0.0001-in layers of electroplated nickel were sent to Battelle Laboratories, Columbus, Ohio for deposition of a 1-micron layer of $Si0_x$ using a proprietary plasma deposition process. The 1-micron layer of $Si0_x$ provided a ϵ that was higher than desired but, as figure 3.1.6-1 shows, the coating thickness can be tailored to achieve different optical values. This figure also shows the differences between bare electroplated nickel and $Si0_x$-coated electroplated nickel. The coating uniformity of the SiO_x around the 2-in-diameter by 12-in-long tubes appeared to be very good. The $Si0_x$ coating also increases the atomic oxygen resistance of the electroplated nickel.

3.1.8 Sol Gel Coatings

Sol gel is a ceramic material that is applied and cured to the exterior surface of the material to be coated. This concept was evaluated because of past experience within Boeing in using the sol gel as a ceramic-based environmental barrier. This concept proved unsatisfactory for several reasons. To achieve satisfactory adhesion on a Gr/Ep tube, a high-temperature flash cure at 700° to 800°F is required, which is not compatible with Gr/Ep. Also the CTE mismatch between the tube and sol gel proved to be too great to withstand the required thermal cycling. Because of those problems and the problems of applying a uniform coating on a tube of any significant length, the sol gel coating was not considered for further evaluation.

3.1.9 Adhesion of Coatings to Graphite/Epoxy Tubes

The coated Al foil was bonded to the Gr/Ep tubes using 0.005-in sheet epoxy and a thin layer of primer applied to the foil to improve the adhesion of the epoxy to the Al foil. The foil anodized in the phosphoric acid solution proved to possess excellent adhesion to the tubes after curing. During peel tests, the 0.002-in Al foil tore before exceeding the shear strength of the epoxy bond. A high shear strength in these bonds is expected because the phosphoric anodizing facilities are used at Boeing solely for maximizing the bonding strength of Al surfaces.

Adhesion of the Al foils to the tubes using either chromic or sulfuric anodized foil or uncoated foil (backside of SiO_2-coated foil) required improvement after initial testing. While the adhesion was adequate, these foils could be peeled intact during peel testing. Upon examination of the failed specimen, it was determined that the Al/primer interface was poor. This was caused by improper primer application. When the required primer is applied in production applications it is sprayed on the selected surfaces to a thickness of 0.00015 to 0.00040-in. The personnel that apply the primer are evaluated weekly to verify their ability to maintain these close tolerances. The primed surfaces are then baked for 1 hr at 250°F and then stored in a freezer until use. Using the production facilities shown in figure 3.1.9-1, the primer was applied to the various Al foils. The adhesion of these foils to Gr/Ep tubes was excellent and comparable to that of the phosphoric anodized foil that was initially made. Adhesion testing of samples before and after thermal cycling is discussed in section 3.3.5.

The 0.001-in electroplated nickel possessed excellent adhesion. The nickel was unaffected by either the tape pull test (as described in section 3.1.6) or scratching

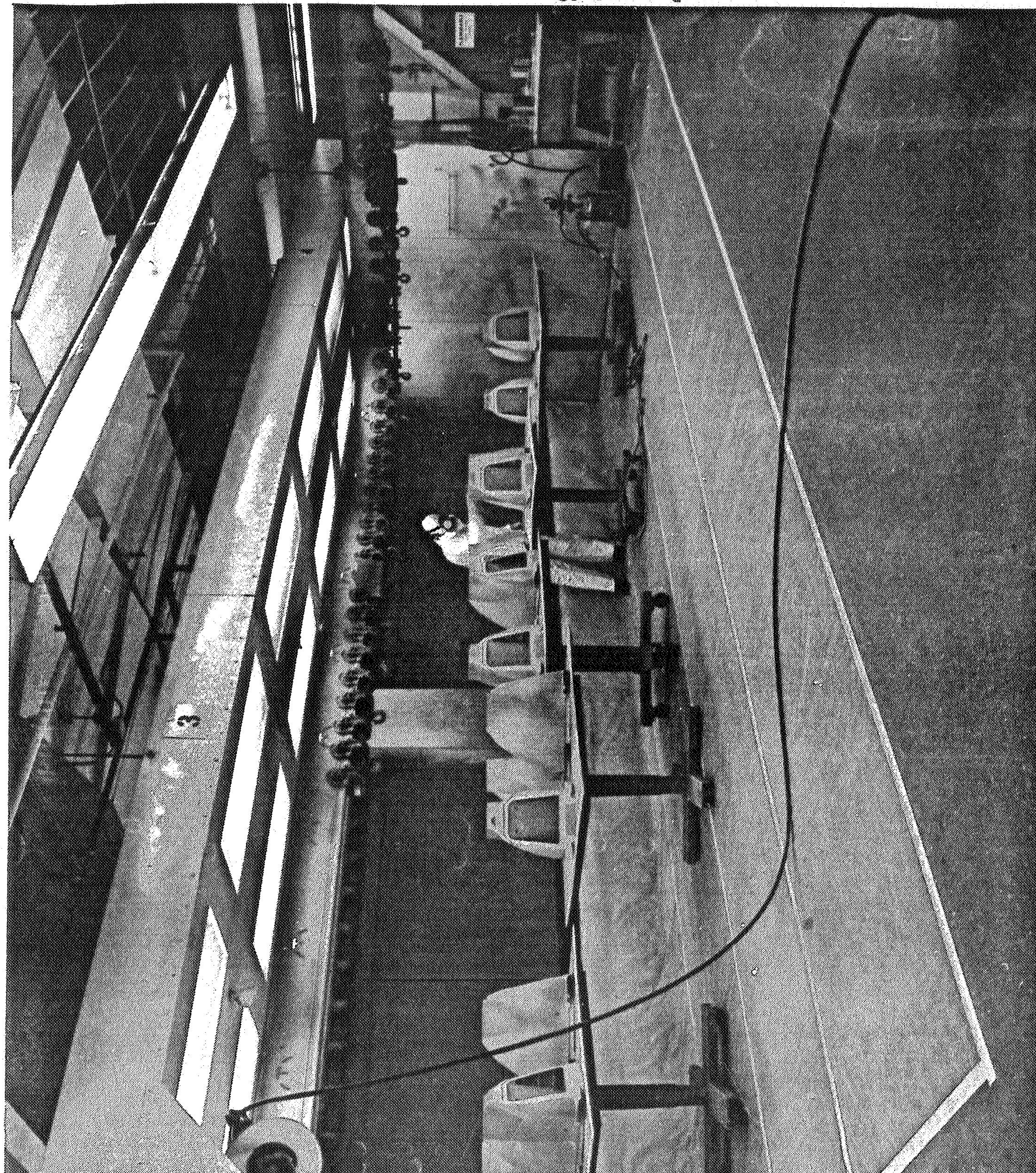

Figure 3.1.9-1 Spray Booth for Primer Application

with an x-acto knife. The thinner electroplated Ni possessed adequate adhesion and passed the tape pull test; however, it could be removed by scratching with an x-acto knife.

3.1.10 Specular Reflectance of Al Surfaces

Because of the requirement for the protectively coated Gr/Ep tubes to possess a nonmirror-like surface for the astronauts to work with, the specular reflectance of a variety of Al- or Ag-coated substrates was determined. Figure 3.1.10-1 shows the results of this testing. The testing was performed at a single wavelength of 633 nanometers using a modified spectrophotometer. The results show that all the foil surfaces are nonspecular with the scratch-brushed sulfuric anodized Al foil and the textured chromic anodized Al foil being the most non specular. These foils scattered almost all the reflected 633 nanometer laser even at an aperture opening of 20 milliradians. NASA LaRC personnel provided the nonspecular silvered Teflon sample, which they have optically evaluated for comparison purposes. The material is similar to the material currently being used as the exterior coating of radiator panels for the Space Shuttle. This figure also shows the effect of texturing the Al foil on the Gr/Ep tubes (similar to the texturing of Al foil on the 8-ft-long tubes delivered to NASA) versus Al foil that had been bonded to the tubes using more conventional fabrication methods. As can be seen, even though the specular reflectance on the unbonded chromic anodized foil is quite low, the texturing decreased the specularity of the foil by over an order of magnitude. Sample #1 was an optical solar reflector that was used to show the specular reflectance of a mirror-like surface.

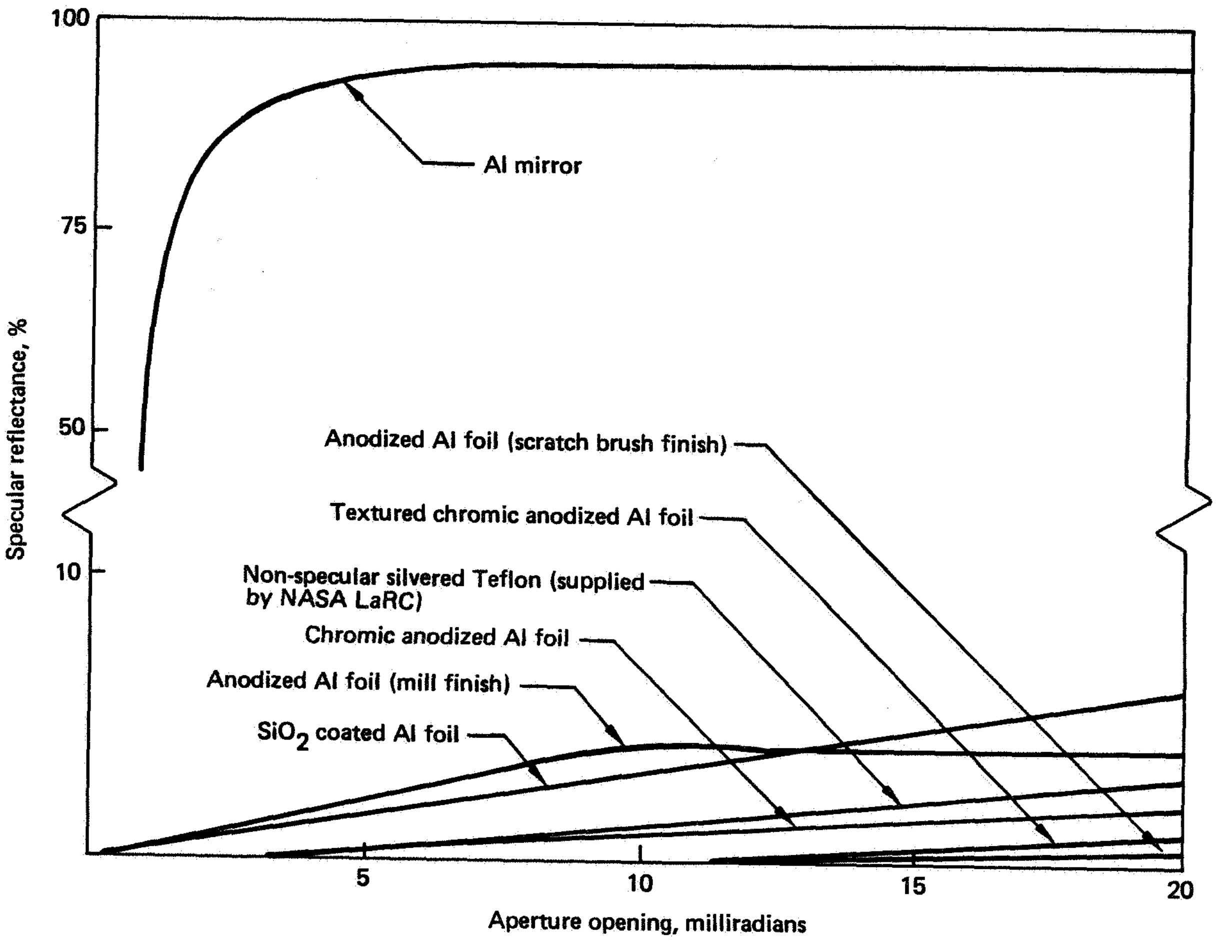

Figure 3.1.10-1 Specularity of Various Aluminum and Silver Surfaces

3.2 EVALUATION TECHNIQUES

The following section describes the test techniques that were used to evaluate the coating properties. These tests include microcracking after thermal cycling, solar absorptance, thermal emittance, and coating adherence. Also discussed is the capability of the optical testing equipment to accurately measure the optical properties of the coated Al foil after it has been bonded to the 2-in-diameter tube.

3.2.1 Microcrack Analysis

The following procedure was used to determine whether thermal cycling had caused microcracks in the Gr/Ep tubes: Saw cut the tube into specimens at least 1-in in length; polish the cut surface starting with 320 grit and finishing with 0.5-micron diamond paste; the cut surface is then examined between 50X and 200X magnification. Microcracks were photographed and the microcrack density determined by averaging the distance between cracks in any single ply. X-ray analysis was also used to determine if any microcracks existed but none were observed at 50X to 200X magnification. Zinc iodide was used as an X-ray penetrant, which would have wicked into any of the microcracks.

3.2.2 Optical Analysis

Solar Absorptance and Specular Reflectance

Solar absorptance (α) measurements were made on a Perkin-Elmer Lambda-9 UV/VIS/NIR Spectrophotometer with 3/16-in diameter beam. A picture and a schematic of this instrument are shown in figure 3.2.2-1. Tests were conducted in accordance with ASTM Standard Method E-424, method A. The measurements are determined from spectra obtained in the total reflectance mode for the spectral range of 0.25 to 2.5-microns. Calculations are based on a 29-point integration over equal energy divisions of the solar spectrum at AM-O. A National Bureau of Standards spectral tile is measured at the same time and serves as a standard material of known spectral reflectance to which all spectra are corrected.

Specular reflectance was measured using a modified bidirectional reflectometer utilizing a 633-nanometer wavelength laser source and a variable aperture system

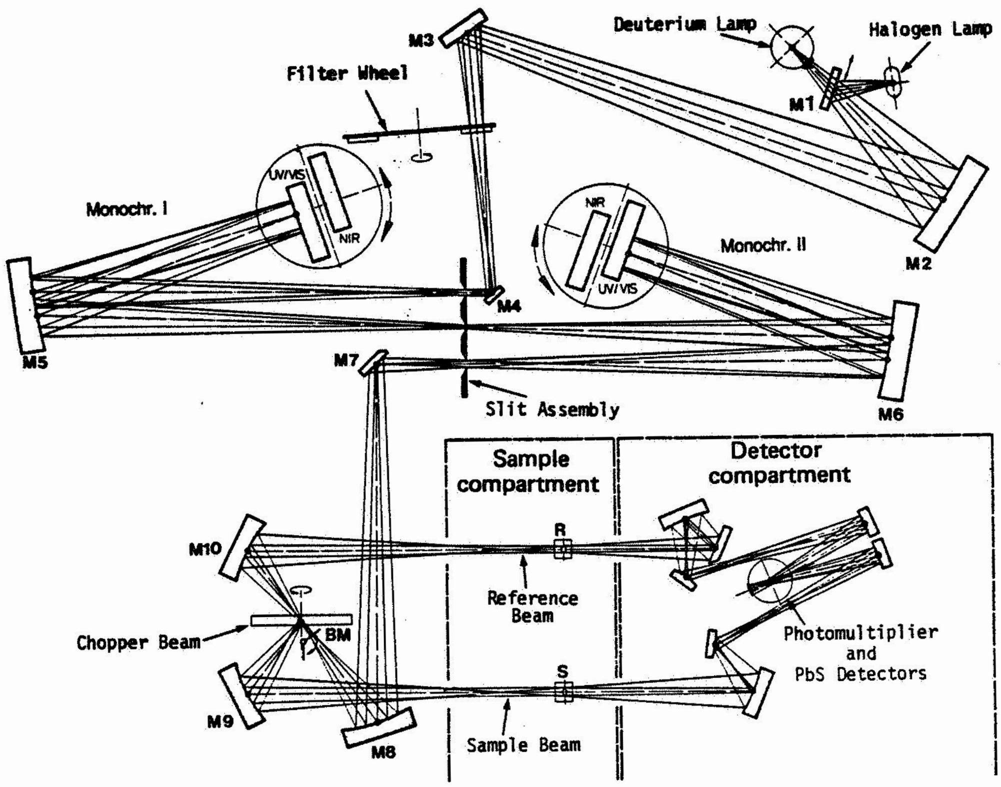

Figure 3.2.2-1 Perkin-Elmer Lambda-9 Spectrophotometer

(1.5 to 20 milliradians) to determine scatter.

Emittance

Total hemispherical emittance (ε) was determined in accordance with ASTM Standard Method E-408, method A, on a Gier-Dunkle Model DB100 Infrared Reflectometer. The instrument is calibrated, prior to each sequence, with NBS reflectance standards suitable to the high and low range of the material being tested. All testing was conducted with the samples at ambient temperature.

Chromic anodized 0.002-in Al foil was used to verify the capabilities of the optical testing equipment to accurately measure curved surfaces, specifically 2-in-diameter tubes. Figure 3.2.2-2 shows a section of tube with the anodized foil bonded to the exterior surface, in the Perkin Elmer sample holder. During testing, the compartment that holds the sample is made light tight by closing the open lid. Figure 3.2.2-3 shows a flat specimen of anodized foil, cut from the same piece that was used to wrap the above tube section with, in the sample holder. An AM-O absorptance test was performed on both samples to determine if there was any additional scattering caused by the relatively small radius of curvature. Figure 3.2.2-4 shows the results of this test. The actual difference in absorptance (26% versus 27%) falls easily within testing scatter. A special tube holding fixture was fabricated for the emittance testing equipment enabling, emittance measuring of 2-in diameter tubes within the same tolerances as just described.

3.2.3 Coating Adherence

The Climbing Drum Peel Test for Adhesives (ASTM D 1781-76) test was used to evaluate the adherence of the Al foil to flat P75S/934 Gr/Ep laminates. The test specimens were 12-in long by 1-in wide, with a bondline of 10-in. This left a 2-in-long piece of unbonded Al foil to be gripped by the "Climbing Drum." Half the specimens were thermal cycled and then the adhesive strength of the cycled specimens were compared to the control specimens to determine the effect of thermal cycling of adhesive strength. Test results and sample preparation are discussed in section 3.3.5.

To evaluate the adherence of the electroplated Ni and the various vacuum deposited coatings, a tape pull test was performed as described in section 3.1.6.

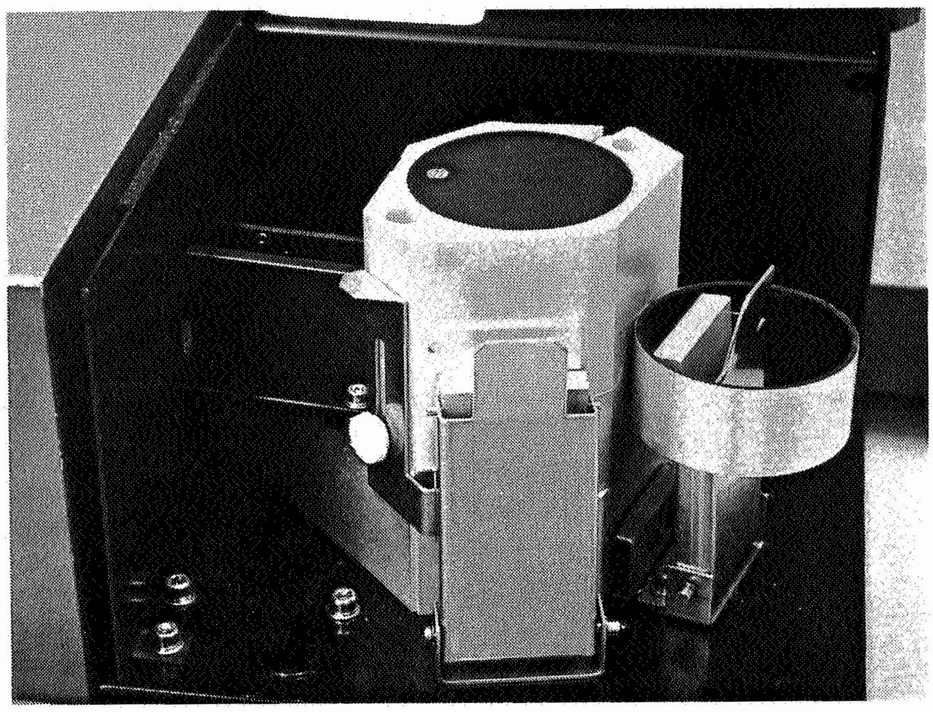

Figure 3.2.2-2 Optical Testing of 2-in-Diameter Tube

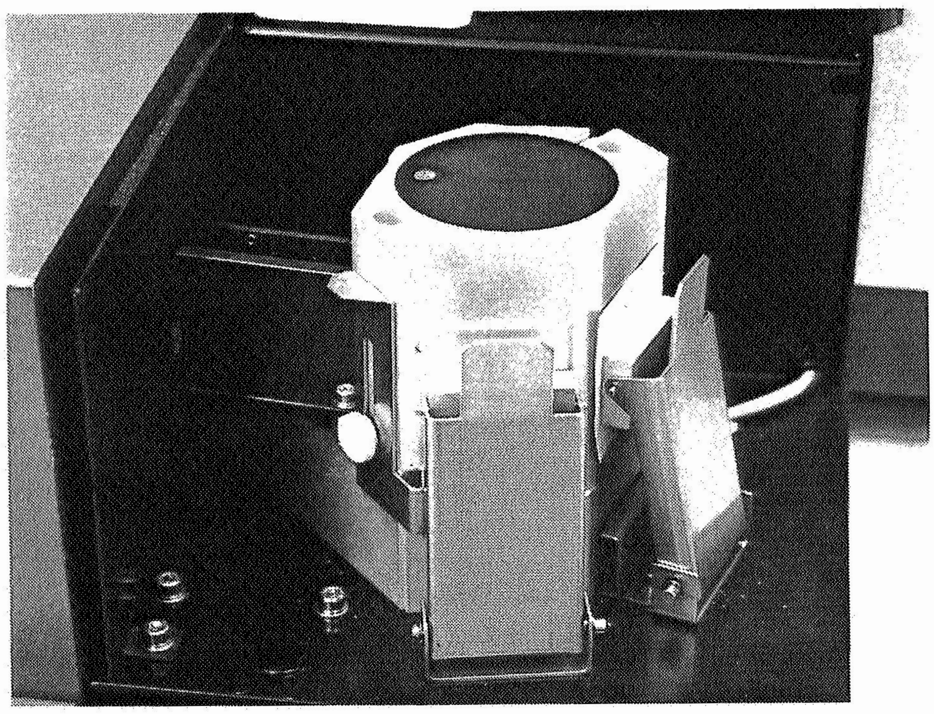

Figure 3.2.2-3 Optical Testing of Flat Foil

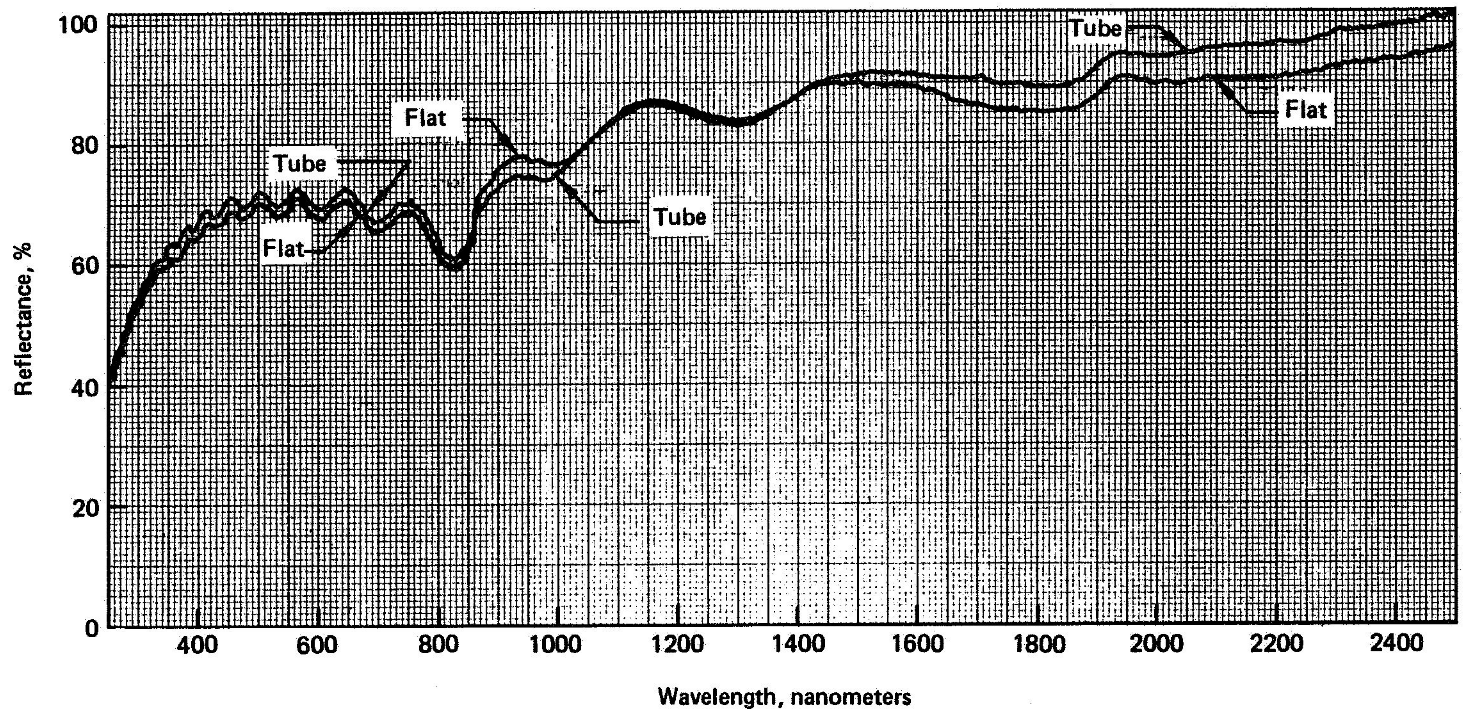

AM-O absorptance of chromic anodized Al foil:
Flat Al foil specimen = 26%
Al foil bonded to Gr/Ep tube = 27%

Figure 3.2.2-4 Comparison of Absorptance of Tube and Flat Foil

3.3 Coating Evaluation Tests

Of the 11 coating concepts discussed in section 3.1, the following 5 coatings were selected for further testing.

a. 1-micron SiO_2/3000 Å Al/Al foil.
b. Phosphoric acid anodized Al foil.
   acid solution/H_2O = 14% by weight
   immersion time = 50 min
   ramp time = 2 min
c. Chromic acid anodized Al foil.
   acid solution/H_2O = 5% by weight
   immersion time = 20 min
   ramp time = 15 min
d. Electroplated nickel
e. SiO_x/electroplated nickel

The first three coating concepts appeared to be the most promising. Not only were the targeted optical values achieved, but the values could be further tailored to achieve different optical values, if required. The electroplated samples were selected for evaluation because of their ease of application, good uniformity, and ability to coat irregular-shaped surfaces. The SiO_x-coated electroplated Gr/Ep tubes possess improved atomic oxygen resistance and higher ε values.

The test plan, (figure 3.0-1) was used to evaluate the above five coatings. These testes included thermal cycling under vacuum, atomic oxygen resistance, and abrasion resistance. All these tests were performed on coated 2-in-diameter P75S/934 Gr/Ep tubes built to the specification described in Section 2.

3.3.1 Thermal Cycling Under Vacuum

The objective of this test was to thermally cycle the various coated tubes (plus one uncoated tube as a control) under a simulated LEO environment. These specimens were thermally cycled under vacuum in Boeing's Space Chamber "B". This chamber is an intermediate-size vacuum chamber with space environment simulation capabilities. The solar simulator built into this chamber provides a 35-

in-diameter, uniform, collimated beam. The light is generated by a bank of 19 2.5-kW xenon lamps. Uniformity and spectral filters provide a beam that is spectrally matched to AM-O; the total incident energy is one solar constant (1350 mW/m^2). The LN_2 shrouds used to approximate the heat sink of black space are constructed of black painted aluminum and are 8-ft in diameter by 18-ft high. Chamber "B" is capable of a working pressure of 1×10^{-9} torr and is loaded from the bottom, with the bottom section capable of being removed so that the test setup may be built up on the floor remote from the chamber. Figure 3.3.1-1 shows a schematic of the chamber and test setup.

The tubes were thermally cycled for a total of 50 cycles while under a vacuum of 10^{-6} torr. Each cycle consisted of opening the douser at the beginning of the cycle to allow the tubes to be radiantly heated by incident solar radiation from the solar simulator, then closing the douser after 57 min, which allowed the tubes to be radiantly cooled by the thermal shroud (without radiation) for 37 min. This cycle closely simulates the Sun/eclipse cycle of the Space Station at LEO. Using this testing technique, each coated tube was allowed to seek its own temperature versus time profile, which is a function of their individual α and ϵ. Changes in optical values, coating and foil adhesion, and microcrack density were determined after the tubes were removed from the vacuum chamber.

The 16 tubes that were cycled included 9 tubes protected with the following coatings:

a. SiO_2/Al/Al foil (two tubes cycled).
b. Phosphoric acid anodized Al foil.
c. Phosphoric acid anodized Al foil on the exterior surface/uncoated Al foil on the interior surface.
d. Chromic acid anodized foil.
e. Electroplated nickel.
f. Flash coating of electroplated nickel.
g. Sulfuric acid anodized foil.
h. Al/Al foil.

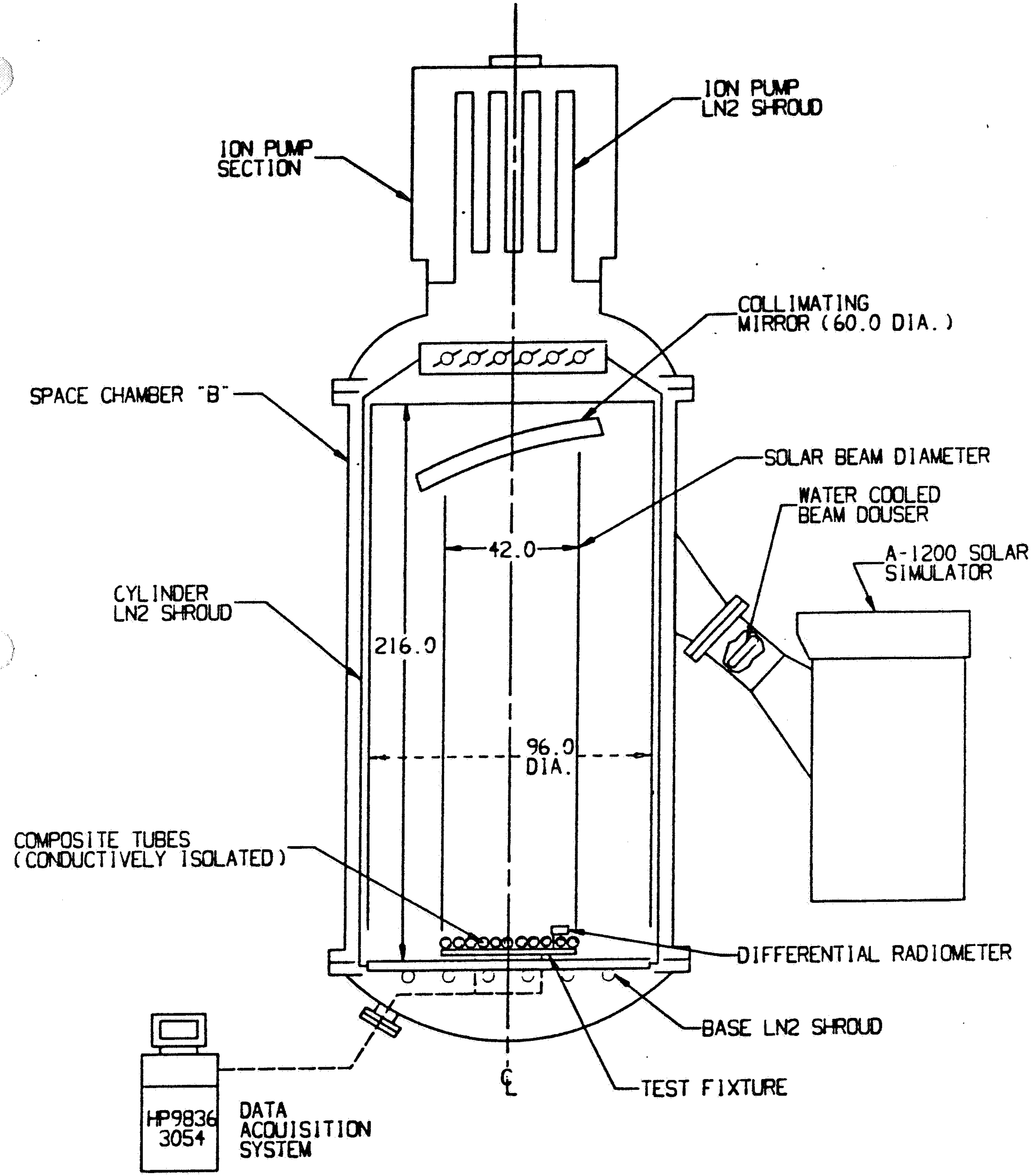

Figure 3.3.1-1 Composite Tube Vacuum Thermal Cycling Test Setup

The Gr/Ep tubes wrapped with sulfuric anodized Al foil and sputtered Al/Al foil were thermal cycled to evaluate their effectiveness even though the optical values weren't within the targeted range. The SiO_x-coated electroplated nickel tubes were not completed in time for this test. Also included in the cycling test were seven uncoated tubes comprised of three different Union Carbide Gr/Ep composites. These were part of a microcrack study, the results of which are discussed in the section 3.3.6.

Because of the feedthrough limitations in the vacuum chamber, only five of the sixteen tubes were instrumented with thermocouples (T/Cs). These tubes were:

a. SiO_2/Al/Al foil.
b. Phosphoric acid anodized Al foil.
c. Phosphoric acid anodized Al foil on the exterior surface/uncoated Al on the interior surface.
d. Electroplated nickel.
e. Uncoated P75S/934 Gr/Ep tube.

Each of the five tubes had three T/Cs bonded to the tube surface with a thermally conductive adhesive. The locations of the T/Cs (shown in figure 3.3.1-2) were: the top and bottom of each tube and on the inside of the top surface. The T/Cs on the top of the exterior surface had radiation shields as shown in figure 3.3.1-3.

Figure 3.3.1-4 is the vacuum chamber base plate showing the location of the 16 Gr/Ep tubes. The tubes were suspended from the test fixture using to prevent conduction between the tubes and fixturing. The base plate is raised up to the chamber to form a vacuum tight seal.

Figure 3.3.1-5 is a picture of the tubes under insolation as seen through a view port in the vacuum chamber. The backside of the tubes were always in the shadow of the simulated solar and, therefore, were continuously radiantly cooled by the -320°F LN_2 thermal shrouds. Tube temperatures were taken every minute for cycles, 1, 2, 25, and 50 and every 5 min for the rest of the cycles.

Because of the tubes proximity to each other (1-in), shielding was placed between the tubes to prevent reflection of the solar radiation from one tube to another

GRAPHITE/EPOXY TUBE THERMAL/VACUUM TEST

TUBE DETAIL

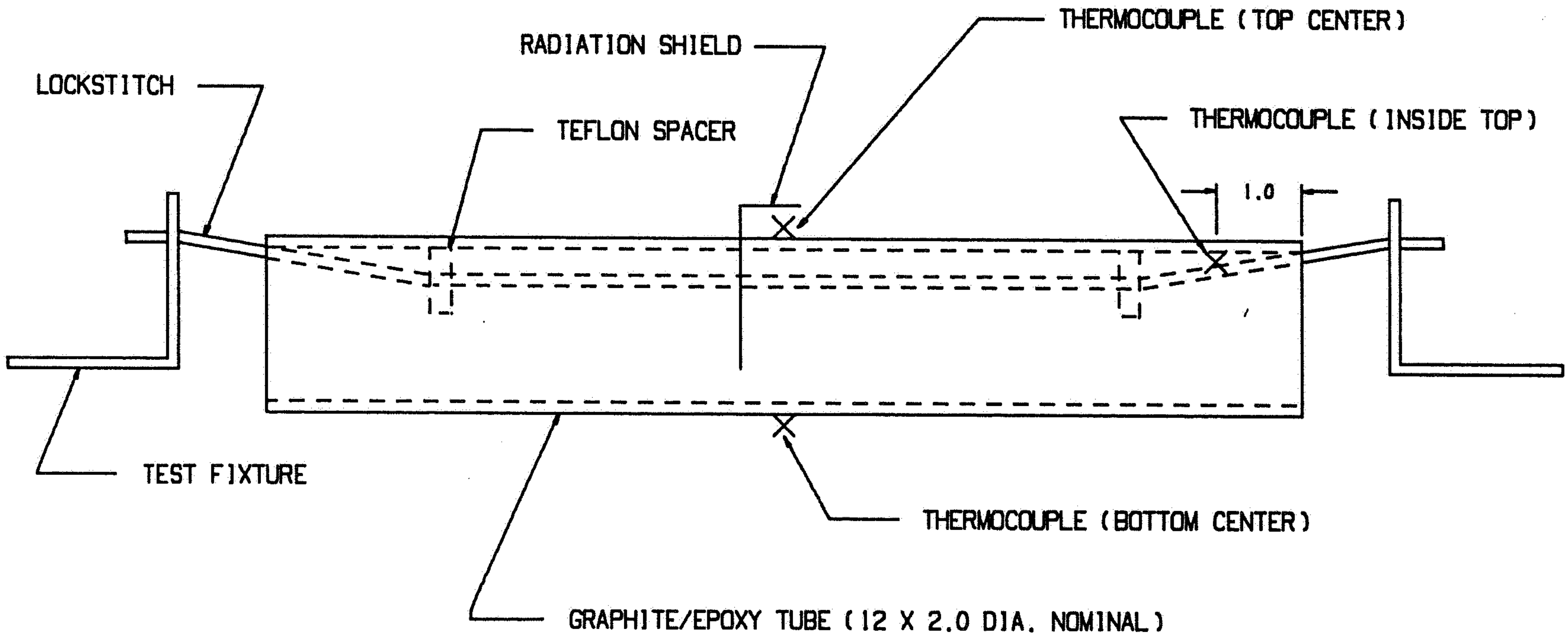

GRAPHITE/EPOXY TUBES - KEY

TUBE #	IDENTIFICATION	THERMOCOUPLE # T.C.	THERMOCOUPLE # T.I.	THERMOCOUPLE # B.C.	TUBE #	IDENTIFICATION	THERMOCOUPLE # T.C.	THERMOCOUPLE # T.I.	THERMOCOUPLE # B.C.
1	PHOSPHORIC ACID	TC02	TC03	TC01	9	CHROMIC			
2	FOIL, BOTH SIDES	TC05	TC06	TC04	10	EP NI			
3	4-2	TC09	TC08	TC07	11	1-2			
4	NI	TC12	TC11	TC10	12	2-2			
5	SI02	TC14	TC15	TC13	13	5-2			
6	P755/934				14	3-2			
7	VACUUM ALUM.				15	SULFURIC ANODIZE			
8	P755/934				16	SI02			

Figure 3.3.1-2 Thermal/Vacuum Test, Gr/Ep Tube Details

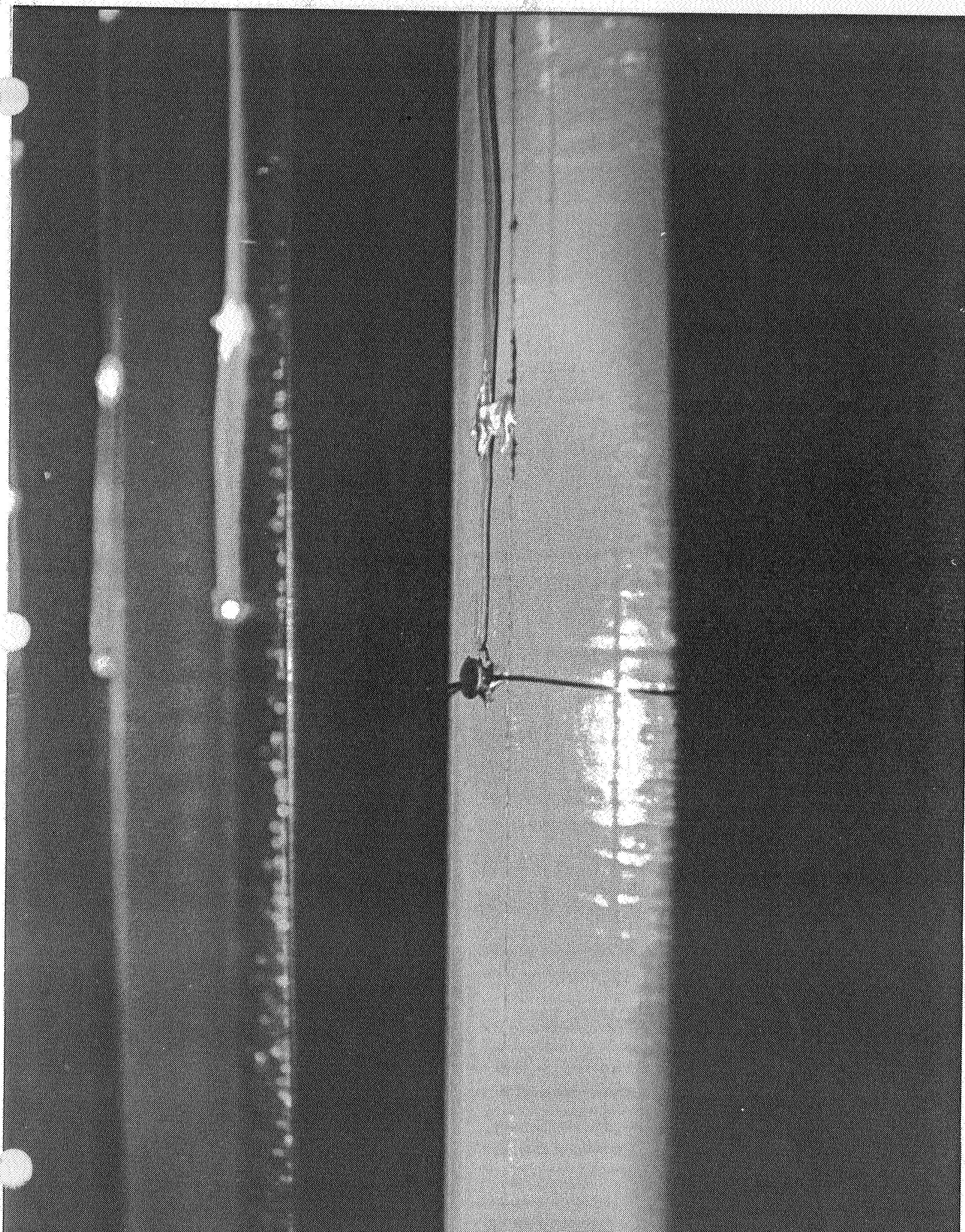

Figure 3.3.1-3 SiO_2/Al/Al Foil Coated Gr/Ep Tube With Radiation Shield

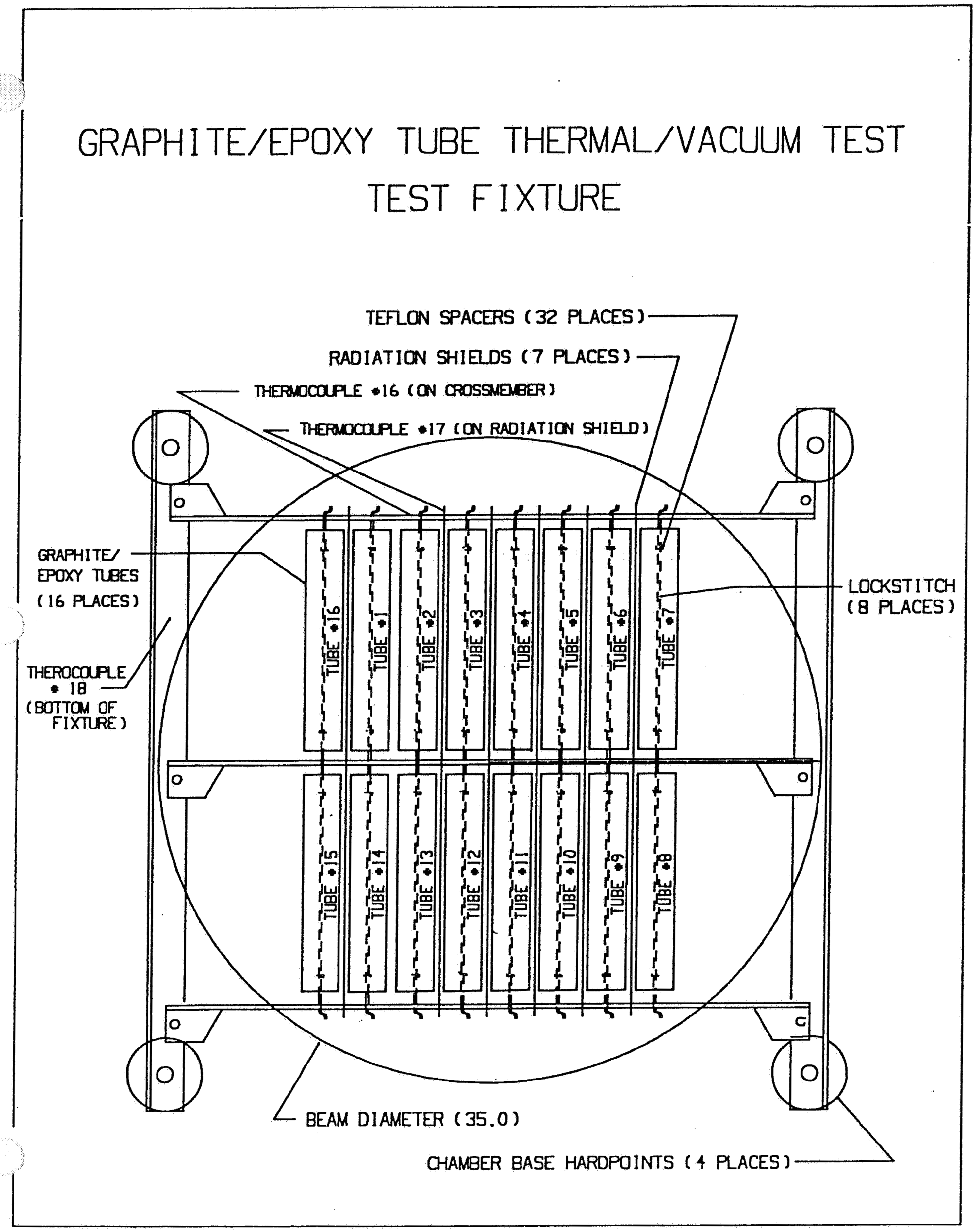

Figure 3.3.1-4 Gr/Ep Tube Thermal/Vacuum Test Fixture

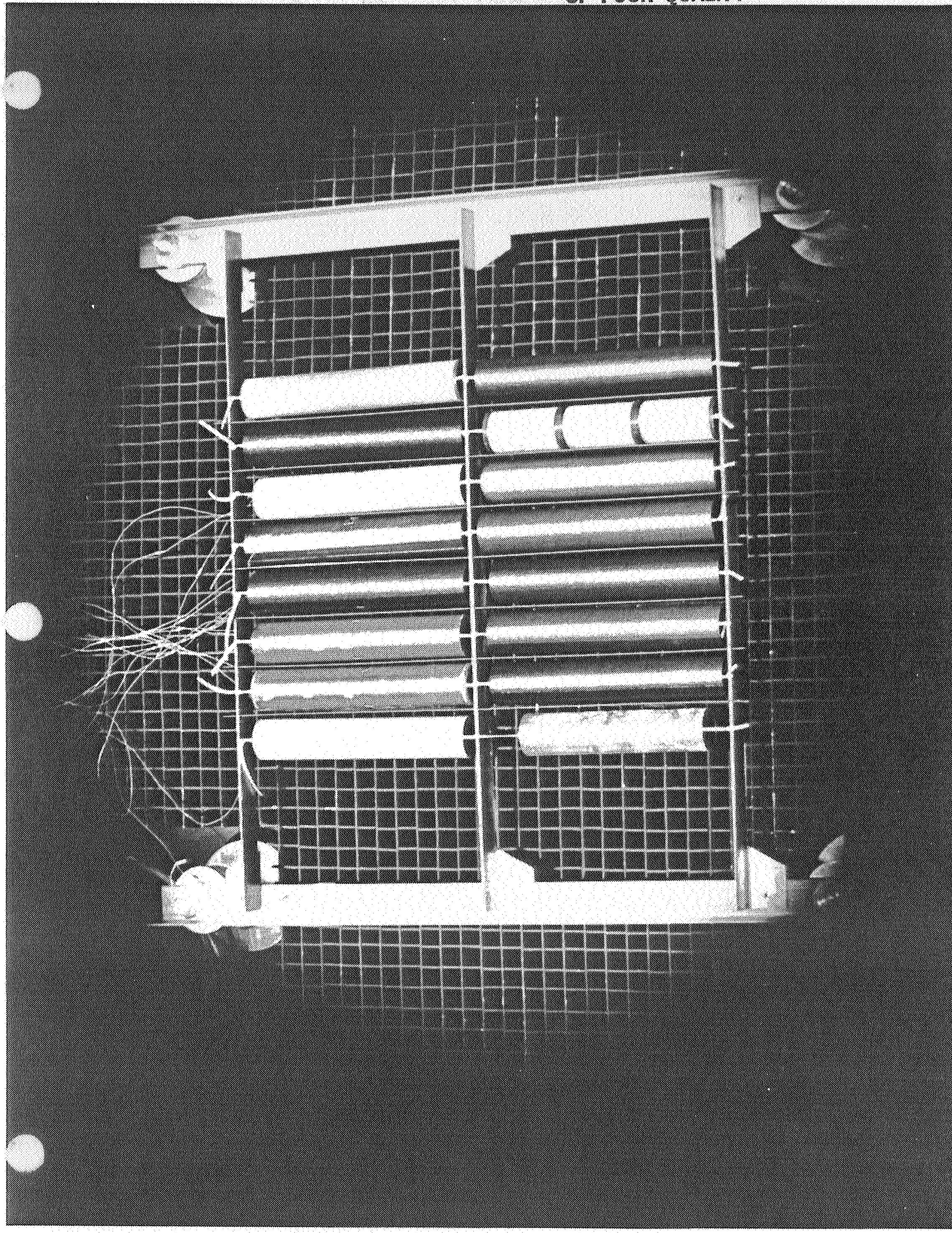

Figure 3.3.1-5 16 Gr/Ep Tubes Under Simulated AM-O Insolation

which would affect the tube temperatures. The shielding consisted of thin Al plate, painted with a black matte finish. The temperature versus time history of one shield was measured (T/C #17) and this was used as a boundary condition during analysis of the tubes.

The temperature versus time profiles recorded by the various T/Cs during simulated LEO testing were used to verify the analytical modeling of the temperature cycling of the tubes. The following paragraphs describe the analytical model and analysis.

3.3.1.1 Thermal Analysis and Test Results

Each tube was analyzed separately, with the analytical model consisting of the tube, its two adjacent shields, and a representation of the background (shroud) surfaces. The tube was circumferentially divided into 36 full-length strip elements. Test data indicated no significant temperature gradients across tube walls; therefore, the model was formed with a single layer of elements, each having a thickness equal to the wall plus coating. Each element was then lumped as a BETA (Boeing Engineer Thermal Analyzer) model node. Each shield was defined as a single node, and the background above and below the tube treated as two additional nodes. The model was treated as two-dimensional, representative of the mid-section of each tube.

Geometric view factors between the tube elements and the shields were computed by handbook formulas, and the additional required view factors (shield-to-shield, shield-to-background, and tube-to-background) were computed by solving standard view summation equations. Radiation exchange factors, including those for tube internal exchange, were obtained via the SCRIPTF program, which is a Boeing developed program to determine the exchange factors.

The values of circumferential conductors between BETA nodes took into account the effect of the foil layers through use of an effective conductivity, based on the weighted average of the Gr/Ep and the aluminum foil conductivities. The conductivity of the $(0_2 \pm 20, 0_2)_s$ layup (shown in figure 3.3.1.1-1) was determined from test data. The nodal capacitance values accounted for the actual material properties in the same way.

Case	Tube surface description		Solar absorptance	Emittance	
	Tube outside	Tube inside		Outside	Inside
1	Bare graphite/epoxy	Bare	.91	.82	.82
2	Phosphoric acid anodized .002" Al foil	Bare	.23	.19	.82
3	Phosphoric acid anodized .002" Al foil	.002" Al foil	.23	.19	.05
4	Elecroplated nickel	Bare	.37	.12	.12
5	SiO_2-Al on .002" Al foil	Bare	.35	.20	.82

Graphite/epoxy:

Density = .064 lb/in^3

Specific heat = .216 btu/lb-^oF @ 47^oC
.225 btu/lb-^oF @ 57^oC

Conductivity (circumferential) = 4.025 x 10^{-5} btu/in-sec-^oF @ 81^oF
3.825 x 10^{-5} btu/in-sec-^oF @ -20^oF

Wall thickness = 0.060 in

Al foil:

Density = .098 lb/in^3

Specific heat = .22 btu/lb-^oF

Conductivity = 220 W/m-K

Thickness = 0.002 in

Figure 3.3.1.1-1 Descriptions and Properties of Thermal Cycled Tubes

The BETA program analysis was carried through two complete cycles for both the test cases and the LEO simulations. The choice of two cycles was a compromise between a need for a sufficient number of cycles to completely "wash out" the effect of possible incorrect initial temperature guesses and a desire to economize on computer time.

Test Results

Figure 3.3.1.1-1 provides the various properties of the modeled tubes. Figure 3.3.1.1-2 to 3.3.1.1-6 show the results of both the analytical analysis and actual test data for each tube that had T/C's.

Differences between predicted and measured temperatures ranged from 5 to 15°F for the bare Gr/Ep tube shown in figure 3.3.1.1-2, to 55°F for the tubes wrapped with phosphoric acid anodized Al foil (figs. 3.3.1.1-3 and 3.3.1.1-4). The use of a two-dimensional analysis could be the cause of some of the difference seen. The end regions of the tube surfaces, inside and outside, had a good view of the support fixture angles (fig. 3.3.1-5). The temperatures of these members, therefore, could have had an important influence on tube end region temperatures, and this effect could have influenced tube control region temperatures by conduction and radiation. The magnitude of longitudinal heat flow effects could vary significantly from tube to tube due to the conduction contribution of the different foils and coatings. This would explain why the bare Gr/Ep tube, which has poor conductance, was accurately modeled, but the tubes wrapped with foil had a larger difference in predicted and actual test values. A large space structure employing tubes such as those analyzed here would probably consist of members with much larger length/diameter ratios than that of the test specimens. Therefore, the two-dimensional analysis approach is considered valid for such members except near their ends, and the on-orbit predictions that follow are assumed to be reasonably accurate.

In addition, the shield temperature history, measured on the shield between the phosphoric anodized foil tube and the bare tube, was used in the analysis of all tubes. If other individual shield temperatures differed from this data, a difference between predicted and measured tube temperatures could be expected.

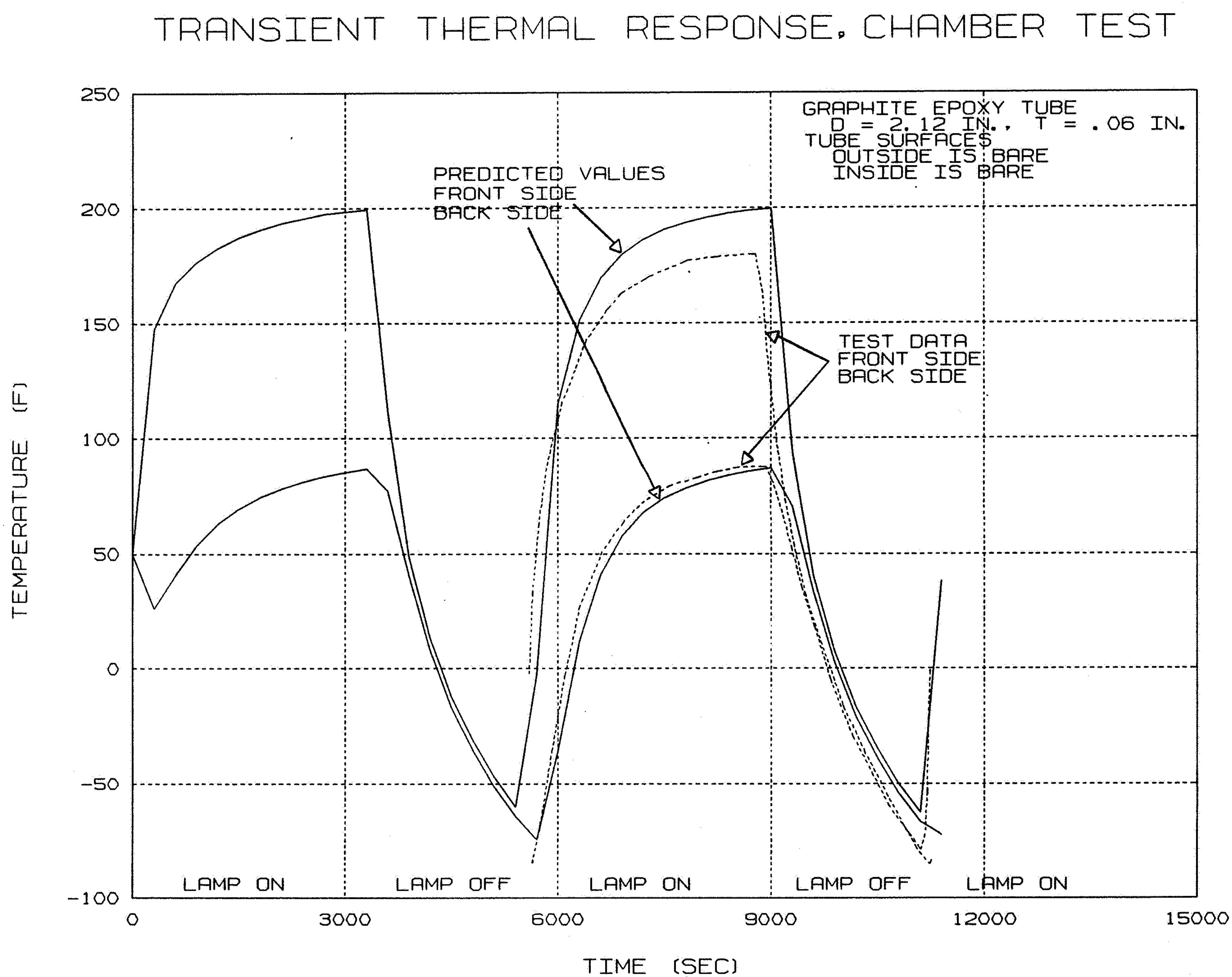

Figure 3.3.1.1-2 Thermal Response of Bare Gr/Ep Tube

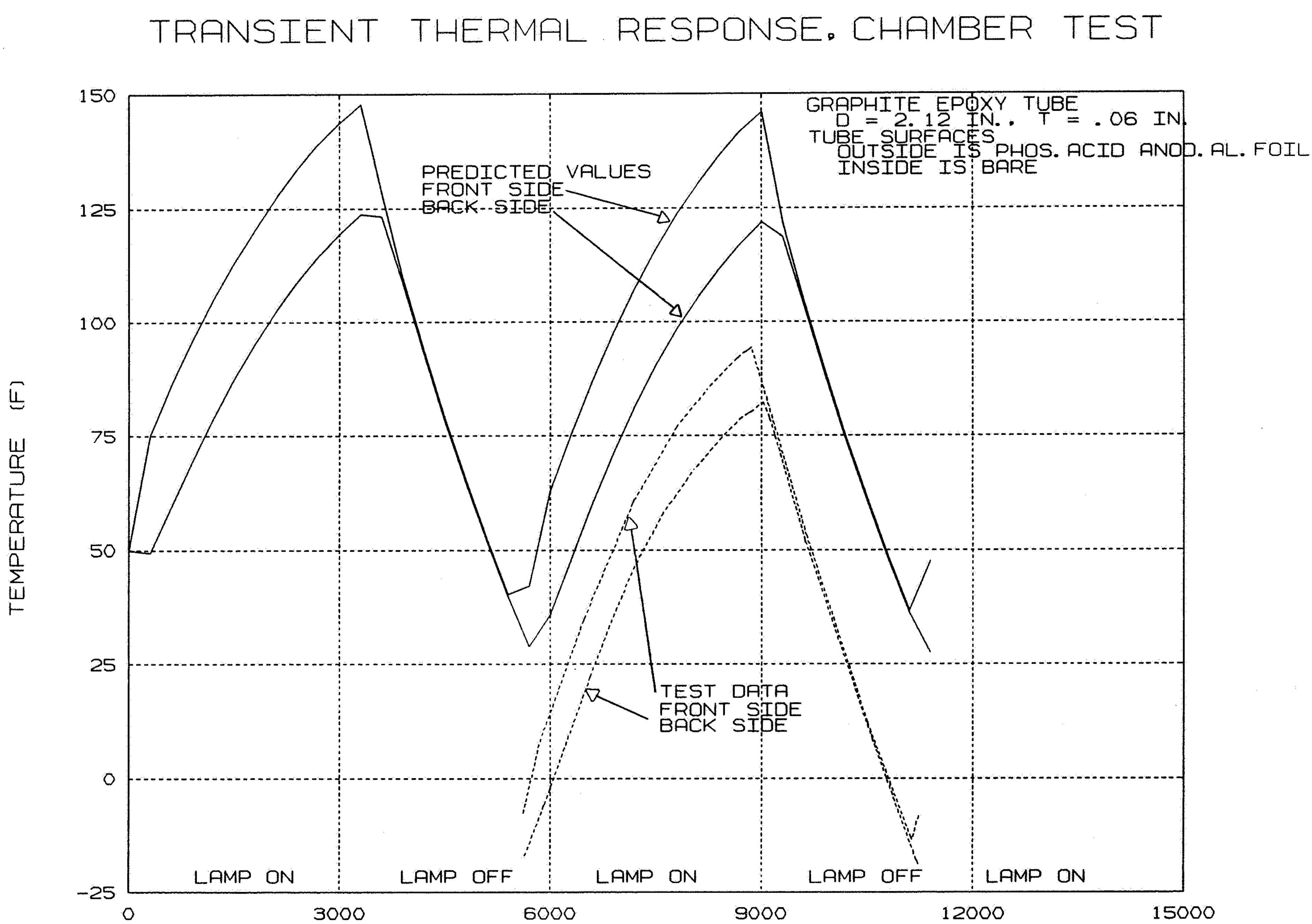

Figure 3.3.1.1-3 Thermal Response of Phosphoric Acid Anodized Al Foil

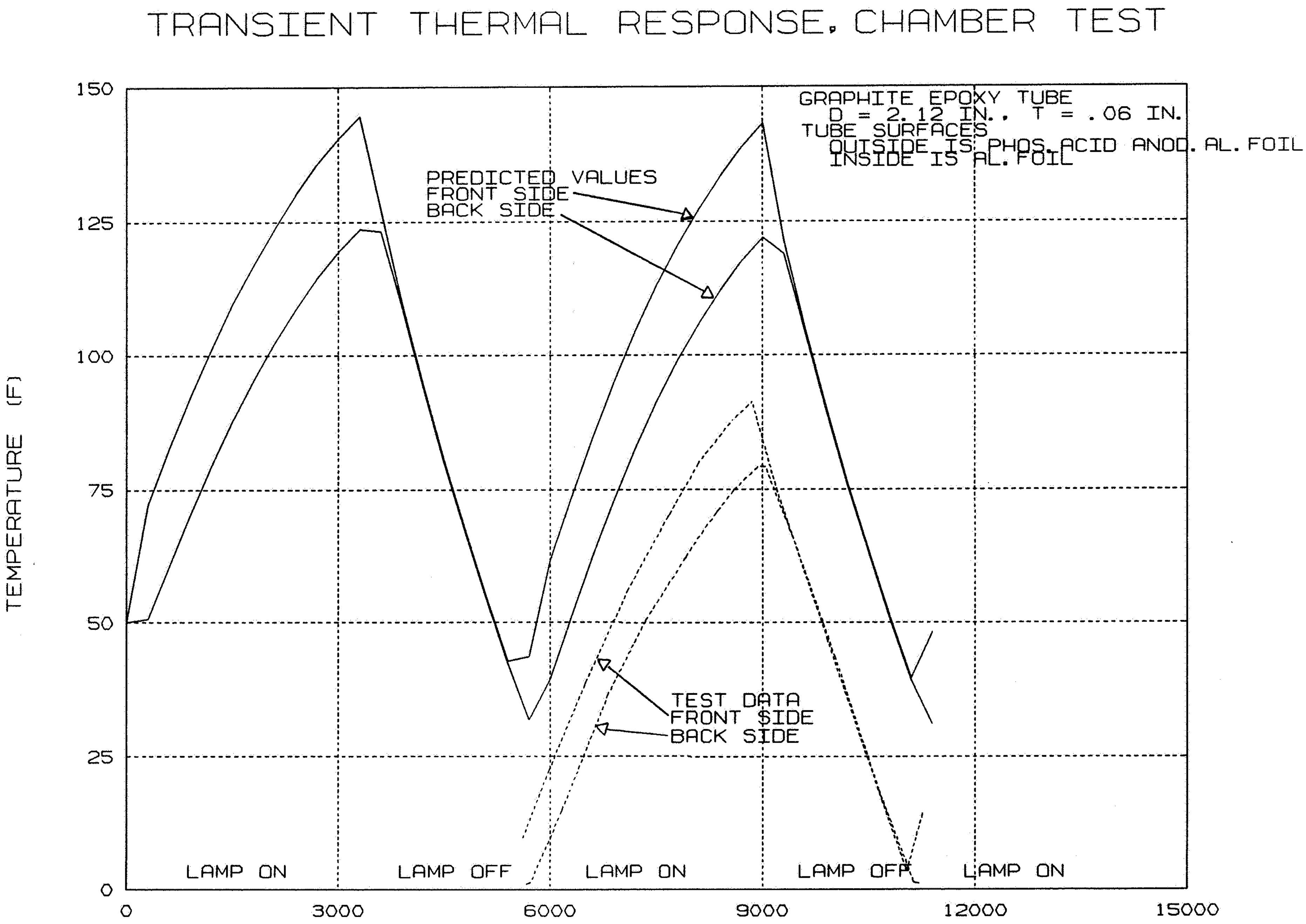

Figure 3.3.1.1-4 Thermal Response of Phosphoric Anodized Al Foil Electroplated With Al Foil on the Interior Surface

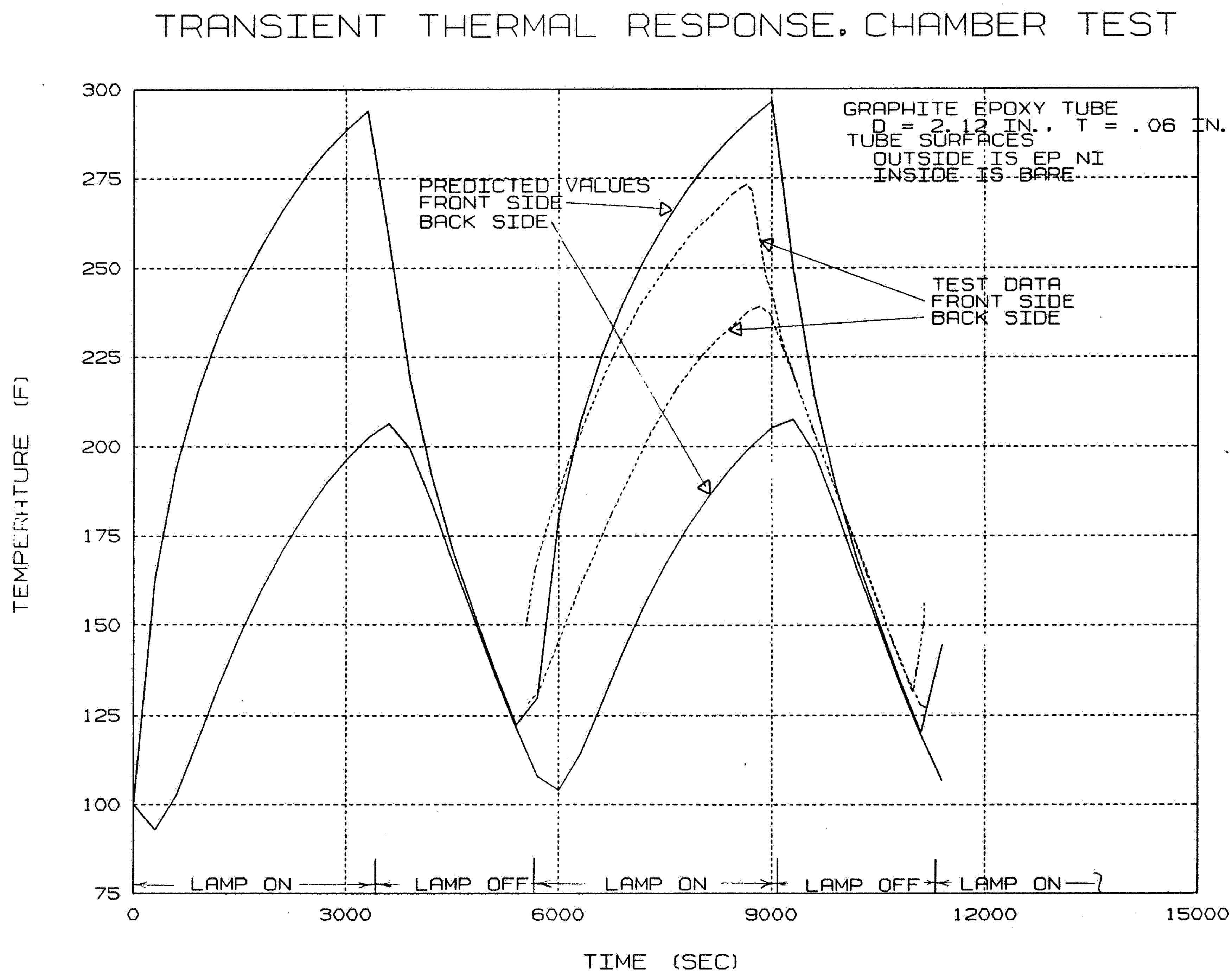

Figure 3.3.1.1-5 Thermal Response of Electroplated Nickel

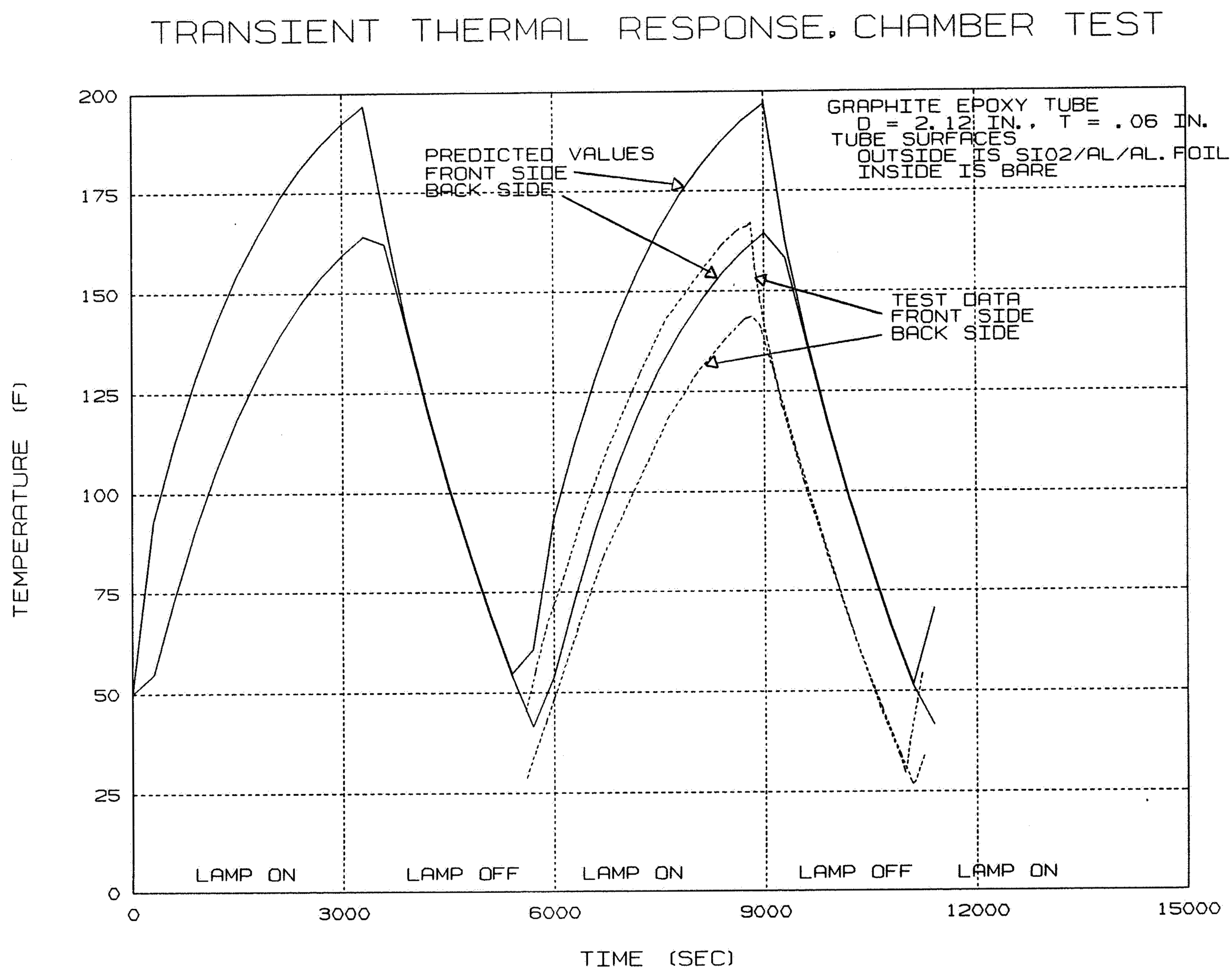

Figure 3.3.1.1-6 Thermal Response of SiO_2/Al/Al Foil

Comparison of the actual tube temperatures, as measured by the 15 thermocouples, between the second and fiftieth cycles disclosed the following results:

a. The maximum and mininum temperature of the phosphoric acid anodized foil increased by 4°F.

b. The maximum and minimum temperature of the SiO_2 coated foil increased by 2°F.

c. There was no change in the temperatures of the uncoated tube and the tube coated with electroplated nickel.

Analysis of the actual tube temperature also determined that -

a. All the tubes had minimal temperature gradients (≤4°F) between the top outside thermocouple and the top inside thermocouple.

b. The bottom (shadowed) temperature was the same as the top temperature at the end of the eclipse portion of the cycle for all five tubes which had thermocouples attached.

c. The bottom (shadowed) temperature was half that of the top temperature (91°F vs 182°F, respectively) for the uncoated tube at the end of the Sun portion of the cycle.

d. The bottom (shadowed) temperature was approximately 15% lower than the top temperature at the end of the sun portion of the cycle for the four coated tubes.

Predictions for the tubes in LEO are shown in figures 3.3.1.1-7 to 3.3.1.1-12. The analysis for these cases differed from the test environment analyses only in the removal of the shield influence and the provision for the entire surface of each tube to view space background having a temperature of -452°F (4K) and an emittance and absorptance of 1.0. Solar radiation was the only heat source. It should be recognized that in LEO, Earth emission and Earth albedo radiation may be significant, depending upon orientation of the body or surface.

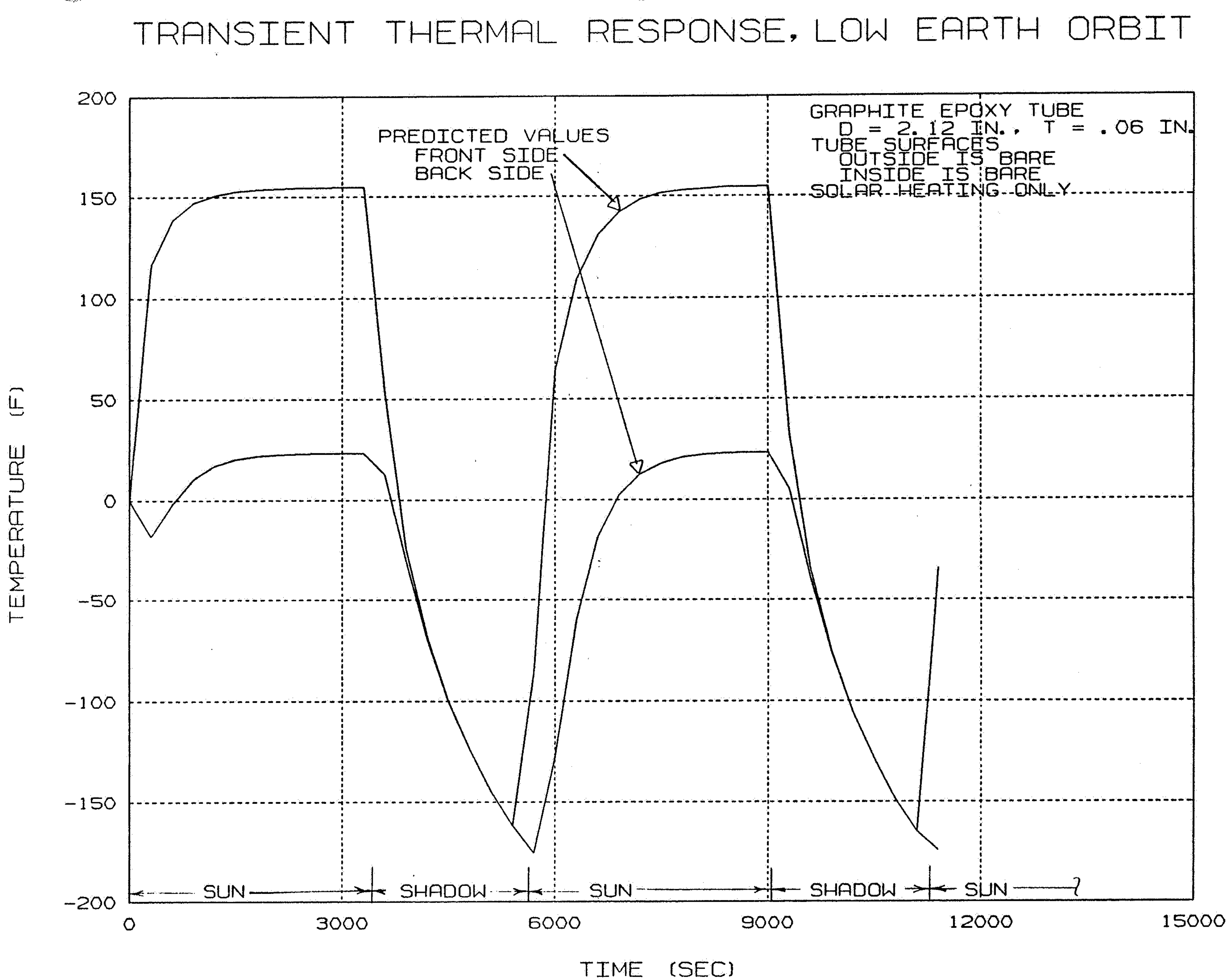

Figure 3.3.1.1-7 Predicted LEO Temperature for Bare Gr/Ep Tubes

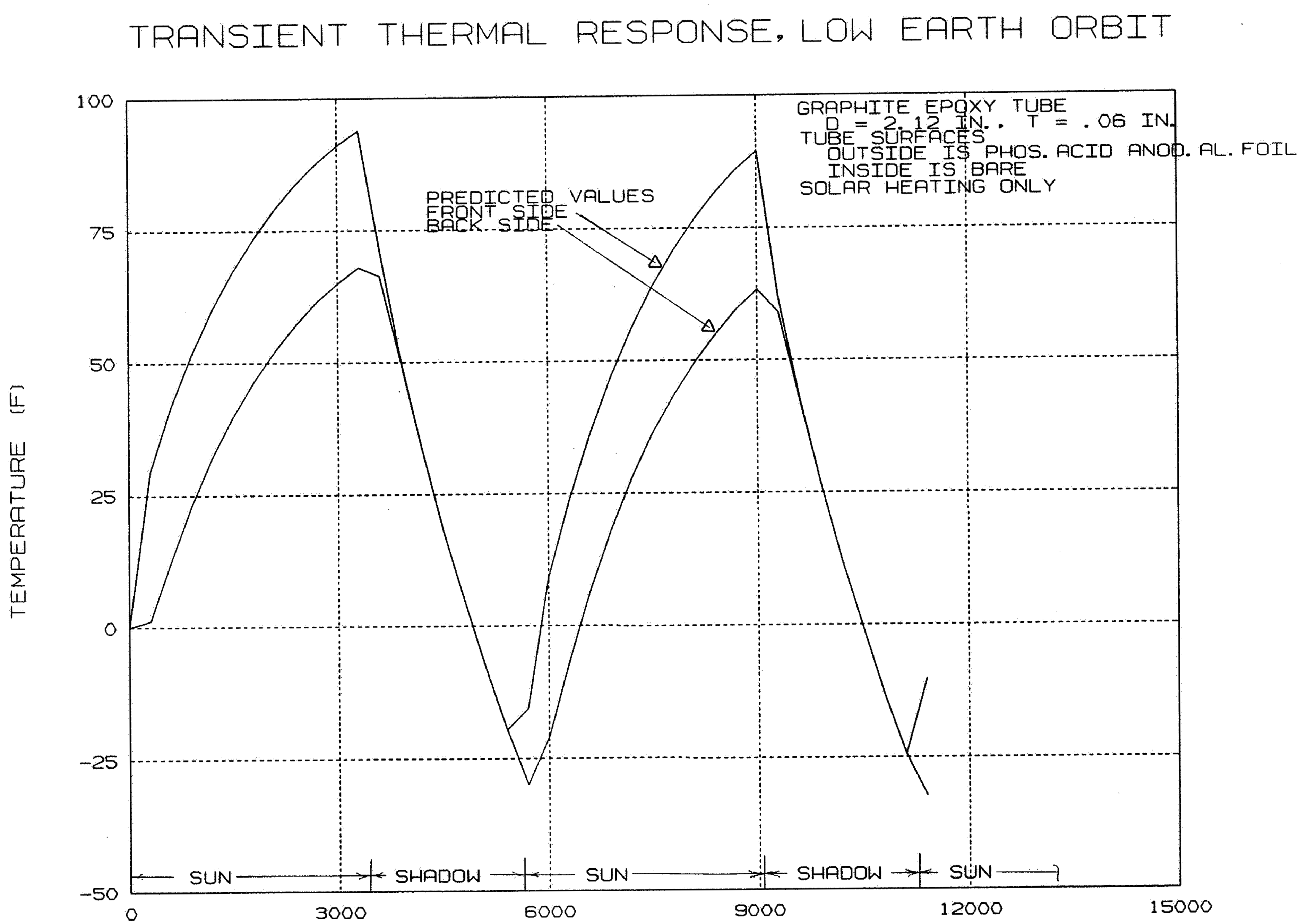

Figure 3.3.1.1-8 Predicted LEO Temperature for Phosphoric Anodized Al Foil

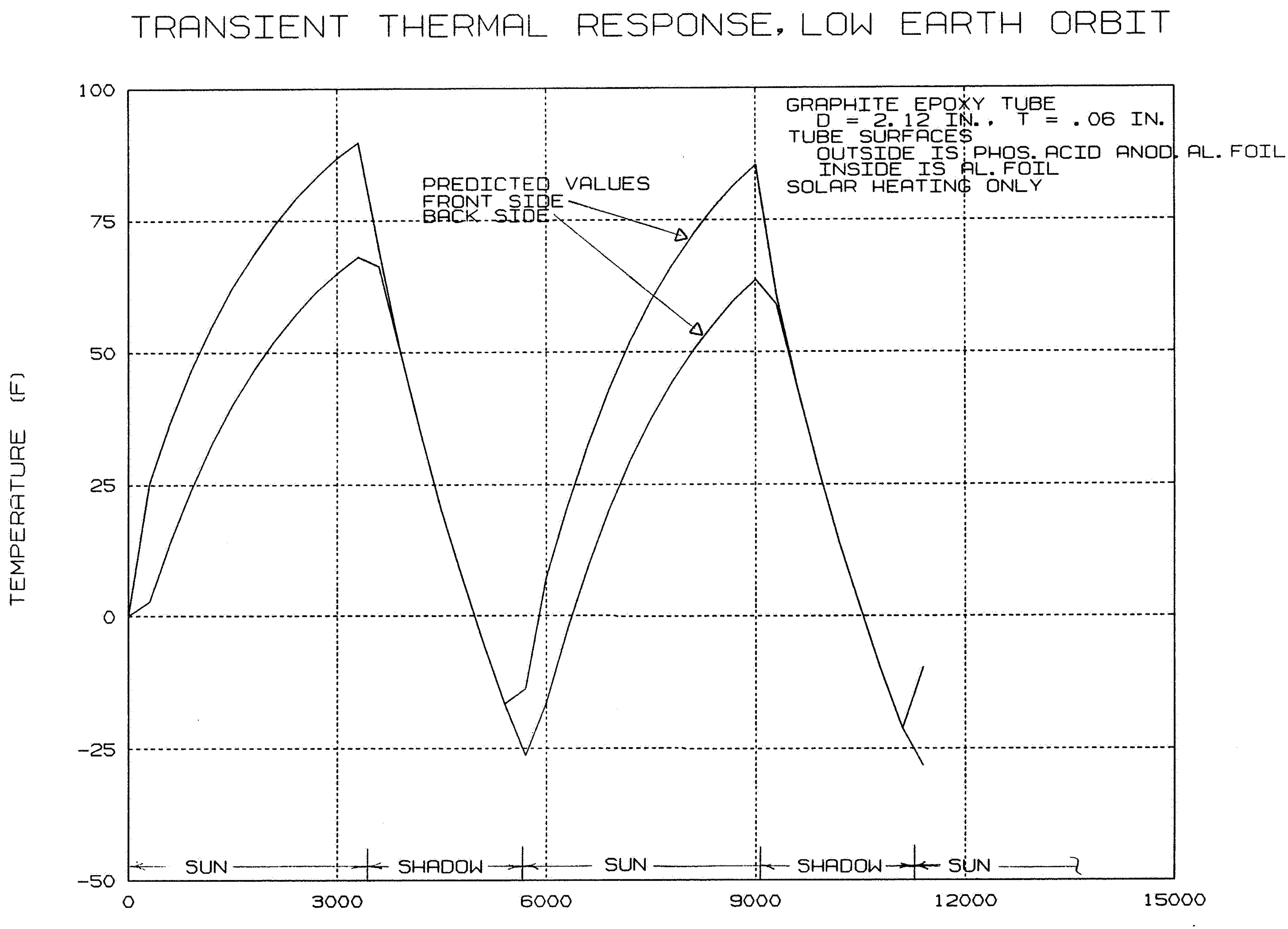

Figure 3.3.1.1-9 Predicted LEO Temperature for Phosphoric Anodized Al With Al Foil on Interior Surface

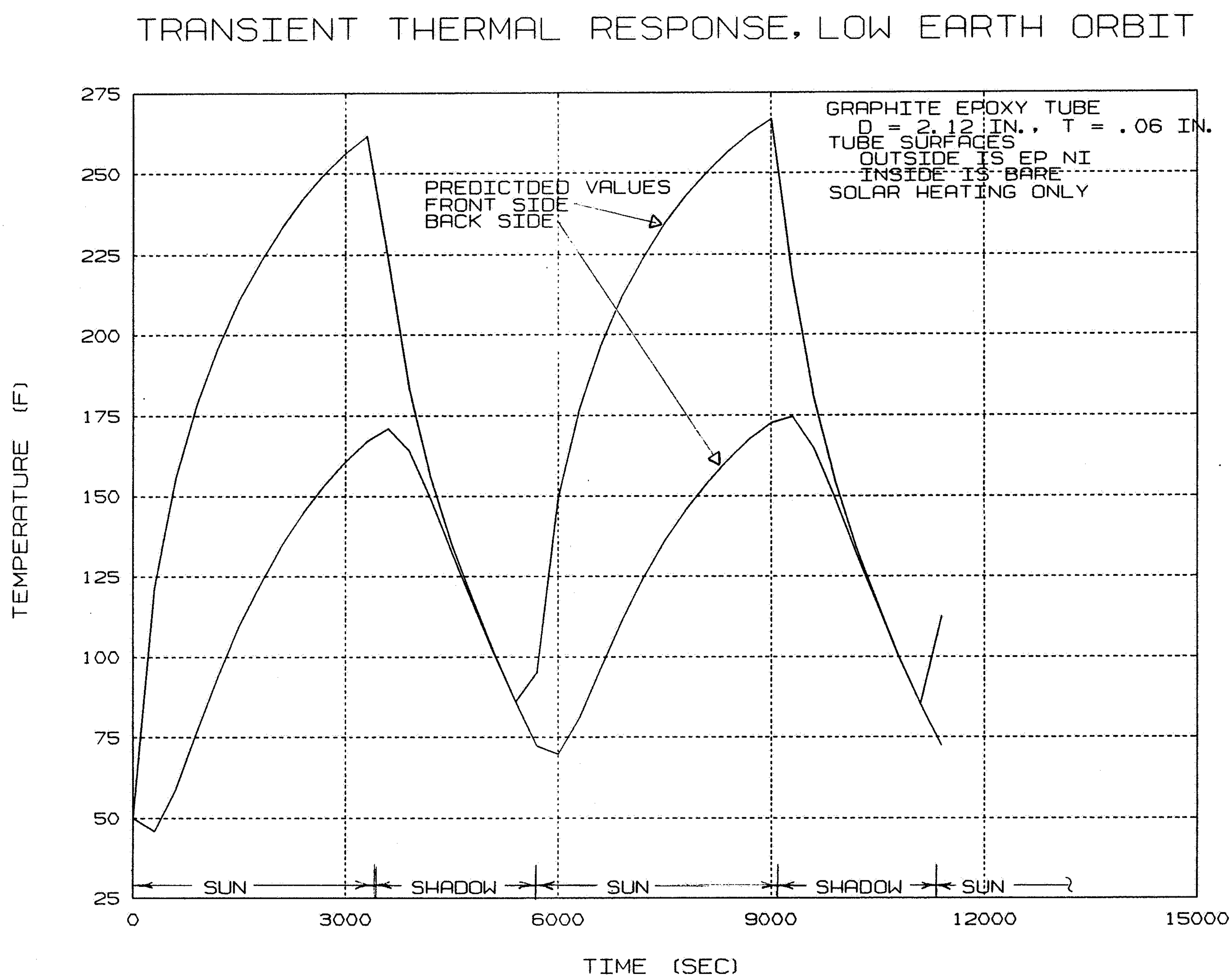

Figure 3.3.1.1-10 Predicted LEO Temperature for Electroplated Nickel

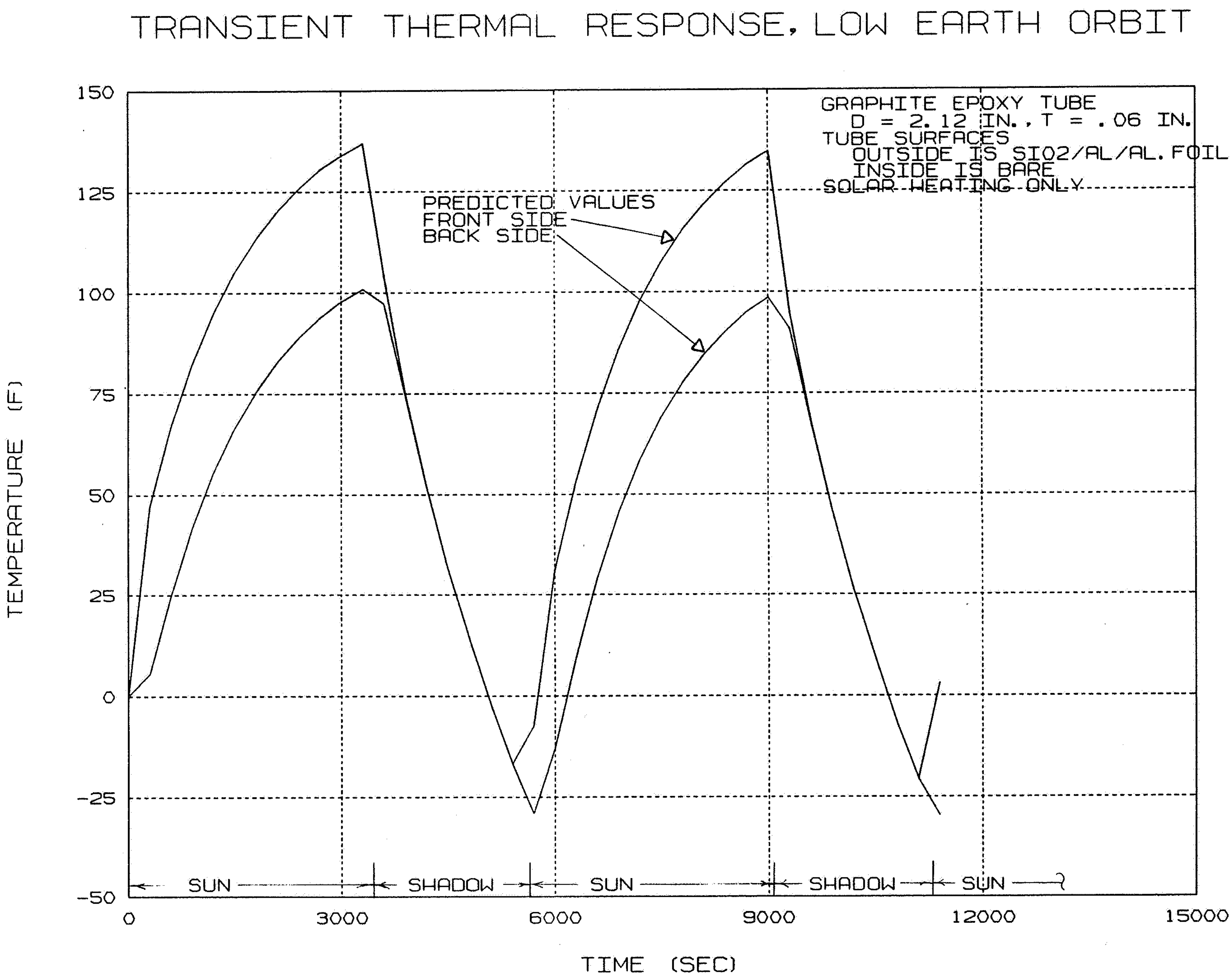

Figure 3.3.1.1-11 Predicted LEO Temperature for SiO_2/Al/Al Foil

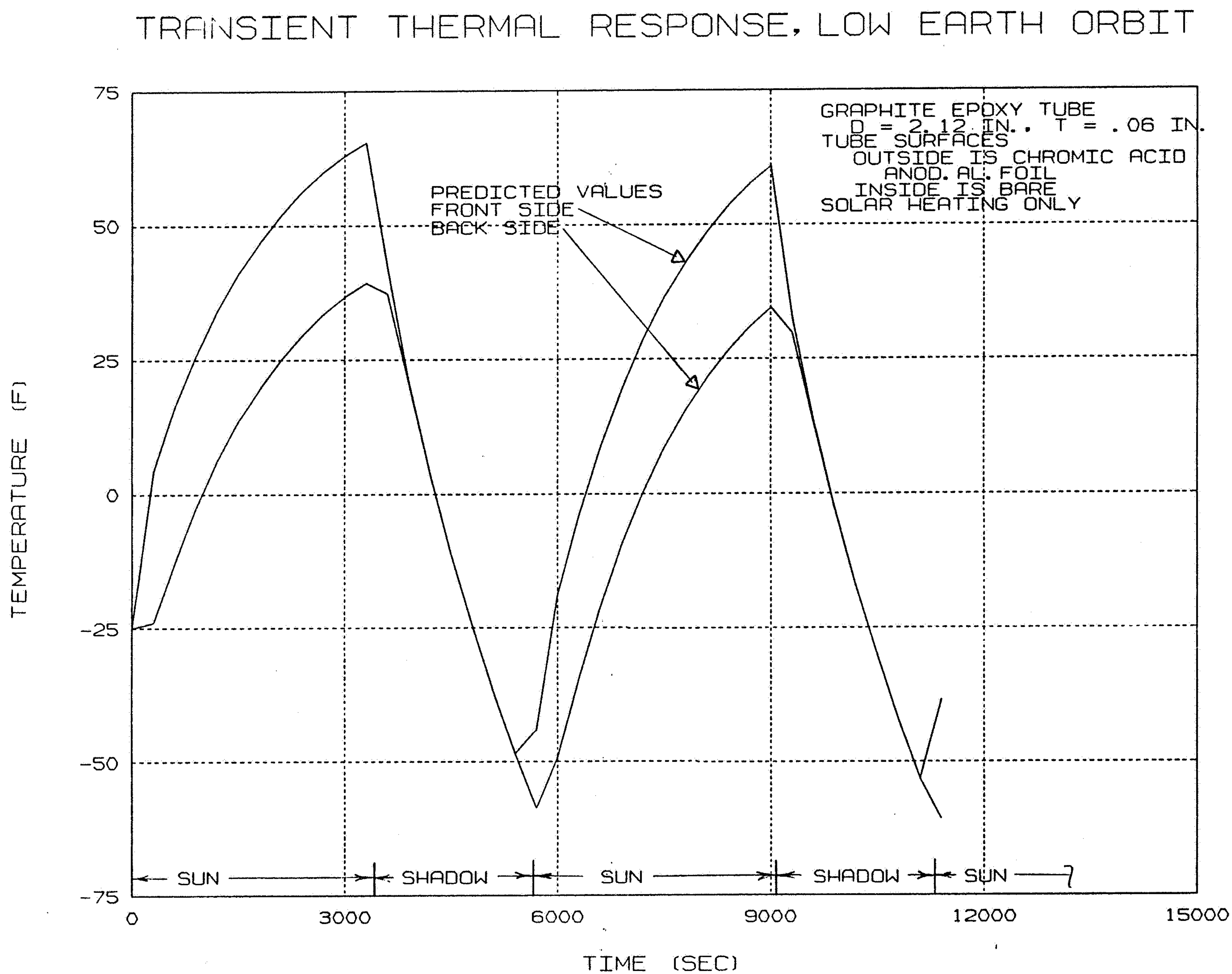

Figure 3.3.1.1-12 Predicted LEO Temperature for Chromic Acid Anodized Al Foil

Figure 3.3.1.1-12 is a temperature profile prediction of a Gr/Ep tube wrapped with the optimized chromic anodized Al foil.

After completion of the cycling, the various tubes were optically evaluated, checked for formation of microcracks, and were evaluated for coating and foil adhesion. 1.5-in-long specimens were cut from each tube for microcrack and optical evaluation. The fresh-cut surface was polished and then examined under 100X and 200X magnification. Photomicrographs of a typical surface are shown in figure 3.3.1.1-13. No microcracks were found. These tubes were further cycled and tested as discussed in section 3.3.6. The samples coated were optically evaluated and all the samples were within $\pm 2\%$ of their control, values which is within the test error tolerances. There was no detectable changes in coating or foil adhesion.

3.3.2 Abrasion Resistance

The specimens were abraided by rubbing two tubes with like coatings together and by rubbing them with simulated astronaut spacesuit materials. Conversation with Hamilton Standard (manufacturer of the space suit) established that the gloves are fabricated from either Kevlar or Nomex with a RTV 167 silicone outer layer and the boots are made from molded RTV silicone with Dacron insteps.

Test Results

The simulated astronaut glove (silicone-coated Kevlar) possessed enough tack that it was impossible to slide the glove across the various tube surfaces. There was no change in optical values or adhesion of the coating caused by handling the tubes with this material.

Abraiding the tubes by lightly rubbing them together caused the SiO_2/Al/Al foil tubes to become darkened along the line of contact. There was no change in either the chromic or phosphoric anodized foil even when the tubes were aggressively rubbed against each other.

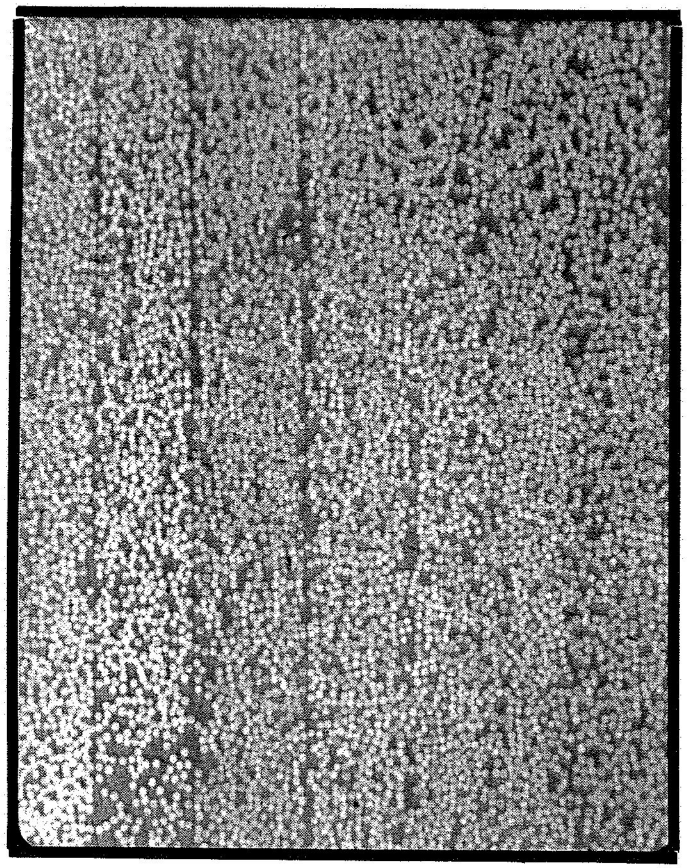

P75S/934 100 X

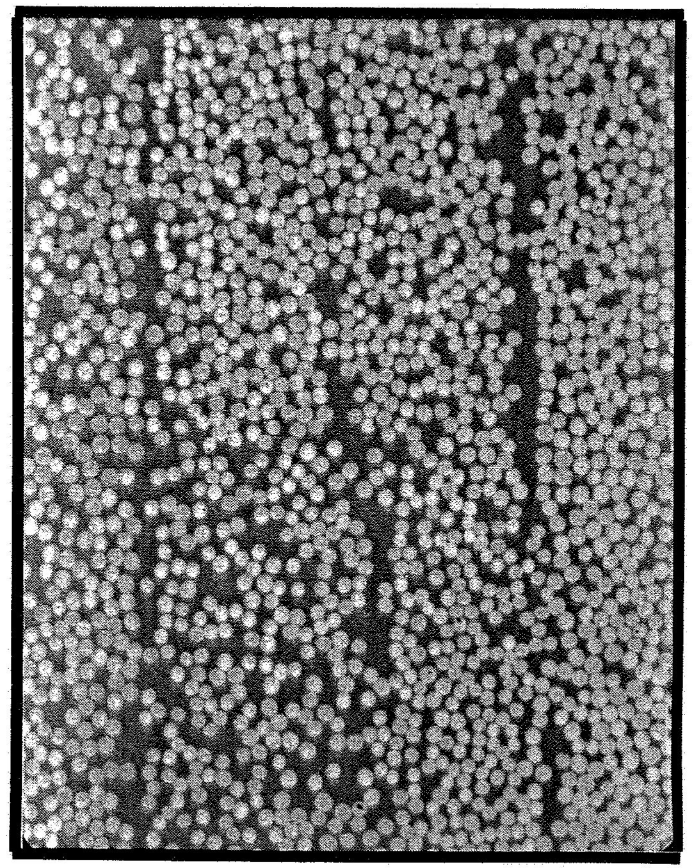

P75S/934 200 X

Figure 3.3.1.1-13 Photomicrographs of P75S/934 Gr/Ep Tubes After Thermal Cycling

3.3.3 Atomic Oxygen Resistance

The Boeing-built large-scale plasma atomic oxygen materials screening (PAOMS) test facility was made available for use under this contract. The facility features controlled test parameters of chamber pressure, oxygen flow rate, sample orientation, and radio frequency (RF) power coupling. Figure 3.3.3-1 shows some of the tube test specimens undergoing atomic oxygen testing in this facility. The RF energy causes the molecular oxygen to disassociate into charged species and neutral atomic oxygen atoms which interact with the coated Gr/Ep tubes positioned in the glow discharge path. Control samples of Kapton-H film were exposed to the plasma during each run thus allowing correlation to shuttle flight test erosion rate data, which is available for Kapton-H materials.

Analysis of flight data from STS-5, which was at an orbital altitude of 305 km, showed that Kapton-H degraded at an average rate of 1.9×10^{-3} mils/hr. Flight data for STS-8, flown at an orbital altitude of 225 km, showed Kapton-H degrading at an average rate of 9.8×10^{-3} mils/hr. Using this data and the known degradation rate of Kapton-H in Boeing's atomic oxygen facility, it was determined that 1 hr in the Boeing PAOMS facility is equivalent to 40 hr and 220 hr of exposure at an altitude of 225 km and 305 km, respectively. This difference in degradation rates between altitudes closely matches the difference in flux rates shown in figure 2.2.3-1. This equivalency is only valid for Kapton-H, but provides an idea of degradation rates for other organic materials.

Test Results

Several configurations of protectively coated tube tested samples were exposed in the PAOMS facility for 11 hr and then removed from the chamber to determine any changes in optical properties and coating adhesion. The specimens were then placed back in the chamber for an additional 22 hr of exposure to achieve a total exposure time of 33 hr. This would be equivalent to 2 months at a 140-mile (225-km) orbit or 10 months at a 190-mile (305-km) orbit for Kapton-H. The coated tubes were placed parallel to the flow tube axis of plasma chamber to minimize any turbulence. The Gr/Ep edges and interior surfaces of the tubes were left exposed to the plasma. Eight Kapton H control samples were simultaneously exposed during the test runs.

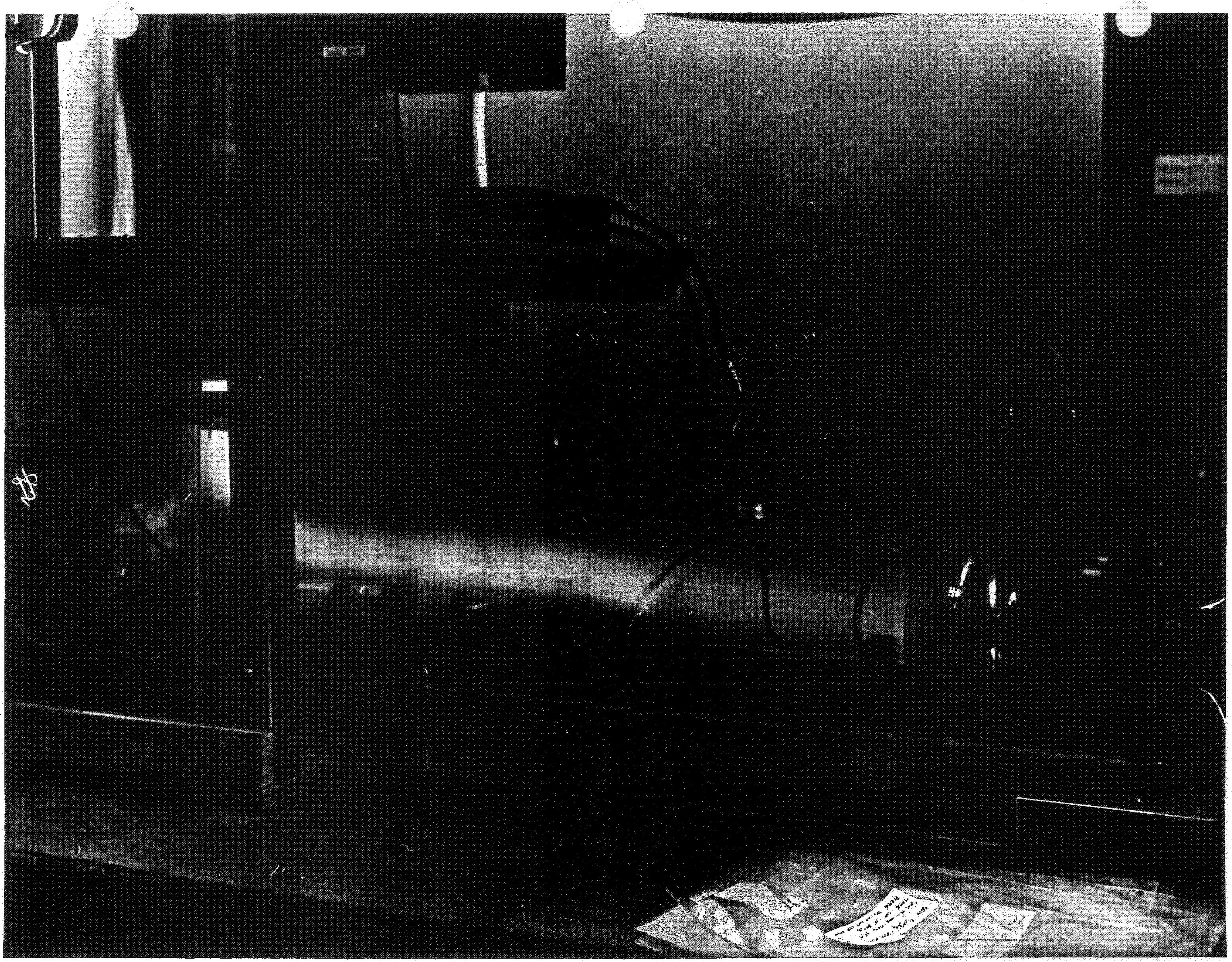

Figure 3.3.3.1 Plasma Atomic Oxygen Material Screening Test Facility

Figure 3.3.3-2 shows the changes in optical properties of the coated tubes. The following changes were noted for the various protective coatings.

a. Extremely poor adhesion of the 0.0001-in layer of electroplated Ni to the Gr/Ep (with and without the SiO_x coating). The samples began to show bubbles within the first hour of exposure. These areas of adhesion loss are shown in figure 3.3.3-3. These specimens were not tested for the additional 22 hr.

b. The 0.001-in layer of electroplated Ni (with and without SiO_x) had a total adhesion loss to the Gr/Ep, but there was no bubbling. The atomic oxygen penetrated between the Ni and Gr/Ep along the entire 1.5-in tube length. The Ni coating was still intact, but could be slid around the tube in one piece. This may have been caused by porosity in the nickel plating. The SiO_x retained its initial optical appearance, but the uncoated Ni specimen became noticably darker.

c. The phosphoric, chromic, and SiO_2 foils had minimal changes in optical appearance when compared to unexposed specimens. There was no loss of adhesion between the Al foil and the Gr/Ep tube on the samples that had the epoxy primer applied per Boeing specification (spray application) to the Al foil prior to the tube fabrication. The one sample that had the epoxy primer brushed onto the foil exhibited several .10-in to .25-in-diameter bubbles in the foil during exposure in the PAOMS.

d. All samples displayed loss of Gr/Ep on the edges and in the interior surfaces. The edges that were once flush with the various coatings had recessed approximately 1/16 of an inch during the 33 hr of exposure. The downstream edges had degraded at approximately the same rate as the upstream edges.

During the atomic oxygen testing of anodized Al foil, one 1.5-in-long tube was punctured to produce an approximately 0.015-in-diameter pin hole through the coating and the foil to simulated the potential damage caused by micrometeroids. After 22 hr of exposure in the PAOMS facility, the tube with the pin hole was removed. A cut was made through the tube where the pin hole in the foil was located. On examination, it was determined that two of the twelve plies of P75S/934 Gr/Ep were eroded away. Figure 3.3.3-4 shows the size of the pinhole

Sample	Before Test		11 Hr Exposure		33 Hr Exposure	
	α	ε	α	ε	α	ε
SiO_2/Al/Al Foil	0.35	0.20	0.34	0.22	0.34	0.21
Chromic Anodized Al Foil	0.29	0.35	0.28	0.38	0.28	0.40
Phosphoric Anodized Al Foil	0.23	0.19	0.18	0.21	0.18	0.19
0.001-in electroplated Ni	0.37	0.11	0.39	0.12	0.41	0.11
SiO_x/0.001-in electroplated Ni	0.49	0.52	0.47	0.48	0.43 to 0.46	0.44
0.0001-in electroplated Ni	0.46	0.13	0.36 to 0.44	0.11	--	--
SiO_x/0.0001-in electroplated Ni	0.53	0.55	0.54	0.50	--	--

Figure 3.3.3-2

Change in Optical Values Caused by Atomic Oxygen Exposure

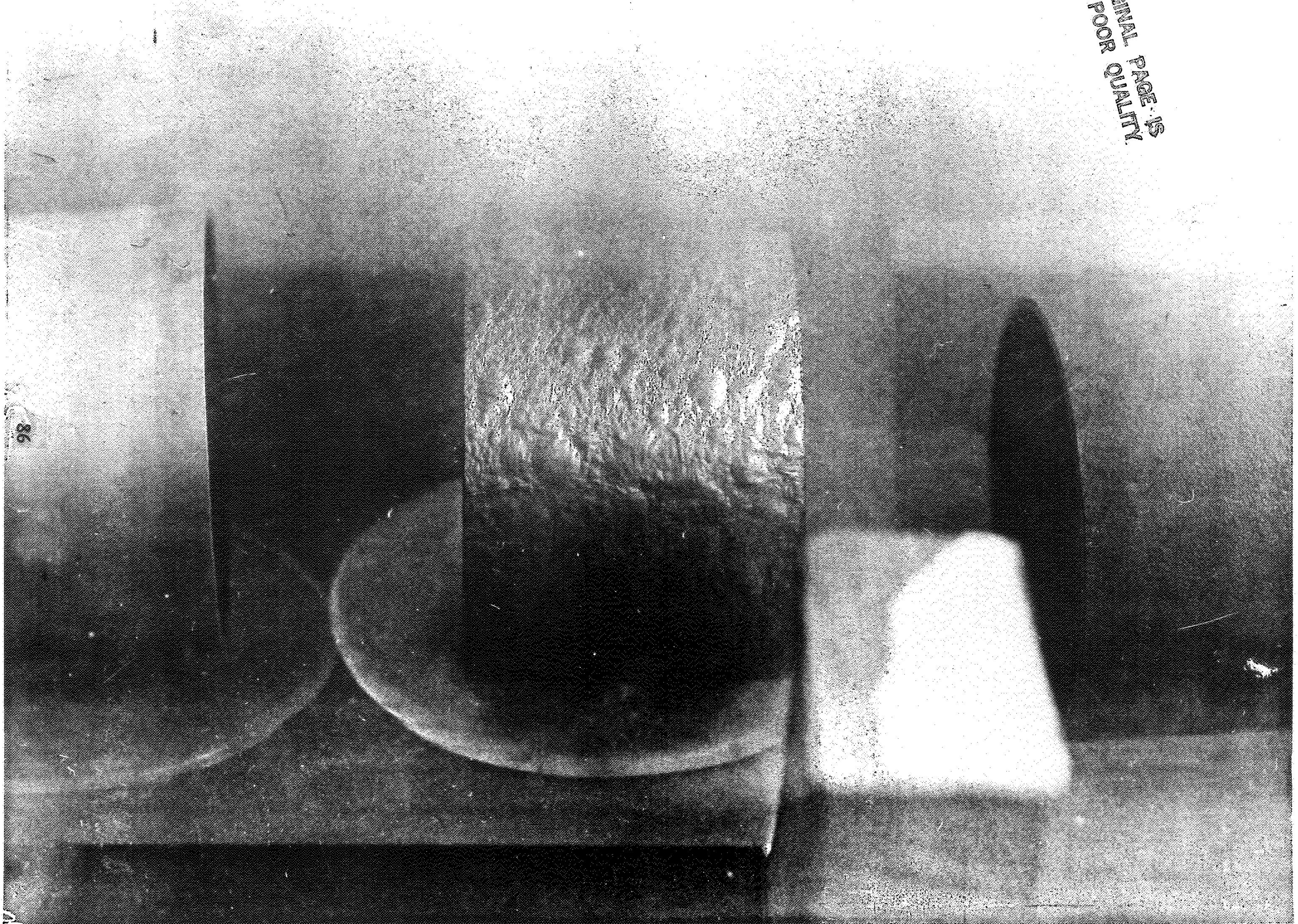

Figure 3.3.3-3 Adhesion Loss of 0.001-in Electroplated Nickel

ORIGINAL PAGE IS
OF POOR QUALITY

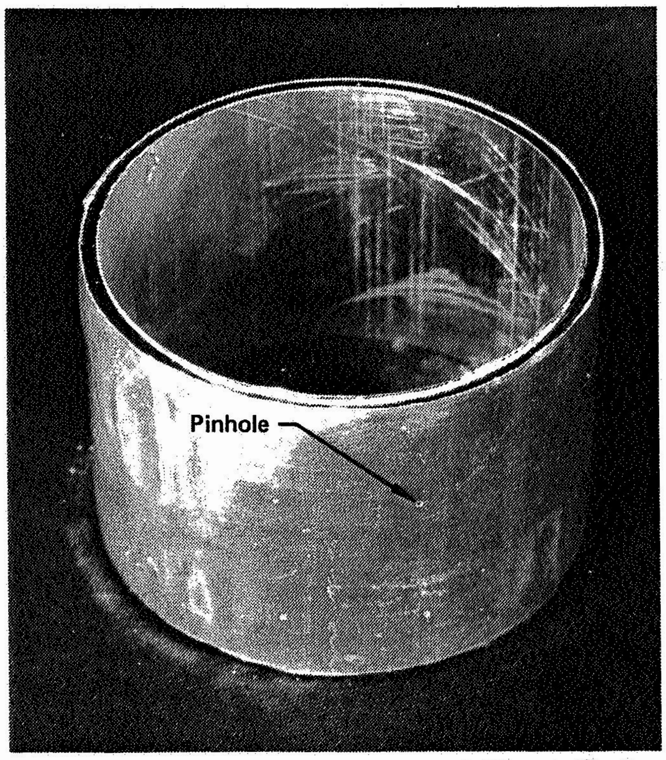

1.4X magnification

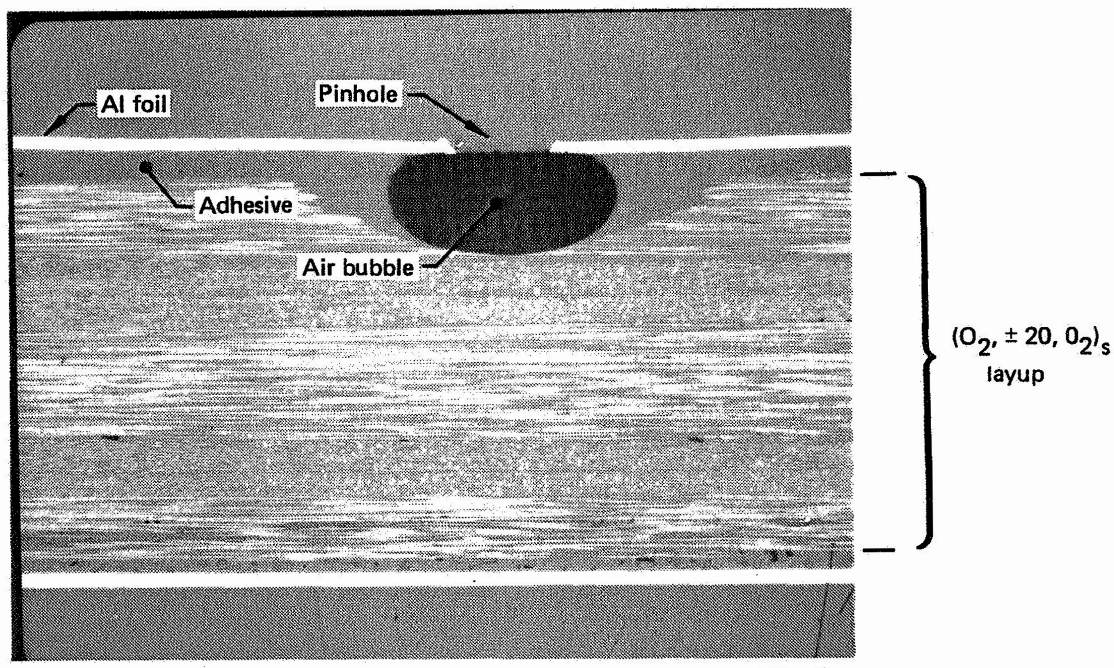

30X magnification

Figure 3.3.3-4 Effect of Pin Holes During Atomic Oxygen Testing and the photomicrograph of the cross-section of the pinhole. (This tube had Al foil bonded to both the interior and exterior surfaces).

Because the Al foil is inert to the effects of atomic oxygen, the pinhole through the foil remains constant. This limits the flux of atomic oxygen to the Gr/Ep. Therefore, it is expected that while continued exposure would erode the Gr/Ep at a constant mass loss, because of the increasing surface area, the rate of penetration would be expected to decrease. No structural testing was performed to determine the effect of the erosion of the Gr/Ep on the mechanical properties of the tube section.

3.3.4 Ultraviolet Resistance

Ultraviolet (UV) testing of the protective coatings was beyond the scope of this program, but similar coatings were exposed to simulated UV testing primarily during the mid-1960s to early 1970s (refs. 4-11). The standard test procedure used was to test the coatings under accelerated UV in vacuum and either remove the specimens from the chamber to monitor optical changes or perform in-situ optical measurements. The in-situ optical measurements provided the opportunity to monitor optical changes during testing without exposing the samples to air. The following paragraphs describe some of the results of this testing:

Work done by D.D. Swofford et al (ref. 4) determined the effects of simulated vacuum/UV space environment on the optical properties of sulfuric acid anodized Al foil. The optical properties of the sulfuric anodized foil were only slightly altered ($\pm$2%) by UV radiation in air. However, the combined UV/vacuum proved to cause yellowing of the anodized foil. There was a gradual increase from an initial $\alpha = 0.16$ to an $\alpha = 0.34$ during the first 700 equivalent sun hours (ESH). Very little change was further noted up to 1344 ESH. The ε remained at 0.83 throughout the testing. The UV source was a mercury arc lamp and the samples were exposed to atmosphere during optical measurements.

Ref. 5 discussed the results of a three year program that included development of high-vacuum space-simulation facility that permitted simultaneous exposure of specimens to electrons, protons and UV radiation. In-situ measurement capabilities of total hemispherical reflectance were also developed. Among the twenty coatings tested were sulfuric anodized Al and a 2.5 micron layer of SiO_2 vacuum deposited onto buffed Al substrates. Figure 3.3.4-1 shows the reflectance changes in the SiO_2 coated substrate following UV exposure and figure 3.3.4-2 shows the reflectance changes in the sulfuric anodized Al after UV exposure. Also, the SiO_2 coated substrate exhibited very little change in reflectance (3%) when exposed to 50-keV electrons at fluences up to 8×10^{15} electrons/cm^2.

3.3.5 Thermal Cycling of Al Foil Bonds

The purpose of this adhesion testing was to determine if there was any change in bond strenghts caused by thermal cycling. Bare Al foil (backside of SiO_2) and chromic anodized Al foil were evaluated. The Al foil had the epoxy primer sprayed onto the backside prior to bonding with .005-in-thick epoxy sheet adhesive to the Gr/Ep substrate. The chromic anodized foil was cured at temperatures of 250°F and 350°F (using the respective epoxy adhesives and primers) to determine if there was any difference in adhesion caused by cure temperature. Three samples of each bond were tested for control values and three samples were subjected to 80 72-min thermal cycles at a temperature range of +250°F to -250°F. The sample size and bond testing technique were discussed in section 3.2.3.

Testing of the control specimens showed that the unanodized foil was able to be peeled off the Gr/EP layup during the peel test while the peel strength of both 250°F and 350°F cured anodized foil exceeded the tensile strength of the 0.002-in foil. The average peel strength of the unanodized foil was 4-in-lb/in of spcimen width. Peel testing of the thermal cycled specimens proved impossible because in all cases the Al foil and the first Gr/Ep layer delaminated from the remainder of the substrate during the thermal cycling process. The CTE mismatch between the foil and the substrate and the CTE mismatch between the 0-deg and 90-deg layers of substrate causes interlaminar shear stresses and a through-the-thickness normal stress within the assembly. At the low temperature of the thermal cycling process, these stresses become large enough near the free edges to cause the delamination. From the presence of the delamination it can be inferred that the Al foil-Gr/Ep bond strength exceeds the interlaminar strength of the Gr/Ep.

There was no delamination of any of the Gr/Ep plys of the foil wrapped tube section that was subjected to the equivalent cycling. This is primarily due to the fact that tubes do not possess free edges, except at the ends.

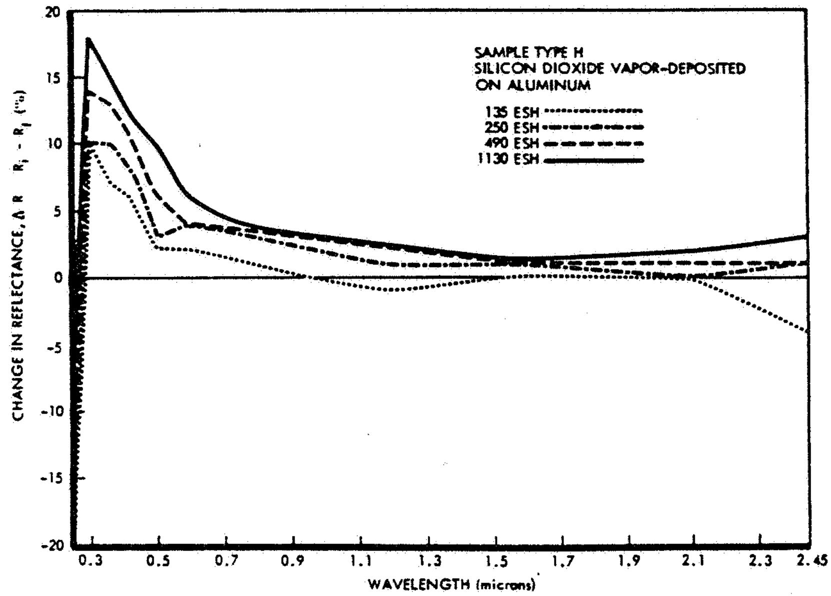

Figure 3.3.4-1 In-Situ Reflectance Changes in SiO_2 Vacuum Deposited on Aluminum

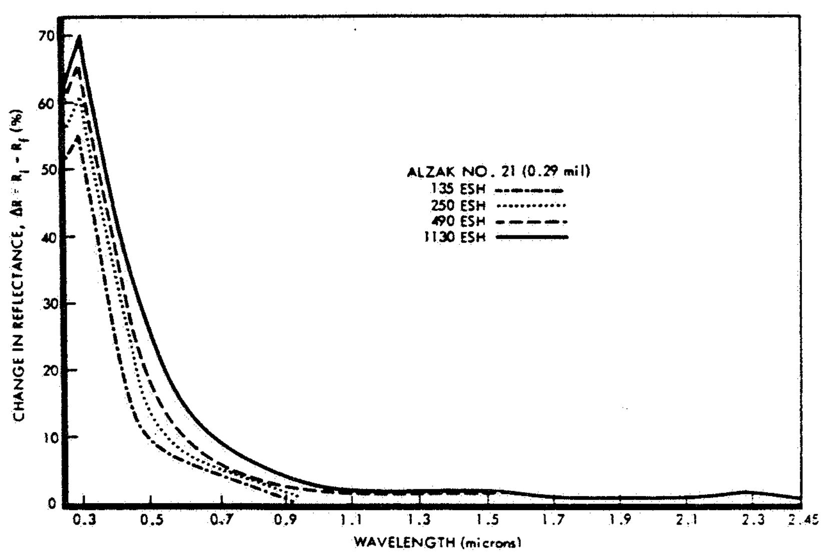

Figure 3.3.4-2 In-Situ Reflectance Changes in Sulfuric Acid Anodized Aluminum

C-2

3.3.6 Resistance to Microcracking of Bare Gr/Ep Tubes

An experimental investigation into the relative toughness of Gr/Ep tubular structures designed for Space Station application was undertaken. The tubes were subjected to a total of 550 thermal cycles to determine if the thermal cycling at LEO would cause the formation of microcracks. Four different prepregs were evaluated:

a. P75S/934 supplied by Fiberite.
b. P75S/1914 supplied by Union Carbide.
c. P75S/1916 supplied by Union Carbide.
d. P75S/1920 supplied by Union Carbide.

The three prepregs supplied by Union Carbide are their "third-generation" epoxy resins impregnated into P75S fibers. The four prepregs were all fabricated by Boeing personnel into 4-ft long by 2-in diameter tubes using a ply sequence of $(0_2, \pm 20, 0_2)_S$. The tubes were then cut into 12-in-long sections.

Two tubes of each prepreg (eight tubes total) were subjected to 50 thermal cycles of simulated LEO exposure. This test was described in section 3.3.1. The temperature extremes were +175°F to -80°F (fig. 3.1.1.1-2). These tubes were then removed from the chamber and subjected to microcrack analysis using 100X and 200X magnification. No microcracks were found in any of the tube surfaces.

Further thermal cycling was initiated. The eight tubes that had been exposed to the 50 cycles of LEO environment were subjected to an additional 500 56-min thermal cycles, which had a temperature range of +120°F to -150°F. This testing was performed in a thermal cycling chamber and not under vacuum as the initial 50 thermal cycles were. After completion of the 500 cycles, the tubes were re-examined to determine if any cracking had taken place. Using 50X to 200X magnification and X-ray analysis as described in section 3.2.1, no microcracks were found in any of the specimens. The P75S/934 tubes were then further cut to provide another cross section of the tube for evaluation, but again no microcracks were found.

Classical laminate analysis was then used to determine the stresses perpendicular to the fibers in each of the layers as these stresses are the cause of transverse matrix cracking. The stress-free temperature of the Gr/Ep was assumed to be the same as the cure temperature, which was 350°F. The following stresses were computed for a laminate (tube) temperature of -150°F with a ply sequence of $(0_2, \pm 20, 0_2)_s$:

0 degree layers, σ_2 = 1800 lb/in^2
$\pm$20 degree layers, σ_2 = 2300 lb/in^2
ultimate, matrix, tensile strength, $F_2{}^T$ = 2800 lb/in^2

As can be seen the stress level in the 20-deg plies is close in value to ultimate tensile strength, but does not exceed it. The ultimate tensile strength was predicted using Boeing design data.

The results of this experimental investigation show that because of the low angle off-axis ply sequence required to meet the stiffness requirements of the Space Station trusses, the microcracking problem of Gr/Ep has been minimized.

3.4 TEST RESULTS AND CONCLUSIONS

a. While the electroplated Ni has the potential of providing conformal coatings to the tubes and any irregular shaped surfaces, such as end fittings, the adhesion loss during exposure to the LEO environment needs to be improved. Perhaps if the edges of the tubes were sealed against atomic oxygen, this problem would be eliminated. Studies should be conducted to determine if the Ni is permeable to atomic oxygen, or if the adhesion loss is caused by the atomic oxygen attacking the bond through the edge of the tubes. The SiO_x coating deposited by Battelle Columbus demonstrated capability to improve the environmental durability of the Ni. The coating also showed promise in improving the capability to tailor the optical properties of the electroplated Ni to meet the targeted values.

b. Both the chromic and phosphoric acid anodized Al foil proved to possess similar environmental durability and possessed excellent adhesion to Gr/Ep when bonded properly. The chromic anodizing can be easily tailored to meet a variety of optical values while it was not proved that the emittance of the phosphoric anodized Al foil could be increased to acceptable levels. Both anodizing techniques have the additional benefit of being produced in large volume without excessive R&D being required.

c. The SiO_2/Al/Al foil proved to also possess environmental durability similar to the anodized foils although the bond strength to the Gr/Ep was not as high. This is because the peel strength of the unanodized Al foil is less than that of the anodized foil (section 3.3.5). During abrasion testing the coating showed signs of optical degradation, but this would be a small percent of the overall area. The major disadvantage is the need to have large area vacuum coaters to deposit these coatings onto Al foil.

d. Microcracks were not found in any of the composite tube structures after undergoing 50 94-min, +175°F to -80°F thermal cycles and 500 56-min, +120°F to -150°F thermal cycles. The tubes were examined for microcracks using 50X to 200X magnification and X-ray analysis. The use of low angle off-axis plies (20 deg) required to meet the stiffness requirements of the Space Station seems to have minimized the microcracking phenomenon.

e. The thermal cycle test data, taken by monitoring the bare and coated tube during cycling, verified the thermal analysis used to predict the time vs temperature profiles of the tubes. This same analysis was used to predict the temperature profiles the various evaluated coatings would undergo in LEO. The predicted temperatures ranged from +65°F to -55°F for the chromic anodized foil wrapped tube to +155°F to -175°F for the bare Gr/Ep tube.

Chromic acid anodized Al foil was selected as the best coating for protecting the Gr/Ep tubes from the LEO environment because of its -

1. Optical tailorability.
2. Excellent adhesion to Gr/Ep.
3. Ease of manufacturing and low cost.
4. Excellent handling properties.

This selection does not imply that other coatings are not suitable for specific applications. No substantial R&D efforts were attempted to improve their properties or optimize processing to assess their full potential as a protective coating for Space Station trusses.

4.0 DELIVERED HARDWARE

Upon completion of Part 1, System Definition, Boeing provided NASA LaRC with four 4-ft-long by 2-in-diameter, P75S/934 Gr/Ep tubes. The layup sequence was $(0_2 \pm 20, 0_2)_s$. Half of each tube was wrapped with adhesively bonded, uncoated Al foil. Two of the tubes were wrapped with 0.0015-in foil and the other two were wrapped with 0.003-in foil.

After the initial screen testing was complete, Boeing supplied NASA LaRC with two samples each of the five selected coatings bonded to 12-in-long by 2-in-diameter Gr/Ep tubes.

At the completion of Part 3, Scale-Up and Assembly, Boeing delivered four 8-ft-long Gr/Ep tubes wrapped with chromic acid anodized 0.002-in Al foil. These tubes are shown in figure 4.0-1. The foil surface had been textured to increase the diffuse reflectance as shown in figure 4.0-2. Also delivered was a space-erectable structural end-fitting (discussed in section 2.1.5). Figure 4.0-3 shows the four tubes latched to the end-fitting.

ORIGINAL PAGE IS
OF POOR QUALITY

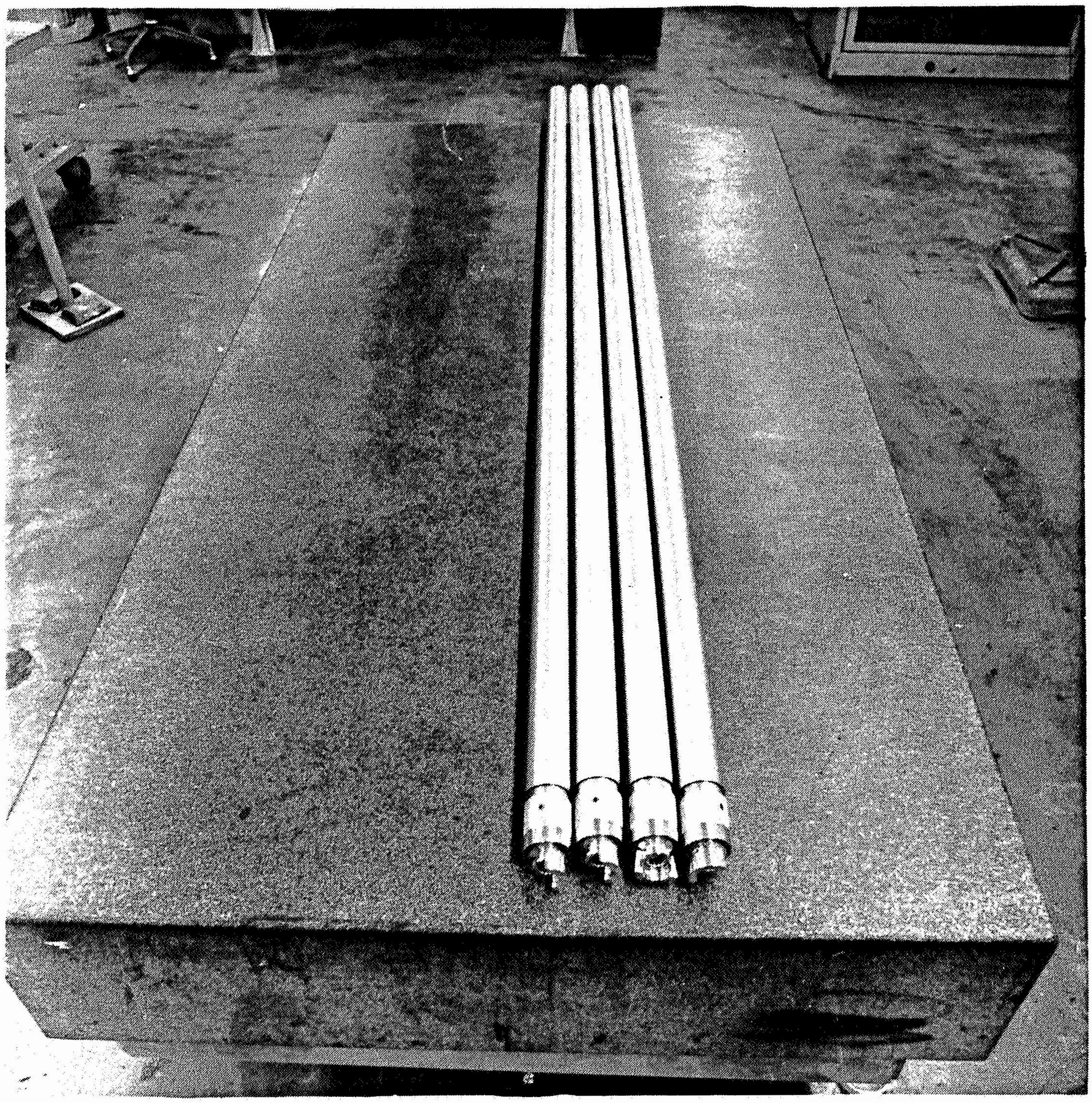

Figure 4.0-1 Four 8-ft-long Gr/Ep Tubes Wrapped With Al Foil

ORIGINAL PAGE IS
OF POOR QUALITY

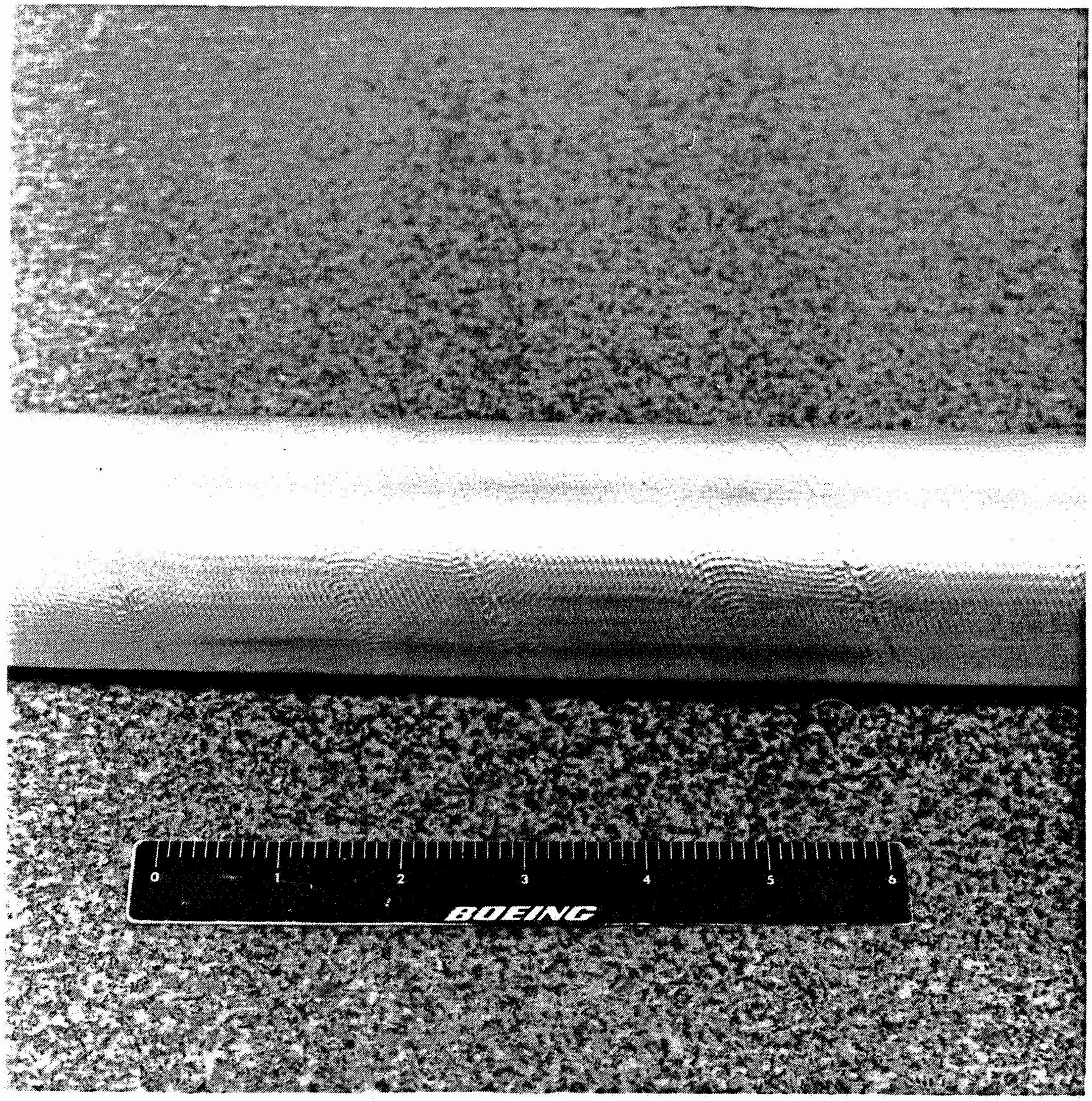

Figure 4.0-2 Chromic Acid Anodized Foil With Textured Surface

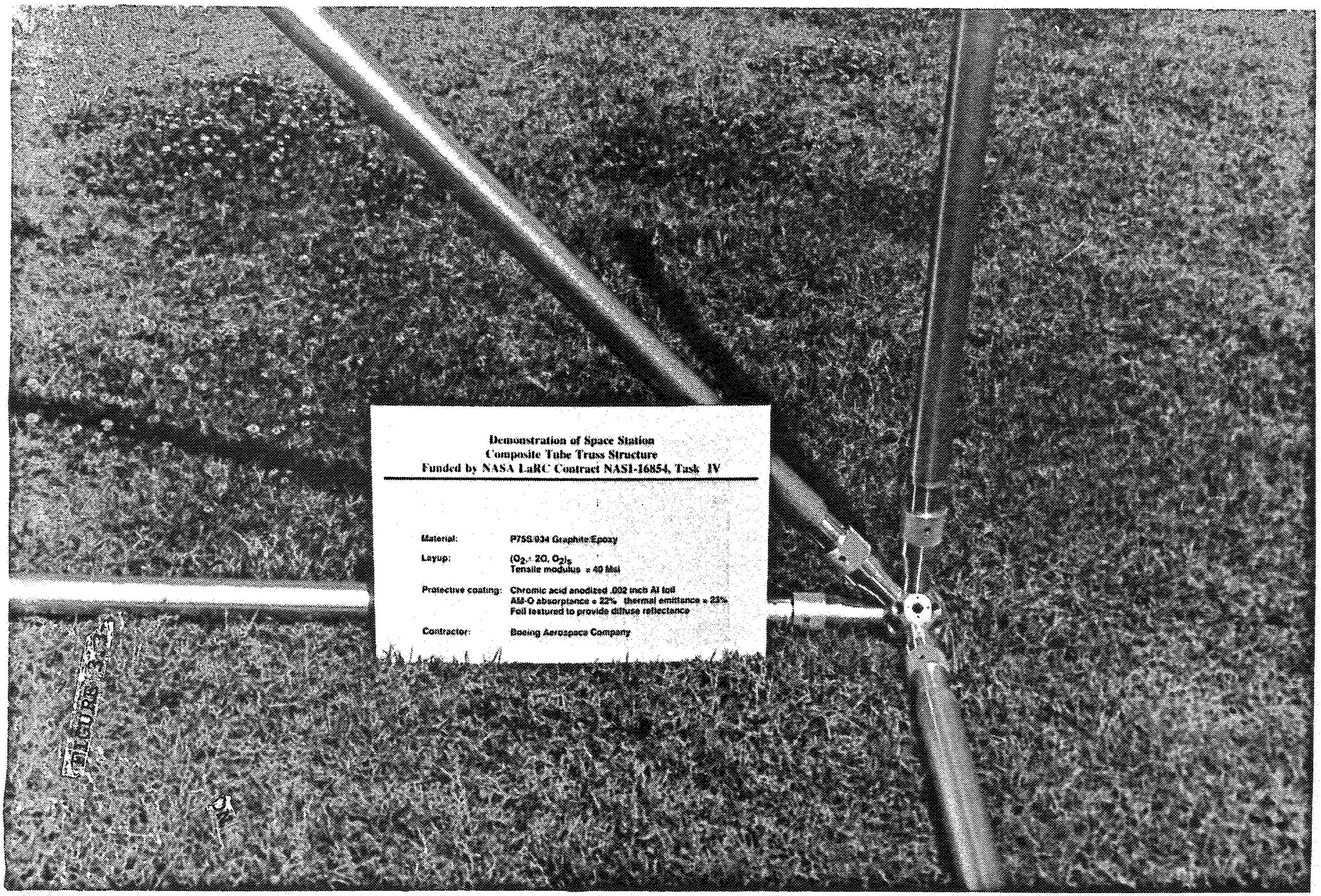

Figure 4.0-3 Four 8-ft Tubes Latched Together

5.0 REFERENCES

1) JSC-19989, "Space Station Reference Configuration Description", Lyndon B. Johnson Space Center, Houston, Texas, August 1984.

2) NAS8-36586, "Technology Readiness for Space Station External Surface Materials," Boeing Aerospace Company, Seattle, Washington, April 1985.

3) Wernick, S. and Pinner, R., "Surface Treatment of Alumium", Vol. 2, 1972, pp. 725.

4) Swofford, D. D. et al, "Effects of Extreme Ultraviolet on the Optical Properties of Thermal Control Coatings," AIAA Progress in Astronautics and Aeronautics, Vol. 21, 1969, pp. 667-695.

5) Brown, R. R. et al, "Electron-Ultraviolet Radiation Effects in Thermal Control Coatings," AIAA Progress in Astronautics and Aeronautics, Vol. 21, 1969, pp. 697-724.

6) Bradford, A. P. and Hass, G., "Increasing the Far Ultraviolet Reflectance of Silicone-Oxide-Protected Aluminum Mirrors by Ultraviolet Irradiation," J. Opt. Soc. Am. 53, 1963, pp. 1096-1100.

7) Weaver, J. H., "Effects of a Vacuum-Ultraviolet Environment on the Optical Properties of Bright Anodized Aluminum," Air Force Materials Laboratory - TR-64-355, January, 1965.

8) Gillette, R. B., "Ultraviolet-Proton Radiation Effects on Solar Concentration Reflective Surfaces," NASA CR-1024, May, 1968.

9) Fogdall, L. B. and Cannaday, S. S., "Proton and Ultraviolet Degradation Tests on HELIOS Spacecraft Materials," Boeing Doc. D180-17868-2, April 1974.

5.0 REFERENCES (Cont'd)

10) Drummeter, L. F. and Hass, G., "Solar Absorptance and Thermal Emittance of Evaporated Coatings," Physics of Thin Films, 1964.

11) Shelton, J. L. and Akers, W. W., "Total Hemispherical Thermal Emittance of Nickel as a Function of Oxide Thickness," AIAA Progress in Astronautics and Aeronautics, Vol. 18, 1966.

Standard Bibliographic Page

1. Report No. NASA CR-178116	2. Government Accession No.	3. Recipient's Catalog No.
4. Title and Subtitle Development of Composite Tube Protective Coatings		5. Report Date July 1986
		6. Performing Organization Code
7. Author(s) H. Dursch and C. Hendricks		8. Performing Organization Report No. D180-29767-1
9. Performing Organization Name and Address Boeing Aerospace Company P.O. Box 3999 Seattle, WA 98124		10. Work Unit No.
		11. Contract or Grant No. NAS1-16854
12. Sponsoring Agency Name and Address National Aeronautics and Space Administration Washington, DC 20546		13. Type of Report and Period Covered Contractor Report
		14. Sponsoring Agency Code

15. Supplementary Notes

Langley Technical Monitor: Lou Teichman
Final Report

16. Abstract This program evaluated protective coatings for graphite/epoxy (Gr/Ep) tubular structures proposed for the Space Station. The program was divided into four parts; System Definition, Coating Concept Selection and Evaluation, Scale-up and Assembly, and Reporting.

System Definition involved defining the structural and environmental properties required of the Gr/Ep tubes. The prepreg and ply sequence selected was a P75S/934 $(0_2, \pm 20, 0_2)_s$ layup which meets the various structural requirements of the Space Station.

Coating Concept and Selection comprised the main emphasis of the effort. Concepts for protectively coating the Gr/Ep tubes included the use of metal foils and electroplating. The program results demonstrated that both phosphoric and chromic acid anodized Al foil provided adequate adhesion to the Gr/Ep tubes and stability of optical properties when subjected to atomic oxygen and thermal cycling representative of the LEO environment. SiO_2/Al coatings sputtered onto Al foils also resulted in an excellent protective coating. The electroplated Ni possessed unacceptable adhesion loss to the Gr/Ep tubes during atomic oxygen testing.

Scale-Up and Assembly involved fabricating and wrapping 8-ft-long by 2-in-diameter Gr/Ep tubes with chromic acid anodized foil and delivering these tubes, along with representative Space Station erectable end fittings, to NASA LaRC.

17. Key Words (Suggested by Authors(s))	18. Distribution Statement
Graphite/Epoxy Anodized Foil Atomic Oxygen Protective Coatings for LEO	Unclassified - Unlimited

19. Security Classif.(of this report)	20. Security Classif.(of this page)	21. No. of Pages	22. Price
Unclassified	Unclassified	100	